

# Statistical Physics of Phase Transitions

## TCM graduate lectures, Michaelmas term 2001

Matthew J. W. Dodgson

First lecture: 5/11/01

- 1. Classical examples:** Mean-field theory of the ferromagnetic phase transition. Van der Waals model/theory of liquid-gas transition. Landau theory of continuous phase transitions; interfaces and domain walls; different order-parameter symmetries.
- 2. Stat. mech. basis of phase transitions.** Why do phase transitions occur? (symmetry, separation of phase space). Simple model of a first-order phase transition. From stat. mech. to MFT: Coarse graining and saddle-point approximation. Example: the Ising model; exact solution for 1D nearest neighbours and for infinite-range; simulations in 2D.
- 3. Effect of thermal fluctuations on ordered phase.** Importance of the thermodynamic limit. Impossibility of symmetry breaking in 1D. Gaussian approximation, continuous symmetry breaking and Goldstone modes. Lower critical dimensions and the Hohenberg-Mermin-Wagner theorem.
- 4. Field theory of phase transitions.** Destruction of mean-field theory by fluctuations near the critical point; diverging specific heat from Gaussian fluctuations. Upper critical dimension and Ginzburg criterion. Perturbation theory and Feynman diagrams. Breakdown of pert. theory below the upper critical dimension.
- 5. Scaling and Renormalization Group approach.** Scale-invariance at the critical point. Review of critical exponents. Renormalization Group transformations; from fixed points to critical exponents and scaling laws. Momentum-shell RG and the Gaussian fixed point. A new fixed point below four dimensions; critical exponents to order  $\epsilon = 4 - d$ .
- 6. The 2D-XY model.** Expansions at low and high temperatures. Spin-waves and vortices as relevant excitations. Simple Kosterlitz-Thouless argument for vortex-pair unbinding transition. Mapping from XY-model to Sine-Gordon model, and RG analysis.

## Books

P. M. Chaikin and T. C. Lubensky, *Principles of Condensed Matter Physics*, (Cambridge University Press, 1995).

Covers much more than just phase transitions, but still manages to introduce much in these lectures in an understandable way.

N. Goldenfeld, *Lectures on Phase Transitions and the Renormalization Group*, (Addison-Wesley, 1992).

Excellent text book on the statistical physics of phase transitions.

S.-K. Ma, *Modern Theory of Critical Phenomena*, (Addison-Wesley, 1976).

Possibly the first textbook explaining field theory and RG of continuous phase transitions. Goes through the basic examples in good detail, but perhaps not the ideal first introduction to the subject.

C. Domb, *The Critical Point*, (Taylor and Francis, London, 1996).

Historical overview of the development of the theory of critical phenomena.

J. Zinn-Justin, *Quantum Field Theory and Critical Phenomena*, (Oxford University Press, 1989).

Heavy going book which covers a lot of the mathematical aspects of the course, as well as showing the links between the theory of phase transitions and quantum field theory.

# Lecture One

## 1 Early understanding of phase transitions

In this lecture we review the classical understanding of phase transitions, dating from over a century ago. We start with the Weiss mean-field theory of ferromagnetism. We then look at the Van der Waals model of a liquid-gas phase transition. Both theories have similar features, in particular a critical end-point to a coexistence line. We therefore look at the general description of this critical point, the Landau theory, and find that a diverging length scale is a characteristic of continuous phase transitions.

### 1.1 Classical theory of the ferromagnetic phase transition

#### 1.1.1 Statistical physics of a magnetic moment: paramagnetism

Consider a classical magnetic dipole moment of fixed strength  $m_0$ , which is free to rotate. In a magnetic field  $\mathbf{B}$  the dipole has an interaction energy,  $E(\theta, \phi) = -\mathbf{m} \cdot \mathbf{B} = -m_0 B \cos \theta$ . In thermal equilibrium the dipole will sample all possible directions with a Boltzmann probability distribution,  $\mathcal{P}(\theta, \phi) = \exp[-\beta E(\theta, \phi)]$  (with  $\beta = 1/T$ ). We can calculate the average magnetic moment in the field direction  $\tilde{m} = \langle m_z \rangle = Z^{-1} \int d\theta d\phi \sin \theta \mathcal{P}(\theta, \phi) m_0 \cos \theta$ , where

$$Z = \int_0^\pi d\theta \int_0^{2\pi} d\phi \sin \theta \mathcal{P}(\theta, \phi) = \frac{4\pi}{\beta m_0 B} \sinh(\beta m_0 B). \quad (1)$$

We quickly find  $\tilde{m}$  by differentiating this “partition function”,

$$\tilde{m} = \frac{1}{Z} \frac{\partial Z}{\partial B} = m_0 \left[ \coth(\beta m_0 B) - \frac{1}{\beta m_0 B} \right] \equiv m_0 L(\beta m_0 B), \quad (2)$$

where we have defined the Langevin function as  $L(x) = \coth(x) - 1/x$ . Usually we are interested in the linear response, i.e as  $B \rightarrow 0$  we should have  $M = \rho \tilde{m} = \chi H$  (where  $H = B/\mu_0$  and  $\rho$  is the density of the magnetic moments). Expanding the Langevin function we find  $\lim_{x \rightarrow 0} L(x) = x/3$  so that we have,

$$\chi = \frac{\mu_0}{3} \rho m_0^2 \beta \propto \frac{1}{T}, \quad (3)$$

(Note, a positive susceptibility is defined as paramagnetic).

An inverse temperature dependence of susceptibility was systematically measured by P. Curie (1895) for a range of paramagnetic substances (oxygen, palladium, and various salts such as  $\text{FeCl}_2$ ).<sup>1</sup> The above derivation, which ignores the interactions between a set of fixed magnetic moments, is due to Langevin (1905). Of course, we have also ignored the quantization of spin and angular momentum. This is important in restricting the allowed values of  $m_z$  of the individual moments. However, the general “Curie law” of  $\chi \propto \frac{1}{T}$  still holds.<sup>2</sup>

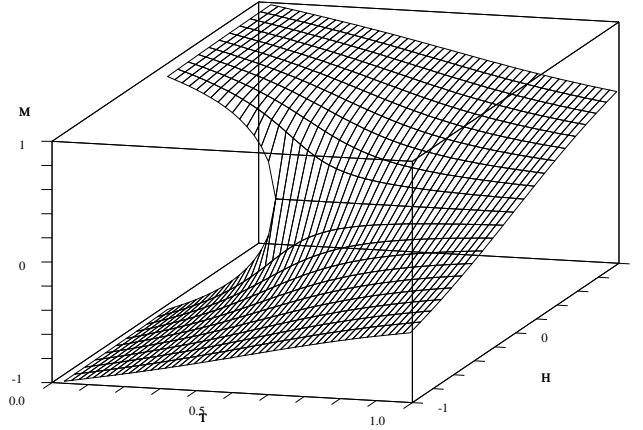


Figure 1: The self-consistent mean-field solution for the magnetization of a ferromagnet as a function of temperature and external field.

### 1.1.2 Weiss mean-field description of ferromagnets

Typical materials contain many such magnetic moments (eg. atomic spins), which have some interaction. A general form which can often be justified (eg. classical dipole interaction, Heisenberg exchange) is the interaction energy,

$$E_{\text{int}} = - \sum_{i < j} V(\mathbf{R}_i - \mathbf{R}_j) \mathbf{m}_i \cdot \mathbf{m}_j. \quad (4)$$

The thermodynamics of this problem is now non-trivial. However, a reasonable approximation is to look at the energetics of a single moment interacting with the average moment on the other spins. This is equivalent to the  $i$ -th moment seeing an effective field,

$$\mathbf{B} = \mu_0 \mathbf{H} + \sum_{i \neq j} V(\mathbf{R}_i - \mathbf{R}_j) \langle \mathbf{m}_j \rangle. \quad (5)$$

This “mean-field theory” was first used by Weiss (1907) to explain the behaviour of ferromagnets observed by Curie. In a ferromagnet the interactions tend to align the spins, so that  $\rho^{-1} \sum_{i \neq j} V(\mathbf{R}_i - \mathbf{R}_j) \equiv \Theta > 0$ , and the magnetization  $M = \rho \langle m_j \rangle$  lies in the same direction as the external field,  $B = \mu_0 H + \Theta M$ . The effective field now enters into the Langevin model for the  $i$ -th moment,

$$M = m_0 \rho L [\beta m_0 (\mu_0 H + \Theta M)]. \quad (6)$$

This is a relation between  $H$  and  $M$ , known as the equation of state. From this, all thermodynamic properties can be obtained! The self-consistent solution of  $M(T, H)$  for this equation is shown in Fig. 1. At low temperatures there is a spontaneous magnetization at zero field. The size of  $M(T, H \rightarrow 0)$  falls continuously to zero at a critical temperature  $T_c$ . We can see this by expanding the inverse Langevin function,<sup>3</sup>

$$\mu_0 H = -\Theta M + \frac{1}{\beta m_0} L^{-1} [M/m_0 \rho] \quad (7)$$

<sup>1</sup>E.C. Stoner, *Magnetism and Matter*, (Methuen, London, 1934).

<sup>2</sup>In this course on phase transitions, we will not be too interested in the effects of quantum mechanics. The reason for this (coarse-graining) will be justified later.

<sup>3</sup>we use the expansion  $L^{-1}(x) = 3x + \frac{9}{5}x^3$

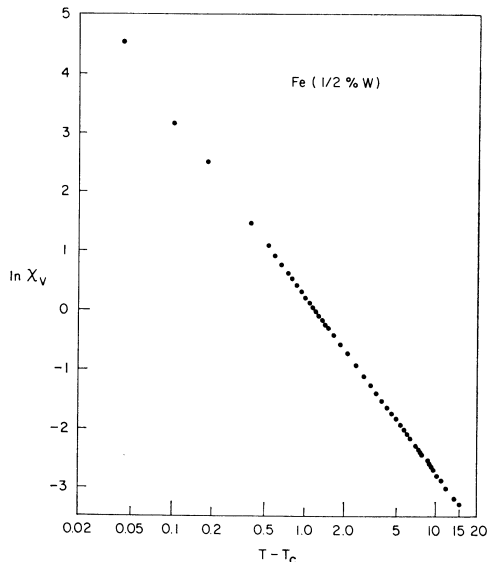


Figure 2: Experimental values of susceptibility of an Iron alloy, from J.E. Noakes et al., J. Appl. Phys. **37**, 1265 (1966). This log-log plot shows a linear dependence over several orders of magnitude. However, the slope is not the classical value of one, but  $\gamma = 1.33 \pm 0.015$ .

$$= \left(-\Theta + \frac{3}{\beta \rho m_0^2}\right)M + \frac{9}{5\beta m_0^4 \rho^3}M^3, \quad (8)$$

and we have a susceptibility near the critical point (or Curie point) of,

$$\chi = \frac{a}{T - T_c}, \quad (9)$$

with  $T_c = \frac{1}{3}\Theta\rho m_0^2$ . This is the famous Curie-Weiss law (observed by Curie and explained by Weiss).

This very simple theory already has a richness of behaviour. The zero field solution below  $T_c$  displays symmetry breaking: There are two equivalent solutions, each of which has a lower symmetry than the interactions in the system. As one passes from positive to negative fields, there is a jump in the magnetization, i.e. the  $H = 0$  line below  $T_c$  marks a first-order phase transition (jump in  $\partial G/\partial H$ ). The critical point itself is very special, where the magnetization has a divergent slope. This also leads to a discontinuity in the specific heat as we increase  $T$  through  $T_c$  at zero field.

Finally we note that Fig. 1 does not show all of the solutions to (6). Considering by hand a graphical solution of the self-consistent equation shows two other solution branches, one of which is unstable, the other which is metastable (a metastable solution has higher free energy than the true solution, and so is probabilistically unfavourable in thermodynamic equilibrium).

### 1.1.3 An experimental discrepancy

The above Curie-Weiss law has proved a very useful way for experimentalists to characterize the high-temperature behaviour of magnetic materials, and it is an experimental fact that in ferromagnets the susceptibility diverges at the Curie temperature. However, when one looks very closely at this divergence one finds that the divergence

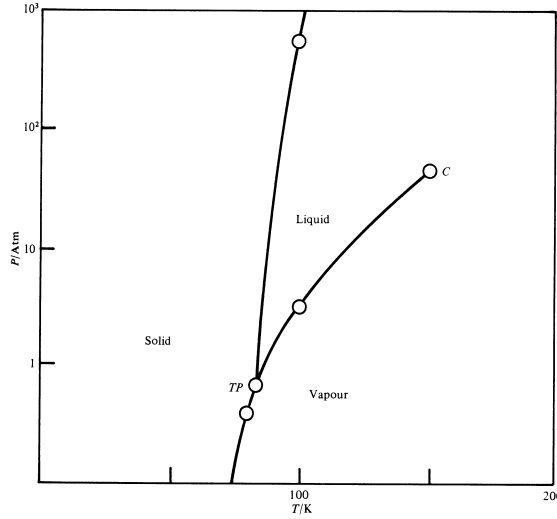


Figure 3: The phase diagram of Argon in the pressure-temperature plane.

has a different form from Curie-Weiss. In Fig. 2, data is shown that obeys a form,

$$\chi = a \left( \frac{T - T_c}{T_c} \right)^{-\gamma}, \quad (10)$$

with  $\gamma \approx 1.33$ , rather than the mean-field prediction of  $\gamma_{\text{MF}} = 1$ . We therefore have a hint that we may need to go beyond mean-field theory. In Lecture 4 we will find out why the mean-field approximation has broken down.

## 1.2 Van der Waals theory of a liquid-gas transition

Fig. 3 shows the phase diagram of Argon. Of interest to us is the boundary between liquid and gas phases. What is the difference between a liquid and a gas? In a liquid the density is approximately fixed in order to minimize the attractive interaction between atoms/molecules. In a gas the density is much lower, but the system gains more entropy. The first understanding of a phase transition between these two states is due to Van der Waals (1873). Consider the energy of pair-wise interactions between identical particles,  $E = \sum_{i < j} V_{\text{int}}(\mathbf{R}_j - \mathbf{R}_i)$ , and let the interaction potential be written as a sum of a long-range attraction (e.g. from the Van der Waals attraction of fluctuating dipoles) and a hard-core repulsion from the particle of radius  $a$ ,  $V_{\text{int}}(R) = V_{\text{attr}}(R) + V_{\text{hc}}(R)$ . For example, an attractive interaction of range  $\lambda$  may be of the form  $V_{\text{attr}}(R) \propto -\exp(-R/\lambda)$ . A typical form for  $V_{\text{int}}(R)$  is shown in Fig. 4.

The thermodynamics of this interacting system is governed by the partition function,

$$Z = \text{Tr} e^{-\beta E} = \int \prod_{i'} d^d R_{i'} e^{-\beta \sum_{i < j} V_{\text{int}}(\mathbf{R}_j - \mathbf{R}_i)}. \quad (11)$$

### 1.2.1 Mean-field theory

If the range of the interaction,  $\lambda$  is much larger than the typical particle separation  $\rho^{-d}$  (where  $\rho = N/V$  is the density), then to a good approximation an individual particle feels the average attractive potential from many ( $\sim \lambda^d \rho$ ) particles. Therefore we can write,

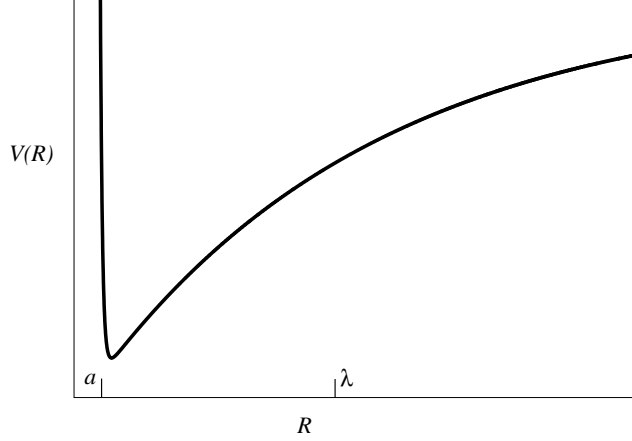


Figure 4: Typical inter-particle interaction potential with a hard-core repulsion and a long-range attraction.

$$\sum_{i < j} V_{\text{att}}(\mathbf{R}_j - \mathbf{R}_i) = \frac{1}{2} \sum_{i \neq j} V_{\text{attr}}(\mathbf{R}_j - \mathbf{R}_i) \approx \frac{1}{2} \sum_i \rho \int d^d r V_{\text{attr}}(r) = -JN^2/V, \quad (12)$$

where we define  $J = \frac{1}{2} \int d^d r V_{\text{attr}}(r)$ . Now the partition function becomes,

$$Z = e^{\beta JN^2/V} \int \prod_{i'} d^d R_{i'} e^{-\beta \sum_{i < j} V_{\text{hc}}(\mathbf{R}_j - \mathbf{R}_i)} = e^{\beta JN^2/V} Z_{\text{hc}}. \quad (13)$$

Van der Waals assumed the effect of the hard core is just to exclude some of phase space, so that,

$$Z_{\text{hc}} = (V - Nb)^N \quad (14)$$

( $b \approx a^d$  is the excluded volume of one particle). This result for  $Z_{\text{hc}}$  is only exact in one dimension, but should be a good approximation at low densities in higher dimensions. The Van der Waals free energy per particle now follows,

$$f(v, T) = -\frac{T}{N} \ln Z = -\frac{J}{v} - T \ln(v - b), \quad (15)$$

where  $v = V/N$  is the volume per particle. Using the formula for pressure,  $P = -\partial f / \partial v|_T$ , we get the Van der Waals equation of state,

$$P(v, T) = -\frac{J}{v^2} + \frac{T}{(v - b)}. \quad (16)$$

The free energy and pressure as functions of volume at fixed temperature are shown in Fig. 5. Note the presence of a critical temperature,  $T_c = (8/27)J/b$  below which there is always a thermodynamically unstable range of volumes (because  $\partial^2 f / \partial v^2 = -\partial p / \partial v$  cannot be negative). In this range the system will need a coexistence of a high-density liquid and a low-density gas. If we instead consider systems of fixed pressure, we need to look at the Gibbs free energy  $G(P, T) = F[V(P, T), T] + PV$ . The result at  $T = 0.75T_c$  is shown in Fig. 6 where we see that as a function of

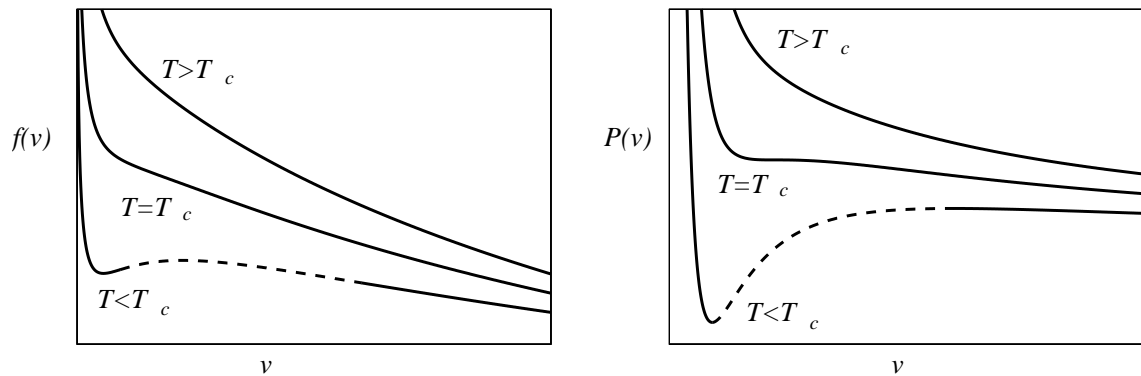


Figure 5: (a) The Van der Waals free energy as a function of volume per particle for temperatures above, below and at  $T_c$ . (b) The pressure  $P = -\partial f / \partial v$  at the same temperatures. Note the unstable region (dashed line) where  $\partial P / \partial v$  is positive.

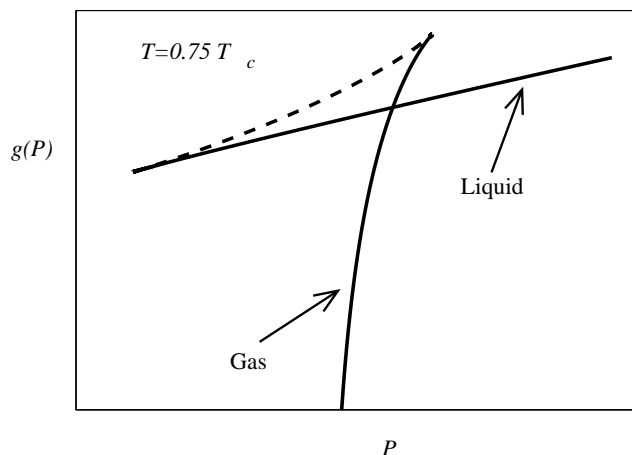


Figure 6: The Gibbs free energy  $g = f + Pv$  of the Van der Waals system at  $T = 0.75 T_c$ . The curve has cusps where  $\partial P / \partial v = 0$ . The equilibrium system takes the solution of lowest  $g$ , so there is a first-order transition where the liquid curve crosses the gas curve.

temperature the Gibbs free energies of the two stable solutions cross each other. The correct thermodynamic phase is the one of lowest  $G$ . It is this which leads to a phase diagram similar to that in Fig. 3 (but without a solid phase). (Note, the coexistence region can also be determined from the  $P$ - $v$  curve using the Maxwell equal-area construction, or from the  $f$ - $v$  curve, using the convexity property of the free energy.)

Again, this simple theory contains a wealth of phenomena: On crossing the coexistence line there is a density jump and a latent heat obeying the Clausius-Clapeyron relation  $\Delta s = \Delta v (dP/dT)$ , which in turn must give a peak in the specific heat. These first-order jumps reduce to zero as the critical end-point of the coexistence line is approached.



### Question 1

Find the location of the critical point  $P_c = P(v_c, T_c)$ , defined by setting the first and second derivatives of (16) to zero. Show that near the critical point,

$$\frac{v - v_c}{v_c} = - \left[ \frac{2}{3} \frac{(P - P_c)}{P_c} \right]^{1/3}. \quad (17)$$

on the critical isotherm  $T = T_c$  (note, the same exponent of  $1/3$  is found for the mean-field ferromagnet on the critical isotherm.) Show that on the coexistence line,

$$v = v_c \pm 2v_c \left( \frac{T_c - T}{T} \right)^{1/2}, \quad (18)$$

with the plus sign for approaching from the gas phase and the minus sign corresponding to the liquid. We see that the density difference  $\Delta v$  between gas and liquid falls continuously to zero at the critical point (again, the same exponent of  $1/2$  is found for the spontaneous magnetic moment in a mean-field ferromagnet). Finally, show that the compressibility

$$\kappa = -\frac{1}{v} \left. \frac{\partial v}{\partial P} \right|_T. \quad (19)$$

diverges at the critical point. Therefore we can expect violent density fluctuations at criticality (observed in carbon dioxide as “critical opalescence” by Andrews in 1863).

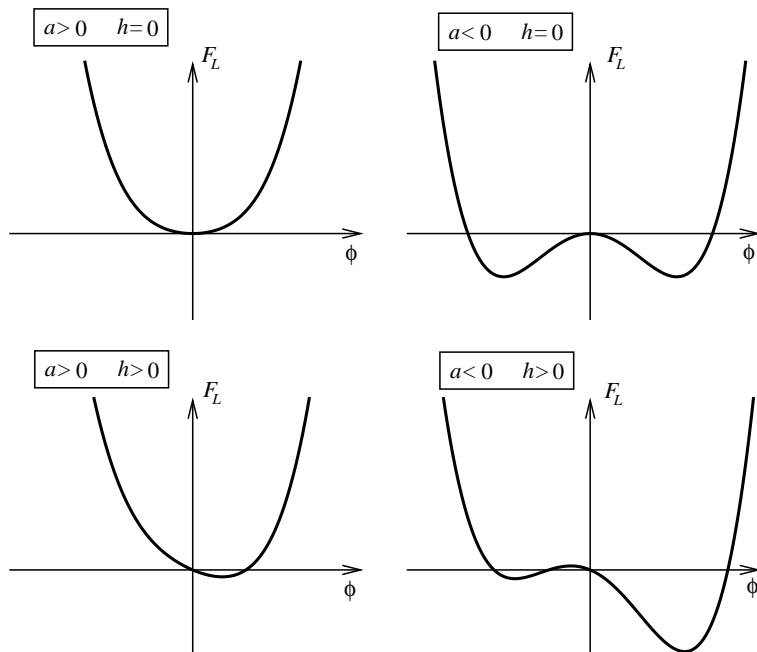


Figure 7: The Landau “free energy” function  $F_L(\phi) = a\phi^2 + b\phi^4 - h\phi$  for different values of the parameter  $a$  and a field  $h$ . For  $a > 0$  and  $h = 0$  there is only one minimum at the origin  $\phi = 0$ . This corresponds to the disordered phase. For  $a < 0$  and  $h = 0$  there are two minima at finite  $\phi$ , and the system orders into one of the states with a spontaneous breaking of symmetry. With a symmetry breaking field  $h > 0$  the  $a > 0$  curve has a minimum at non-zero  $\phi$ , while for  $a < 0$  the degeneracy of the minima is lifted.

### 1.3 Landau theory of critical point

Both examples above share the feature of a coexistence line ending in a critical point. In each case the coexisting phases have a quantity (i.e. the magnetization or the density) that is different, but where the difference goes to zero at the critical point. Apart from the qualitative similarities, there are certain quantities that are exactly the same in both systems, e.g. the exponent of the vanishing magnetization/density difference. These features can be explained with a simple phenomenological model due to Landau (1937).<sup>4</sup>

The critical point is to be regarded as a continuous phase transition (the thermodynamic functions of state such as entropy, energy, volume are continuous), which separates two phases of different symmetry. Usually the low-temperature phase has a lower symmetry than the high-temperature phase. Landau suggested that such transitions are characterized by an order parameter  $\phi$  which is nonzero in the less-symmetrical phase, and zero in the symmetrical phase. (For the ferromagnet  $\phi = \mathbf{M}$ , a vector, while for the liquid-gas transition  $\phi = v_{\text{gas}} - v_{\text{liq}}$ , a scalar.) The Landau theory then assumes that the free energy  $F_L$  of the system is a function of this parameter, and that the thermodynamically stable state will have the value of  $\phi$  that minimizes this function, i.e.  $F = \min[F_L(\phi)]$ .

As the order parameter goes to zero at the transition  $T_c$ , we can expand  $F_L(\phi)$

<sup>4</sup>The standard exposition is in L.D. Landau and G.M. Lifshitz, *Statistical Physics*, (Pergamon Press, Oxford 1958).

near the phase transition,

$$F_L(\phi) = F_0 + a\phi + b\phi^2 + c\phi^3 + d\phi^4 + \dots, \quad (20)$$

where the coefficients depend on temperature and other external parameters in a smooth way. Now, as we need the minimum of  $F_L$  to be at  $\phi = 0$  above the transition, we can immediately set  $a = 0$ . The rest are in general nonzero. Often, however, we have a symmetry  $\phi \rightarrow -\phi$  in the problem (e.g. for the ferromagnet), in which case we can set all coefficients with odd powers to zero. We then arrive at the simplest form valid near  $T_c$ ,

$$F_L(\phi) = F_0 + a\phi^2 + b\phi^4. \quad (21)$$

The general shape of this function is shown in Fig. 7. Note that we need  $b > 0$  to have a solution (or higher order terms are needed). We see in Fig. 7 that when  $a > 0$  the solution is at  $\phi = 0$  while for  $a < 0$  the solution is  $\phi = \phi_0 \equiv \sqrt{-a/2b}$ . Therefore the continuous phase transition occurs when  $a$  changes sign. To lowest order near  $T_c$  the coefficient has the temperature dependence  $a(T) = (T - T_c)a'$ . This leads to the required continuous drop in order parameter,

$$|\phi| = \phi_0 \equiv \left(\frac{a'}{2b}\right)^{1/2} (T_c - T)^{1/2}, \quad T_c > T. \quad (22)$$

In general the order parameter will couple to a field with a contribution to the free energy of  $-h\phi$ . Now minimizing  $F_L$  leads to the equation of state,

$$h = 2a'(T - T_c)\phi + 4b\phi^3. \quad (23)$$

Note that this is the same as the expansion of the equation of state near the Curie point of a ferromagnet with  $h$  the magnetic field, and near the critical point of the Van der Waals fluid with  $h$  the difference of the pressure from the critical pressure  $p_c$ .

### 1.3.1 First-order transitions

This Landau phenomenology can also be used to describe first-order transitions, although in this case there is no requirement for the order parameter to be small at the transition. Therefore the above expansion of (20) is not justified. Nevertheless it is instructive to look at the system,

$$F_L(\eta) = F_0 + a\eta^2 + b\eta^3 + c\eta^4, \quad (24)$$

which does not have the symmetry  $\eta \rightarrow -\eta$ . Now the system may develop two minima at the same time, and the stable phase is the one of lowest  $F_L$ . Although this model demonstrates some general features of a first-order transition, we emphasize that it has no general applicability as  $\eta$  may not be small, unlike the case for continuous transitions.

### 1.3.2 Universal dependence of susceptibility, entropy and specific heat

The susceptibility is the prefactor of the linear response to the field, and it diverges at the continuous transition,

$$\chi = \lim_{h \rightarrow 0} \frac{\partial \phi}{\partial h} = \begin{cases} \frac{1}{2a'}(T - T_c)^{-1}, & T > T_c, \\ \frac{1}{4a'}(T_c - T)^{-1}, & T_c > T. \end{cases} \quad (25)$$

While the free energy is just a constant in the high temperature phase where  $\phi = 0$ , at low temperatures we have  $F = \min[F_L(\phi)] = F_0 - (a'^2/4b)(T_c - T)^2$ . Thus the free energy is continuous at the transition, but so is the entropy,

$$S = - \left( \frac{\partial F}{\partial T} \right) = \begin{cases} S_0, & T > T_c, \\ S_0 + \frac{a'^2}{2b}(T - T_c), & T_c > T. \end{cases} \quad (26)$$

Notice, however, that there is a kink in the entropy. This is realized as a discontinuity in the specific heat,

$$c_h = T \left( \frac{\partial S}{\partial T} \right)_h = \begin{cases} c_{h,0}, & T > T_c, \\ c_{h,0} + \frac{a'^2}{2b}T, & T_c > T. \end{cases} \quad (27)$$

All of these features are realized close enough to the critical point in the mean-field theories of ferromagnets and the liquid-gas transition (as well as binary alloys, superfluids, superconductors etc.).

### 1.3.3 Interfaces and domain walls

So far we have assumed that the order parameter takes the same value everywhere in space. Physically, however, we may guess that on quenching down in temperature to below a continuous transition, the system might start to break the symmetry in different directions in different regions of space. We can allow for such inhomogeneities within the phenomenological Landau picture, using a position dependent order parameter  $\phi(\mathbf{r})$ . The expansion of the free energy will now include derivatives of the powers of  $\phi$ . Let us only consider very long wavelength distortions, in which case we may include only the first and second derivatives. We can write this in the form,

$$F_L[\phi(\mathbf{r})] = F_0 + \int d^d r \left[ a\phi^2(\mathbf{r}) + b\phi^4(\mathbf{r}) + g|\partial_{\mathbf{r}}\phi|^2 \right]. \quad (28)$$

This should be minimized subject to any boundary conditions, which can be expressed in the differential equation,

$$h(\mathbf{r}) = 2a\phi(\mathbf{r}) + 4b\phi^3(\mathbf{r}) - 2g\partial_{\mathbf{r}}^2\phi, \quad (29)$$

where we have included a space-dependent field.

In the liquid-gas problem we may have on the coexistence line an interface separating a liquid in one region from a gas in another region (both phases being in equilibrium). This is just like a scalar order parameter with the symmetry broken in two different directions in different regions separated by an interface, or “domain wall”. In the simplest case imagine a flat interface separating  $\phi = -\phi_0$  as  $x \rightarrow -\infty$  from  $\phi = \phi_0$  as  $x \rightarrow +\infty$ . To solve the differential equation for the order-parameter profile we need to scale out the dimensions, and write

$$\tilde{\phi} = \phi/\phi_0, \quad \tilde{x} = \sqrt{\frac{a}{g}}x, \quad (30)$$

which gives a dimensionless equation for the interface,

$$\tilde{\phi} + \tilde{\phi}^3 = \frac{\partial^2}{\partial \tilde{x}^2} \tilde{\phi}. \quad (31)$$

In other words, the solution to this,  $\tilde{\phi}_i(\tilde{x})$  is a solution for all temperatures close to the critical point, with an interface width of  $\tilde{x}_0$  (see Fig....). This translates to a physical width of

$$x_0 = \sqrt{\frac{g}{a}} \tilde{x}_0 = \frac{g^{1/2} \tilde{x}_0}{a_0^{1/2}} (T_c - T)^{-1/2}. \quad (32)$$

Therefore we see that the width of an interface between domains diverges as the critical temperature is approached. (The reason is the vanishing energy scale for raising  $\phi$  away from  $\pm\phi_0$  which allows for the energy of the derivative term to be reduced by increasing the length of this “defect”.) This is our first glimpse of the divergence of an important length scale that is the defining feature of the critical point.

The interface also costs an energy,

$$\begin{aligned} F_i &= \int d^d r \left[ a\phi^2(\mathbf{r}) + b\phi^4(\mathbf{r}) + g|\partial_{\mathbf{r}}\phi|^2 \right] - F_L[\phi_0] \\ &= L^{d-1} \frac{|a|^{3/2} g^{1/2}}{2b} \int_{-\infty}^{\infty} d\tilde{x} \left[ \frac{1}{2} - \tilde{\phi}^2(\tilde{x}) + \frac{1}{2} \tilde{\phi}^4(\tilde{x}) + (\partial_{\tilde{x}} \tilde{\phi})^2 \right] \\ &\propto (T_c - T)^{3/2}, \end{aligned} \quad (33)$$

which vanishes as  $T_c$  is approached.

### 1.3.4 Different order parameter symmetries

The above example of an interface was for a scalar order parameter (i.e. where the field  $\phi$  is just a real number). This is the simplest example of an order parameter with a discrete symmetry ( $+$   $\rightarrow$   $-$ ). It corresponds to the two member group  $Z_2$ . Experimental realizations of phase transitions that break this symmetry are uniaxial ferromagnets, alloy disordering on a bipartite lattice, and the liquid-gas transition on the coexistence curve.

On the other hand, the classical ferromagnet we considered at the beginning of this lecture has a vector order parameter, and a free energy at zero field that is symmetric under rotations in three dimensions. This is a continuous symmetry (of the group  $O_3$ ), and has very different properties which may be seen if we consider the above problem of an interface. If we impose the analogous boundary conditions of  $\mathbf{M} = -\mathbf{M}_0$  as  $x \rightarrow -\infty$  and  $\mathbf{M} = \mathbf{M}_0$  as  $x \rightarrow +\infty$  then the system can minimize its energy by a continual change in  $\mathbf{M}$  which is always in the minimum of the potential, but costs an energy in the derivative of the spatial dependence which decreases as the system size increases. These long-wavelength distortions (known as Goldstone modes) can be quite destructive of the ordered phase if thermally activated, which we will consider in more detail in Lecture 3.

Finally we note for completeness another continuous symmetry  $O_2$  which is broken in easy-plane ferromagnets, and also in superfluids and superconductors in the form of a complex order parameter (this is really the group  $U(1)$ ).

# Lecture Two

## 2 Statistical mechanics of phase transitions

In this lecture we look at the understanding of why phase transitions occur from the perspective of statistical physics. We start with some general observations on phase transitions. We then look at the justification of Landau theory in terms of the coarse-graining of thermal fluctuations in microscopic degrees of freedom. Finally we look at one of the most important model systems: the Ising model, which we solve in 1D for nearest neighbour interactions and in any dimension for infinite range interactions. We end the lecture looking at a numerical simulation of the 2D Ising model, for which a nice graphical user interface has been made public on the web.

The basis of our understanding of thermodynamics is statistical physics. This tells us that for a system with microscopic degrees of freedom  $\varphi_{\text{mic}}$  (e.g. positions of particles, spins) in equilibrium with a thermal bath at temperature  $T$ , all configurations are sampled over long enough times, with a Boltzmann probability distribution of  $\mathcal{P}_{\text{B}}(\varphi_{\text{mic}}) = \exp[-\beta H(\varphi_{\text{mic}})]$ , where  $H$  is the energy of the configuration  $\varphi_{\text{mic}}$ .<sup>5</sup> Any property  $A$  of the system is then given by

$$\langle A \rangle = Z^{-1} \text{Tr}_{\varphi_{\text{mic}}} A(\varphi_{\text{mic}}) \exp[-\beta H(\varphi_{\text{mic}})] \quad (34)$$

(by “trace” we mean a complete sum over all possible configurations of  $\varphi_{\text{mic}}$ ). In principle then, if we know the function  $H(\varphi_{\text{mic}})$  we know all of the thermodynamic properties. In practice, as we will see, new and subtle concepts are required to understand the phenomena of systems with quite simple forms of  $H(\varphi_{\text{mic}})$ .

### 2.1 Why do phase transitions occur?

A phase transition separates two phases with some different property. This implies that there are different regions of “phase space” (that is, the allowed configuration space of  $\varphi_{\text{mic}}$ ) which are characterized by different values of some  $A(\varphi_{\text{mic}})$ . On one side of the transition the system has overwhelming probability to have  $A(\varphi_{\text{mic}}) = A_1$  while on the other side the most likely value is  $A_2$ . When a phase transition is tuned by temperature it can often be viewed in the following way: The low temperature phase allows the system to minimize the energy  $H$  which maximizes the probability  $\mathcal{P}_{\text{B}}(\varphi_{\text{mic}})$ . However, this minimization makes constraints on the possible configurations. A higher energy phase with more configurational space may dominate once the temperature is enough to flatten the effect of  $\mathcal{P}_{\text{B}}(\varphi_{\text{mic}})$ . That is, this phase has more entropy, and the entropic advantage will win out above the phase transition.

Now we see why transitions often occur where the low temperature phase has a broken symmetry. For example in a ferromagnet, the energy can be minimized by pointing all the spins in the same direction (which has to be chosen spontaneously). This however is a big constraint on the possible configurations, which is why a phase with average zero magnetic moment will dominate the probabilities at high enough

---

<sup>5</sup>We consider here a purely classical system with precisely defined classical configurations. Of course, the world is quantum, and the microscopic configurations should be the eigenstates of the total system. Eventually, however, we are interested in properties in the “classical regime”, where quantum effects should be decoherent, and the quantum and classical treatments lead to the same physical properties (c.f. the correspondence principle).

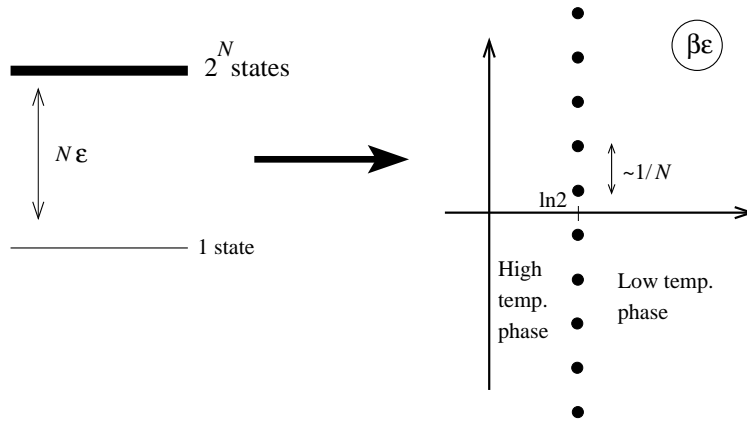


Figure 8: The zeros of the partition function of our simple model in the complex- $\beta$  plane. Note that they lie on a line crossing the real axis at the transition temperature of the infinite system. In the limit of  $\ln N \rightarrow \infty$  the density of zeros diverges and the line becomes a branch cut between the solutions in the high and low temperature phases.

temperature. The fact of the symmetry change means that the transition must occur at a single point (it is all or nothing with symmetry), rather than any smooth crossover between the two phases.

### 2.1.1 Simple model of a first-order transition

#### Question 2

We can illustrate the above points with an extremely simple model. Consider a system with a choice of  $2^N + 1$  configurations, one of which has zero energy, while the other  $2^N$  configurations all cost an energy  $\epsilon N$ . Write down the partition function and find the free energy as  $N \rightarrow \infty$ . Find the transition temperature, and the latent heat. Find the zeros of the partition function in the complex- $\beta$  plane. What happens to the zeros as  $N \rightarrow \infty$ ?

Despite the over-simplicity of this model, it does demonstrate the features of entropy competing with energy, and realizes what we mean by a region of phase space becoming dominant. It means that its contribution to the partition function grows faster with  $N$  than other regions of phase space. The true phase transition only occurs in the  $N \rightarrow \infty$  limit, also known as the thermodynamic limit. This simple model allows us to illustrate another point: the fact that the characteristics of a phase transition are determined by the analytic structure of  $Z(\beta)$  in the complex  $\beta$ -plane.<sup>6</sup> In our simple model the zeros lie on a line  $\text{Re}(\beta) = 1/s$  in the complex  $\beta$ -plane (see Fig. 8). Also, the density of zeros increases with  $N$ , while the distance of the nearest zero to the real axis falls to zero as  $1/N$ . In the thermodynamic limit this line of zeros becomes a branch cut which separates the two phases.

This resolves the paradox of how to get non-analytic behaviour at a transition in what appears to be an analytic function  $Z(\beta)$ . The required discontinuities only occur in the thermodynamic limit when the density of zeros diverges on a line in the

<sup>6</sup>This was possibly first introduced for the 2D Ising model in C.N. Yang and T. Lee, Phys. Rev. **97**, 404 (1952). See also the recent paper, P. Borrmann, O. Mülken, and J. Harting, Phys. Rev. Lett. **84**, 3511 (2000).

complex plane that meets the real axis at the transition point. The way the density of zeros depends on the distance from the real axis determines all of the characteristics (first-order versus continuous, how the specific heat diverges, etc.) of the transition (Grossman and Rosenhauer 1967). Unfortunately it turns out that it is rarely possible to calculate the positions of these zeros, and so it is not the most common way to analyse phase transitions.

## 2.2 From stat-mech to Mean-Field Theory

A question raised but not answered in the last lecture is what is the physical meaning of the Landau free energy? Let us remind ourselves of the definition of the true free energy,

$$e^{-\beta F(T)} = Z = \text{Tr}_{\varphi_{\text{mic}}} \exp[-\beta H(\varphi_{\text{mic}})]. \quad (35)$$

How do we describe the order parameter  $\phi$  in this approach? It is clear that the order parameter should be an averaged quantity. For example, we may have an order parameter that is simply the average value of the microscopic field,  $\phi = \langle \varphi_{\text{mic}} \rangle$ . However, in the above formulation, this average is fixed at a given temperature, and can only be altered by adding a field to  $H(\varphi_{\text{mic}})$ . This would give a free energy as a function of field,  $F(T, h)$ , and we can make a Legendre transform of this to get  $G(T, \phi) = F(T, h(\phi)) + h\phi$ . We can see that the Landau free energy  $F_L(\phi, T)$  is not the true free energy  $G(\phi, T)$  because of the thermodynamically unstable solutions that exist in  $F_L$ .

### 2.2.1 Coarse graining

Another problem is how to describe the spatial variations  $\phi(\mathbf{r})$  when there is no spatial dependence in  $G(\phi, T)$ ? The answer lies in coarse-graining. We therefore keep some long-wavelength spatial dependence by only averaging up to some fixed resolution length. To implement the coarse graining we define a block size  $l = 1/\Lambda$  where  $l$  is much greater than the underlying microscopic discretization  $d$ . For a block centred at  $\mathbf{r}$  we define the order parameter

$$\phi(\mathbf{r}) = \frac{1}{l^d} \int_{\text{block}(\mathbf{r})} d^d r' \varphi_{\text{mic}}(\mathbf{r}'). \quad (36)$$

Now there will be many configurations in a given block that lead to the same averaged order parameter. We therefore define the Landau free energy as arising from the partial trace over all those microscopic configurations that still lead to a given set of coarse grained order parameters. Mathematically this may be written,

$$e^{-\beta F_L[\phi(\mathbf{r}), T]} = \text{Tr}_{\varphi_{\text{mic}}} \delta \left[ \phi(\mathbf{r}) - \frac{1}{l^d} \int_{\text{block}(\mathbf{r})} d^d r' \varphi_{\text{mic}}(\mathbf{r}') \right] \exp[-\beta H(\varphi_{\text{mic}})]. \quad (37)$$

We are then able to write the full partition function as,

$$\begin{aligned} Z = e^{-\beta F[T]} &= \text{Tr}_{\phi(\mathbf{r})} e^{-\beta F_L[\phi(\mathbf{r}), T]} \\ &= \int D\phi(\mathbf{r}) e^{-\beta F_L[\phi(\mathbf{r}), T]}, \end{aligned} \quad (38)$$

where  $\int D\phi(\mathbf{r}) = \int \prod_{\mathbf{r}} d\phi(\mathbf{r})$  is a functional integral. Note that the Landau free energy could not be confused with the microscopic Hamiltonian because of the temperature dependence in  $F_L[\phi(\mathbf{r}), T]$  that has arisen after the coarse graining.



This definition of the Landau free energy explains some important features. First it allows for unstable solutions, which will not appear after the final trace. Secondly we see the justification that  $F_L[\phi(\mathbf{r})]$  should be an analytic function, as the partial trace is only over a finite number of degrees of freedom. The singularities at the phase transition only appear after the final trace over an infinite system.

### 2.2.2 The saddle-point approximation

One assumption of the Landau theory remains unexplained: the need to take the minimum value of the Landau free energy. In the definition (38) we see that the true free energy has contributions from all possible configurations of  $\phi(\mathbf{r})$ . The mean-field theory is only a “saddle-point” approximation to the functional integral appearing in (38). If we expand in the form  $F_L[\phi(\mathbf{r})] = F_L[\phi_0] + \delta F_L[\phi(\mathbf{r})]$ , where  $\phi_0$  minimizes  $F_L$ , then we can write,

$$F = F_L[\phi_0] - T \ln(Z_{\text{fluc}}). \quad (39)$$

The Landau mean-field theory consists of ignoring the fluctuation term,  $Z_{\text{fluc}} = \int D\phi(\mathbf{r}') e^{-\beta \delta F_L[\phi(\mathbf{r})]}$ . We will consider when this actually works in Lecture 3.

### 2.2.3 Landau theory is a classical field theory

The problem of evaluating functional integrals over a “field” such as  $\phi(\mathbf{r})$  is known as a classical field theory. Using the form of  $F_L[\phi(\mathbf{r}), T]$  justified near a continuous phase transition, the partition function has the form,

$$Z = \int D\phi(\mathbf{r}') \exp \left[ -\beta \int d^d r [a(T)\phi^2(\mathbf{r}) + b\phi^4(\mathbf{r}) + g|\partial_{\mathbf{r}}\phi|^2] \right]. \quad (40)$$

This is a well-studied problem in classical field theory, often known affectionately as  $\phi^4$ -theory (pronounced “phi four”). It is surprisingly non-trivial, and we will be looking at many aspects of it during this course. Despite being a classical field, this problem has much in common with the quantum field theories found in many-body perturbation theory used in particle physics and in solid-state physics.

## 2.3 Example: the Ising model

We now turn to a simple model microscopic system known as the Ising model. This consists of up and down spins defined on a lattice (as with a spin- $\frac{1}{2}$  particle), which we represent by the values  $\sigma_i = \pm 1$ . With ferromagnetic nearest-neighbour interactions we have,

$$H[\sigma_i] = -J \sum_{\langle ij \rangle} \sigma_i \sigma_j, \quad (41)$$

where the sum is over the links between adjacent sites. This has a partition function,

$$Z = \sum_{\sigma_1=\pm 1} \sum_{\sigma_2=\pm 1} \dots \sum_{\sigma_N=\pm 1} e^{\beta J \sum_{\langle ij \rangle} \sigma_i \sigma_j}. \quad (42)$$

(The mapping of this to a lattice gas was shown in Yong Mao’s lectures.) There is no general solution for  $Z$  in three dimensions. A beautiful yet complex solution has been found in two dimensions (Onsager 1944). In one dimension, it is rather easy to solve.

### 2.3.1 Solution in one dimension

In one dimension the spins lie on a linear chain, so that the energy can be written,

$$H[\{\sigma_i\}, J] = -J \sum_i \sigma_i \sigma_{i+1} = -J \sum_i \nu_i \quad (43)$$

where  $\nu_i = \sigma_i \sigma_{i+1}$  can take the values  $\pm 1$ . With open boundary conditions there are no restraints between the different  $\nu_i$  and we have

$$Z_N = \text{Tr}_{\nu_i} e^{\beta J \sum_{i=1}^{N-1} \nu_i} = \left( \sum_{\nu=\pm 1} e^{\beta J \nu} \right)^{N-1} = (2 \cosh \beta J)^{N-1} \quad (44)$$

and the free energy per spin is

$$f = -\frac{T}{N} \ln Z = -T \ln (2 \cosh \beta J), \quad (45)$$

which is a smooth function for all temperatures. This means there is no phase transition in the 1D Ising model, despite what a mean-field treatment would have told us. The physical reason for this will be given in the next lecture. At this stage we just note the low and high temperature limits,

$$f \approx \begin{cases} -J - T e^{-2J/T}, & T \ll J, \\ -T \ln 2 - \frac{J^2}{2T}, & J \ll T. \end{cases} \quad (46)$$

Differentiating (45) gives us the entropy,

$$s = -\frac{\partial f}{\partial T} = \ln(2 \cosh \beta J) - \beta J \tanh \beta J, \quad (47)$$

and the heat capacity,

$$c = -T \frac{\partial^2 f}{\partial T^2} = \frac{(\beta J)^2}{\cosh^2 \beta J}. \quad (48)$$

This last result we plot in Fig. 9. Note that despite the lack of a phase transition, there is a well defined peak in the specific heat near  $T \approx J$  associated with the loss of ordering between neighbouring spins at this temperature. This is called a ‘‘Schottky anomaly’’.

How does the 1D Ising system respond to a magnetic field? Including a ‘‘Zeeman splitting’’ in the energy leads to,

$$H[\{\sigma_i\}, J, h] = - \sum_i [J \sigma_i \sigma_{i+1} + h \sigma_i]. \quad (49)$$

Now we can’t use the above trick, so we need a more sophisticated solution. We write the Hamiltonian as a sum over terms that are symmetric in  $\sigma_i$  and  $\sigma_{i+1}$ ,

$$H[\{\sigma_i\}, J, h] = - \sum_i \left[ J \sigma_i \sigma_{i+1} + \frac{h}{2} (\sigma_i + \sigma_{i+1}) \right] = - \sum_i \tilde{K}(\sigma_i, \sigma_{i+1}). \quad (50)$$

The function  $\tilde{K}$  can be thought of as a  $2 \times 2$  matrix, as the arguments can only take two values,

$$\tilde{K}(\sigma, \sigma') = \begin{bmatrix} J + h & -J \\ -J & J - h \end{bmatrix}. \quad (51)$$

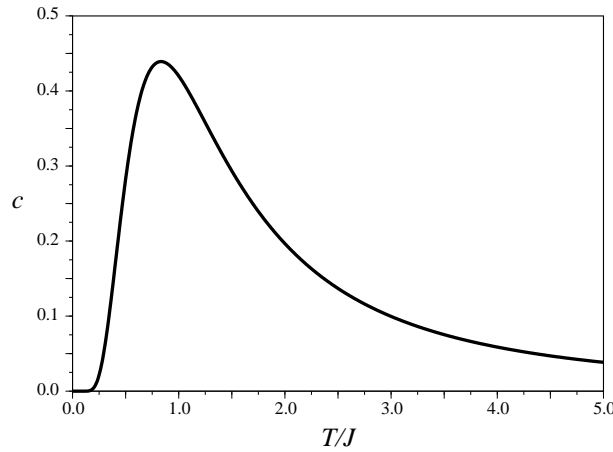


Figure 9: The heat capacity per spin of the 1D Ising model as calculated in these notes. The peak near  $T \approx J$  is known as a “Schottky anomaly”, and is associated with the ordering of neighbouring spins, despite the fact that there is no phase transition to an ordered phase.

The exponential of this matrix will be particularly useful, and is known as a “transfer matrix”,  $e^{\tilde{K}(\sigma, \sigma')}$ . We now choose periodic boundary conditions so that we can write the partition function as,

$$\begin{aligned} Z_N &= \text{Tr}_{\sigma_i} e^{\beta \sum_i \tilde{K}(\sigma_i, \sigma_{i+1})} \\ &= \sum_{\sigma_1=\pm 1} \sum_{\sigma_2=\pm 1} \dots \sum_{\sigma_N=\pm 1} e^{\beta \tilde{K}(\sigma_1, \sigma_2)} e^{\beta \tilde{K}(\sigma_2, \sigma_3)} \dots e^{\beta \tilde{K}(\sigma_N, \sigma_1)}. \end{aligned} \quad (52)$$

Note that this is in the form of a matrix multiplication,  $M_{\alpha\beta} M_{\beta\gamma} \dots M_{\zeta\alpha} = \text{Tr}(M^N) = \sum_{\alpha} (\lambda_{\alpha})^N$  where  $\lambda_{\alpha}$  are the eigenvalues of  $M$ . Therefore we only need the two eigenvalues of  $e^{\tilde{K}(\sigma, \sigma')}$ , which are

$$\lambda_{\pm} = e^{\beta J} \cosh \beta h \pm \left[ e^{2\beta J} \sinh^2 \beta h + e^{-2\beta J} \right]^{\frac{1}{2}}, \quad (53)$$

and we have  $Z_N = \lambda_+^N + \lambda_-^N$ . In the large  $N$  limit the largest eigenvalue will dominate and give the “exact solution”.

### Question 3

**Find the magnetization of the 1D Ising model in a field  $h$ , and show that the susceptibility follows the Curie law at high temperatures, but has a much stronger divergence as  $T \rightarrow 0$ .**

### 2.3.2 The infinite-range Ising model

In contrast to the above model where mean-field theory clearly does not apply, we look at a similar system where the mean-field theory is exact. Instead of nearest-neighbour interactions, consider the opposite extreme where each spin has the same ferromagnetic interaction with each other spin,

$$H = -\frac{J}{2N} \sum_{i \neq j}^N \sigma_i \sigma_j - h \sum_{i=1}^N \sigma_i. \quad (54)$$

The factor  $1/N$  is needed to keep the energy extensive in  $N$ . To solve this we note that we can write the double sum as  $\sum_{i \neq j}^N \sigma_i \sigma_j = \sum_{i,j}^N \sigma_i \sigma_j - \sum_{i=1}^N \sigma_i^2 = \left( \sum_{i=1}^N \sigma_i \right)^2 - N$ .

Writing the total spin as  $S = \sum_{i=1}^N \sigma_i$  we then have,

$$H(S) = -\frac{J}{2N}S^2 - hS + \text{const.}, \quad (55)$$

and

$$Z_N = \sum_{\sigma_1=\pm 1} \sum_{\sigma_2=\pm 1} \dots \sum_{\sigma_N=\pm 1} e^{\frac{\beta J}{2N}S^2 + \beta h S}. \quad (56)$$

The  $S^2$  in the exponent is a pain, as without it we could write  $\sum_{\sigma_1=\pm 1} \dots \sum_{\sigma_N=\pm 1} e^{aS} = (\sum_{\sigma} e^{a\sigma})^N = (2 \cosh a)^N$ . Therefore we use a trick so that only linear terms in  $S$  appear in the exponential. We can write a Gaussian function as an integral,

$$e^{bS^2} = \frac{1}{\sqrt{4\pi b}} \int_{-\infty}^{\infty} dt e^{-t^2/4b} e^{tS}, \quad (57)$$

so that the partition function is,

$$\begin{aligned} Z &= \text{Tr}_{\sigma_i} \sqrt{\frac{N}{2\pi\beta J}} \int dt e^{-\frac{N}{2\beta J}t^2} e^{(t+\beta h)S} \\ &= \sqrt{\frac{N}{2\pi\beta J}} \int dt e^{-\frac{N}{2\beta J}t^2} [2 \cosh(t + \beta h)]^N. \end{aligned} \quad (58)$$

This trick is the basic form of the Hubbard-Stratonovich transformation. Now we really can use the “steepest-descent” approach, as when we take  $N \rightarrow \infty$  the Gaussian is very sharply peaked (like a delta function). The cosh contains an exponential which may shift this peak. By differentiating the integrand we see that the peak is centred at  $t = t^*$  which satisfies,

$$t^* = \beta J \tanh(t^* + \beta h). \quad (59)$$

Similarly we can calculate the magnetization  $\langle \sigma \rangle = (1/\beta N Z) \partial Z / \partial h$ , which is found to be  $\langle \sigma \rangle = \tanh(t^* + \beta h)$  obeying the same relation above. This is very similar to the mean-field theory of the classical ferromagnet we saw in lecture 1, only the Langevin function is replaced by a tanh (which just reflects the fact that the spin only takes two values, rather than pointing at any angle). All of the same analysis applies, with a phase transition at the point  $T_c = J$ .

Note that the infinite-range model does not care about the dimension, as each spin interacts with each other spin regardless of where it is in space. In fact, the nearest-neighbour model only starts to resemble the infinite-range model as the dimension becomes very large, as we will see in the following lectures.

### 2.3.3 Numerical simulation of 2D Ising model

In the lecture we will see a numerical simulation of the 2D Ising model, where we can look directly at the sort of configurations seen at a given temperature. This is just for illustrative purposes, as the properties of the transition are known exactly from Onsager’s solution. However, looking at the evolving configurations in the simulations gives us a lot of intuition on the nature of the phase transition, eg. fluctuations with a characteristic length scale, and the ideas of scaling.

# Lecture Three

## 3 Thermal fluctuations in the ordered phase: How to kill a phase transition

In this lecture we describe the impossibility of phase transitions in finite systems or in infinite systems of low dimensionality.

### 3.1 Importance of the thermodynamic limit.

As we saw in the example in Lecture 2, the required discontinuity in a thermodynamic variable (i.e. a derivative of the free energy) at the phase transition is impossible unless we take the number of degrees of freedom to infinity. We can demonstrate this quite generally for an Ising-like system with  $N$  fields  $\sigma_i$  that can take the values  $\pm 1$ , and a Landau free energy  $F_L[\{\sigma_i\}, T, X]$  which is analytic in all arguments ( $X$  represents some external parameters). Then the partition function,

$$Z = \sum_{\sigma_1=\pm 1} \sum_{\sigma_2=\pm 1} \dots \sum_{\sigma_N=\pm 1} e^{-\beta F_L[\{\sigma_i\}, T, X]}, \quad (60)$$

is just a finite sum of an analytic function, which remains an analytic function of  $T$  and  $X$ . Also the partition function is bounded,  $0 < Z < 2^N \exp(-\beta F_{L, \min}[\{\sigma_i\}, \beta, X])$ . Therefore the free energy  $F = -T \ln Z$  is a smooth function. The only way this argument can break down is when the number of fields summed over goes to infinity.

The argument for a continuous field  $\phi$  that can take an infinite number of values between  $-\infty$  and  $+\infty$  needs a bit more care. In this case we have,

$$Z = \int d\phi_1 \int d\phi_2 \dots \int d\phi_N e^{-\beta F_L[\{\phi_i\}, T, X]}. \quad (61)$$

For this to make any sense at all we must have  $F_L[\{\phi_i\}, T, X]$  an increasing function of all of the  $\phi_i$  so that the integrals converge. In this case we can show that each integral of an analytic function remains an analytic function,<sup>7</sup> so as long as there is only a finite number of fields  $\phi_i$  then  $Z$  must remain analytic.

Similarly we can also show that there cannot be any spontaneous symmetry breaking (associated with the low-temperature side of a phase transition) in a system of finite size. In the absence of symmetry-breaking fields we have

$$\begin{aligned} \langle \phi_j \rangle &= \frac{1}{Z} \int \prod_{i'} d\phi_{i'} \phi_j e^{-\beta F_L[\{\phi_i\}]} \\ &= -\frac{1}{Z} \int \prod_{i'} d\phi_{i'} -\phi_j e^{-\beta F_L[\{-\phi_i\}]} \\ &= -\langle \phi_j \rangle. \end{aligned} \quad (62)$$

Therefore  $\langle \phi_j \rangle = 0$ . It is hard to see how the conclusion could be any different even in the thermodynamic limit. However, it is a subtle case of taking the right order

---

<sup>7</sup>Using the mathematical theorem that  $f(z) = \int_{-\infty}^{\infty} d\phi g(\phi, z)$  is an analytic function of  $z$  in the domain  $D$  where  $g(\phi, z)$  is analytic (with  $\phi$  on real axis) as long as the integral is convergent. This is proved on p. 99-100 of E.C. Titchmarsh, *The Theory of Functions*, (Oxford University Press, 1939).

of limits. To see this, imagine we include a small symmetry breaking field,  $h$ . Then compare the probabilities for the state to be  $\{\phi_i^A\}$  or in  $\{\phi_i^B\} = \{-\phi_i^A\}$ . The difference in energy between the two states will be  $\Delta F_L = -h \sum_i (\phi_i^B - \phi_i^A) = 2h \sum_i \phi_i^A$ , so that the ratio of probabilities is

$$\frac{\mathcal{P}_A}{\mathcal{P}_B} = e^{2\beta h N \langle \phi \rangle}, \quad (63)$$

where  $\langle \phi \rangle = \frac{1}{N} \sum_i \langle \phi_i \rangle$ . If we let  $N \rightarrow \infty$  we see that  $P_A/P_B \rightarrow 0$ , which means that the system will only sample those configurations with positive “magnetization”  $\langle \phi \rangle$ . Only after this limit should we take the field to zero, to see if the magnetization falls to zero (a paramagnet) or if it goes to a non-zero value (a ferromagnet). To summarize we can write:

$$\begin{aligned} \lim_{N \rightarrow \infty} \lim_{h \rightarrow 0+} \langle \phi \rangle &= 0 \text{ always,} \\ \lim_{h \rightarrow 0+} \lim_{N \rightarrow \infty} \langle \phi \rangle &= \begin{cases} +M, & \text{FM,} \\ 0, & \text{PM.} \end{cases} \end{aligned} \quad (64)$$

How should we understand this for a system with zero field? First, consider a discrete symmetry. In a finite system, while the probability distribution may be peaked at  $\phi = \pm M$ , there is a finite probability for the system to have any magnetization between these two peaks. Dynamically, if we place the system in a configuration with  $+M$ , it is only a matter of time before the system will also sample  $-M$ . What happens in the thermodynamic limit is that the relative probability of the intermediate states falls to zero, so that the two symmetry broken phases become “ergodically” separate.

For a continuous symmetry there is always a path between states of different symmetry which is of equal probability. In this case, spontaneous symmetry breaking can only occur in the thermodynamic limit because of the small chance that all degrees of freedom move collectively in this direction. For other directions there are still energy barriers which may prevent the drift to other symmetry broken states.

Of course, the thermodynamic limit is only a necessary condition for spontaneous symmetry breaking. We will see in this lecture that the symmetry breaking also depends on the dimension and order-parameter symmetry of the system in question.

## 3.2 Absence of symmetry breaking in one dimension

We saw in the last lecture that the 1D Ising model has no phase transition, i.e. the ferromagnetic phase only exists at  $T = 0$ . This is a general feature of 1D systems: a symmetry broken phase will always be unstable to a mixture of phases. This was understood by Landau (1950) in terms of the domain wall that must separate two different phases.<sup>8</sup> This domain wall will only cost a finite energy in one dimension, e.g. in the Ising model the interface between a region of up spins and a region of down spins costs an energy  $J$ . Simply put, an object that costs an energy  $\epsilon$  that can be placed anywhere, will be present on average with a density proportional to the Boltzmann factor  $e^{-\epsilon/T}$ . Clearly the presence of a finite density of domain walls means we must have an equal mixture of up and down spins at any temperature, and therefore no symmetry breaking.

---

<sup>8</sup>see L.D. Landau and G.M. Lifshitz, *Statistical Physics*, (Pergamon Press, Oxford 1958). The absence of an ordered phase in one dimension was first realised by Peierls (1934), see R. Peierls, *Surprises in Theoretical Physics* (Princeton University Press, 1979).

An alternative (but equivalent) argument is to look at the free energy of a system with one domain wall compared to a system with none. While it costs an energy  $J$  for the wall, there is an entropy gain for the  $N$  sites we can place the wall, so that the free energy is

$$F_{\text{d-w}} = F_0 + J - T \ln N, \quad (65)$$

which will always be less than  $F_0$  for large enough  $N$ . Therefore even in the thermodynamic limit the symmetry broken phase is unstable to the creation of interfaces between different phases.

Having said that there is no symmetry breaking in one dimension, how did we find a finite temperature transition in the 1D infinite-range Ising model? We need a caveat that with long-range interactions the domain wall may have infinite energy, so that the entropy is not enough to favour domain-wall proliferation.

We can try a similar argument for a domain wall in two dimensions. Now the wall encloses a nucleated domain of one phase within another phase. Consider a wall of length  $n$  bonds. The number of ways to start and end at the same point is less than  $z^n$  where  $z$  is the coordination number of the bonds. Therefore the entropy of walls of fixed length  $n$  is bounded by  $S(n) < \ln(Nz^n)$  so that the free energy is more than  $F_{\min} = nJ - T \ln(N) - nT \ln(z)$ . As only large domain walls with  $n = sN$  (for some finite fraction  $s$ ) will force an introduction of the absent phase, we write  $F_{\min} = sN[J - T \ln(z)] - T \ln(N)$ . We therefore see that for small enough temperatures the free energy of macroscopically large domain walls is positive in the thermodynamic limit, and a *discrete* symmetry breaking can survive in two dimensions. We will therefore define a “lower critical dimension”  $d_{\text{lc}}$  such that for  $d \leq d_{\text{lc}}$  there can be no phase transition at finite temperature. For the Ising model (and other discrete symmetry phase transitions) we have shown that  $d_{\text{lc}} = 1$ .

We have emphasized the discreteness of the symmetry breaking for the above argument to apply. For a continuous symmetry we recall that an interface between two phases will stretch over as large a distance as possible to minimize its energy. In other words, long-wavelength distortions become important, which calls for a different approach to test the stability of a symmetry broken phase.

### 3.3 Lower critical dimension with continuous symmetries

The simplest example of a system with continuous symmetry breaking is the Landau theory for a 2D-vector order parameter, or equivalently, a complex scalar order parameter. This has the free energy,

$$F_{\text{L}}[\phi(\mathbf{r})] = \int d^d r \left[ \frac{a}{2} |\phi(\mathbf{r})|^2 + \frac{b}{4} |\phi(\mathbf{r})|^4 + \frac{g}{2} |\partial_{\mathbf{r}} \phi|^2 \right] \quad (66)$$

Unfortunately, the thermodynamic properties of this phi-four model cannot be solved exactly. We see this by rewriting the free energy in Fourier space,

$$F_{\text{L}}[\phi(\mathbf{k})] = \frac{1}{2} \int \frac{d^d k}{(2\pi)^d} (a + gk^2) |\phi_{\mathbf{k}}|^2 + \frac{b}{4} \int \frac{d^d k_1}{(2\pi)^d} \frac{d^d k_2}{(2\pi)^d} \frac{d^d k_3}{(2\pi)^d} \phi_{\mathbf{k}_1} \phi_{\mathbf{k}_2} \phi_{\mathbf{k}_3}^* \phi_{\mathbf{k}_1 + \mathbf{k}_2 - \mathbf{k}_3}^* \quad (67)$$

where we define  $\phi(\mathbf{r}) = \int \frac{d^d k}{(2\pi)^d} e^{i\mathbf{k} \cdot \mathbf{r}} \phi_{\mathbf{k}}$ . The partition function can be evaluated as a trace over the Fourier components of  $\phi$ ,

$$Z = \int \prod_{\mathbf{k}'} d\phi_{\mathbf{k}'} d\phi_{\mathbf{k}'}^* e^{-\beta F_{\text{L}}[\phi_{\mathbf{k}}]} \quad (68)$$

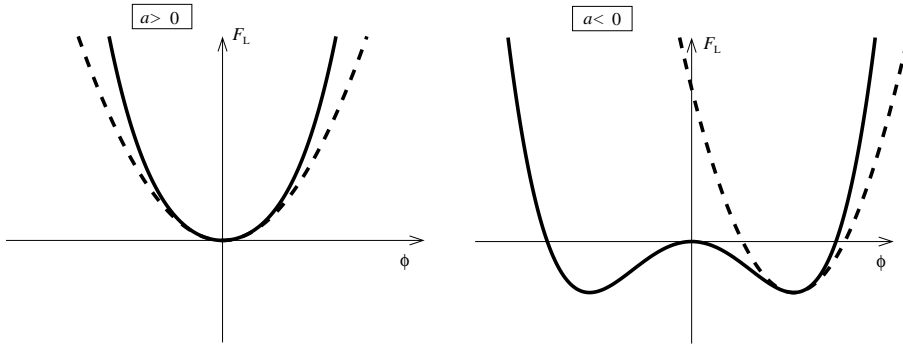


Figure 10: Illustration of the Gaussian approximation for temperatures above  $T_c$  ( $a > 0$ ) and below  $T_c$  ( $a < 0$ ). The full line shows the actual Landau potential, while the dashed line shows the expansion around the minimum to second order. Putting this approximate form into the Boltzmann factor gives a Gaussian integral for the partition function, hence the name of this approximation (it is sometimes also called the harmonic approximation).

We now see that the quadratic terms are “diagonal” in the Fourier components, but the quartic term generates “interactions” between different components. This problem is therefore hard, but an easy problem exists if we can set  $b$  to zero (with  $a$  fixed greater than zero). This is known as the Gaussian approximation above  $T_c$ . For the problem below  $T_c$  we can still use the same type of approximation, but we should expand about one of the minima in the Landau potential. Expanding only to second order again gives a Gaussian theory which is diagonal in the Fourier components. This approximation is illustrated in Fig. 10.

### 3.3.1 Important tool: the Gaussian model

The Gaussian model,

$$F_{b=0}[\phi_{\mathbf{k}}] = \frac{1}{2} \int \frac{d^d k}{(2\pi)^d} (a + gk^2) |\phi_{\mathbf{k}}|^2, \quad (69)$$

is a trivial, solvable model because each Fourier component is independent. It also helps that we can write Gaussian integrals in closed form. So we easily find the partition function to be

$$Z \propto \prod_{\mathbf{k}} \frac{Tl^{-d}}{(a + gk^2)}, \quad (70)$$

where  $l = \Lambda^{-1}$  is the small length cut-off (discreteness of underlying lattice), and the free energy density is

$$f = -T \int \frac{d^d k}{(2\pi)^d} \ln \left( \frac{Tl^{-d}}{(a + gk^2)} \right) \quad (71)$$

(with an upper limit to the integral at  $k = \Lambda$ ), which is analytic for all  $a > 0$ . There is clearly no symmetry breaking in this model, with  $\langle \phi \rangle = 0$ . We will be interested in fluctuations around this average. For a given  $\mathbf{k}$  and  $\mathbf{k}'$  we have the correlation,

$$\langle \phi_{\mathbf{k}} \phi_{\mathbf{k}'}^* \rangle = 2(2\pi)^d \delta^d(\mathbf{k} - \mathbf{k}') T \frac{1}{(a + gk^2)}. \quad (72)$$

This is of course just a restatement of the equipartition theorem.



### 3.3.2 Correlations in the Gaussian model

Back in real space, we define the correlation function between fluctuations as,

$$\begin{aligned} S(\mathbf{r} - \mathbf{r}') &\equiv \langle [\phi(\mathbf{r}) - \langle \phi(\mathbf{r}) \rangle] [\phi^*(\mathbf{r}') - \langle \phi^*(\mathbf{r}') \rangle] \rangle \\ &= \langle \phi(\mathbf{r}) \phi^*(\mathbf{r}') \rangle - \langle \phi(\mathbf{r}) \rangle \langle \phi^*(\mathbf{r}') \rangle \\ &= G(\mathbf{r} - \mathbf{r}') - |\varphi|^2, \end{aligned} \quad (73)$$

where the structure function  $G(\mathbf{r} - \mathbf{r}') = \langle \phi(\mathbf{r}) \phi^*(\mathbf{r}') \rangle$  is often called the propagator and  $\varphi = \langle \phi \rangle$  is the order parameter, and is zero in this system (where  $a$  is positive). The correlation function should always go to zero at large distances, so that a measure of order in the system is the long-length behaviour of the propagator: If the propagator goes to zero then the system can only have short-range order. If the propagator goes to a non-zero constant at large distances, then we must have a non-zero order parameter, and the system has long-range order.

For the propagator we use the Fourier transform to find,<sup>9</sup>

$$G(\mathbf{r} - \mathbf{r}') = \langle \phi(\mathbf{r}) \phi^*(\mathbf{r}') \rangle = 2T \int \frac{d^d k}{(2\pi)^d} \frac{e^{i\mathbf{k} \cdot (\mathbf{r} - \mathbf{r}')}}{(a + gk^2)}. \quad (75)$$

To gain some intuition on this integral, we should scale out the parameters. Defining the length scale  $\xi(T)$  by  $g/a(T) = \xi^2(T)$ , and integrating over a dimensionless variable  $\mathbf{q} = \mathbf{k}\xi$  we have

$$G(\mathbf{r}) = \frac{2T}{a\xi^d} \int \frac{d^d q}{(2\pi)^d} \frac{e^{i\mathbf{q} \cdot \mathbf{r}/\xi}}{(1 + q^2)}. \quad (76)$$

The integral is well behaved at small  $\mathbf{q}$ . At large  $q$  without the exponential the integral would only be convergent for  $d = 1$ . For  $d = 2$  there would be a log divergence, while for higher  $d$  there would be an algebraic divergence. Clearly this divergence is cut off by the exponential factor. As the exponential goes to 1 when  $\mathbf{r}$  goes to zero, the correlation function should “diverge” at small distances. In fact the divergence will be cut off by the discretization length  $l$ . For large distances  $\mathbf{r} > \xi$ , the exponential is oscillating much faster than any other variations, and the correlation function should fall rapidly to zero (in fact exponentially). This behaviour is demonstrated if we explicitly calculate the integral for dimensions one, two and three, with the results:

$$G_{d=1}(\mathbf{r}) = \frac{T}{a\xi} e^{-r/\xi}, \quad (77)$$

$$G_{d=2}(\mathbf{r}) = \frac{T}{\pi a \xi^2} K_0(r/\xi), \quad (78)$$

$$G_{d=3}(\mathbf{r}) = \frac{T}{4\pi a \xi^2} \frac{1}{r} e^{-r/\xi}. \quad (79)$$

( $K_0(x)$  is a modified Bessel function that is logarithmic for small arguments and exponentially decaying for large arguments.) In higher dimensions we will get the

---

<sup>9</sup>Notice that for a generalized  $n$ -vector model with  $\Phi(\mathbf{r}) = [\phi_1, \phi_2, \dots, \phi_n]$  the only change is in the prefactor proportional to  $n$ ,

$$\langle \Phi(\mathbf{r}) \cdot \Phi(\mathbf{r}') \rangle = nT \int \frac{d^d k}{(2\pi)^d} \frac{e^{i\mathbf{k} \cdot (\mathbf{r} - \mathbf{r}')}}{(a + gk^2)}. \quad (74)$$

same exponential decay at large distances with the characteristic length always  $\xi(T)$  which diverges as  $a(T) \rightarrow 0$ . At small distances the algebraic divergence is cut off so that the average fluctuation at a given point in space is determined by the discretization length,

$$G(0) = \langle |\phi(\mathbf{r})|^2 \rangle \sim \frac{T}{a\xi^2 l^{d-2}}. \quad (80)$$

Notice that  $a\xi^2 = g$  so that these fluctuations do not diverge as  $a \rightarrow 0$  (apart from in 1D, but we know there is no transition in this case).

The Gaussian model can be a good approximation to the full phi-four theory for positive  $a$  as long as the fluctuations  $\langle |\phi(\mathbf{r})|^2 \rangle$  are small enough that  $a\langle |\phi(\mathbf{r})|^2 \rangle \ll b\langle |\phi(\mathbf{r})|^2 \rangle^2$ . From the above result this gives the condition on temperature,

$$T \ll \frac{agl^{d-2}}{b}. \quad (81)$$

However, if we include the temperature dependence  $a = a'(T - T_c)$ , we find that the condition is actually for high temperatures,

$$T \gg \frac{T_c}{1 - x}, \quad (82)$$

where  $x = b/a'gl^{d-2}$  must be less than one for the Gaussian approximation to apply. Therefore, perhaps surprisingly, it is the high temperature limit where the Gaussian approximation works best.

### 3.3.3 Gaussian approximation at low temperatures: Absence of ordered phase with continuous symmetry in one and two dimensions

We now consider the problem (66) again, this time with positive  $b$  and negative  $a$ . Then the minimum Landau free energy is at  $\phi = \phi_0 = \sqrt{|a|/b}$ , where we have made the arbitrary choice of phase such that  $\phi_0$  is real. To look at fluctuations around this minimum we write the order parameter as  $\phi = \phi_0(1 + \delta)e^{i\theta}$ . Notice that fluctuations in the phase  $\theta$  only cost energy from the spatial variation, so that the energy goes to zero as the wavelength of a phase excitation goes to infinity. Such a “massless” mode will always exist if there is a continuous symmetry breaking, and is called a Goldstone mode. The energy of such Goldstone modes can be written in the form of an “elastic hamiltonian”,

$$F_L[\theta] = \frac{\varepsilon}{2} \int d^d r |\partial_{\mathbf{r}} \theta|^2, \quad (83)$$

for some elastic stiffness  $\varepsilon$ .

#### **Question 4**

Show that in the small  $\delta$  and  $\theta$  limit,

$$F_L^G[\delta, \theta] = \int d^d r \frac{|a|^2}{b} \delta^2 + \frac{g|a|}{2b} \{ |\partial_{\mathbf{x}} \delta|^2 + |\partial_{\mathbf{x}} \theta|^2 \}, \quad (84)$$

so that the elastic stiffness of the phase fluctuations is  $\varepsilon = g|a|/b$ . Calculate the propagator for the phase

$$G_{\theta}(\mathbf{r}) = \langle \theta(\mathbf{r}) \theta(\mathbf{0}) \rangle = \frac{T}{\varepsilon} \int \frac{d^d k}{(2\pi)^d} \frac{e^{i\mathbf{k} \cdot \mathbf{r}}}{k^2}. \quad (85)$$

for dimensions 1, 2, and higher. Then, ignoring the contribution from  $G_\delta(\mathbf{r})$  and using the property of Gaussian distributions<sup>10</sup> to write  $\langle e^{i[\theta(\mathbf{r})-\theta(0)]} \rangle = e^{-\frac{1}{2}\langle [\theta(\mathbf{r})-\theta(0)]^2 \rangle}$ , show that,<sup>11</sup>

$$G(\mathbf{r}) = \begin{cases} \phi_0^2 e^{-\frac{T}{\varepsilon\pi}r}, & d = 1, \\ \phi_0^2 \left(\frac{r}{l}\right)^{-\frac{T}{2\pi\varepsilon}}, & d = 2, \\ \phi_0^2 \exp\left[\frac{T}{\varepsilon} \frac{c_d}{r^{d-2}} - \frac{T}{\varepsilon} \frac{c_d}{l^{d-2}}\right], & d \geq 3. \end{cases} \quad (86)$$

These results, and the ones for  $T > T_c$ , are summarized in Fig. 11. For  $d = 1$  the propagator decays exponentially with a correlation length  $\xi_-(T) = \varepsilon\pi/T \approx g|a|/bT$ , and the system only has short range order at all non-zero temperatures. For  $d = 2$ , while the propagator goes to zero at large distances, implying the lack of long-range order, the decay is “algebraic”. This means that there is no characteristic length scale to the correlations. This algebraic order is known as “quasi-long-range order”. For all higher dimensions we see the propagator goes to the constant non-zero value of  $G(r \rightarrow \infty) = \exp[-c^d T/\varepsilon l^{d-2}]$ , and the system has long-range order. To summarize we say that the  $O_2$  [or  $U(1)$ ] broken symmetry has a lower critical dimension of  $d_l = 2$ . Note that this is higher than for the Ising symmetry: the continuous symmetry makes the effect of thermal fluctuations more violent. We will have more to say about the special case of two dimensions in Section 3.3.4 and again in Lecture 6.

Similar reasoning for a lower critical dimension applies for all systems with one or more continuous symmetries, where you can write the energy of excitation waves in the elastic form of (83). However, note that the algebraic quasi-long-range order in 2D does not occur with co-dimensions of the continuous symmetry greater than one [e.g. for the classical spin system, with an  $O(3)$  symmetry].

Notice that the destruction of symmetry breaking came from a divergence in the propagator integrals at small  $k$ . In other words the lack of continuous symmetry breaking at or below two dimensions is due to the thermal activation of the low-energy long-wavelength modes (Goldstone modes).

### 3.3.4 Can there be a phase transition at the lower critical dimension?

For  $d = 2$  compare the correlations at low temperature,

$$G_{T \rightarrow 0}(\mathbf{r}) = \phi_0^2 \left(\frac{r}{l}\right)^{-\frac{T}{2\pi\varepsilon}}, \quad (87)$$

<sup>10</sup>If we have a distribution  $P(x) = e^{-x^2/2\sigma}$  so that  $\langle x^2 \rangle = \sigma$  then we can write  $\langle e^{ix} \rangle = z^{-1} \int dx e^{-x^2/2\sigma} e^{ix} = z^{-1} \int dx e^{-\frac{1}{2\sigma}(x-i\sigma)^2} e^{-\sigma/2} = e^{-\langle x^2 \rangle/2}$ .

<sup>11</sup>These results were first derived by T.M. Rice, Phys. Rev. **149**, A1889 (1965), who used them to show that there is no long-range order in superfluids and superconductors in one and two dimensions. A more rigorous quantum mechanical derivation was then published by P.C. Hohenberg, Phys. Rev. **158**, 383 (1967), and for ferromagnetic order in spin systems by N.D. Mermin and H. Wagner, Phys. Rev. Lett. **17**, 1133 (1966). Although Hohenberg probably influenced Mermin and Wagner, and the two papers were submitted at similar dates, the different years of publication has led many people to attribute the statement of “no ordered state at nonzero temperature in one and two dimensions” to the last paper, but we shall name it the “Hohenberg-Mermin-Wagner” theorem.

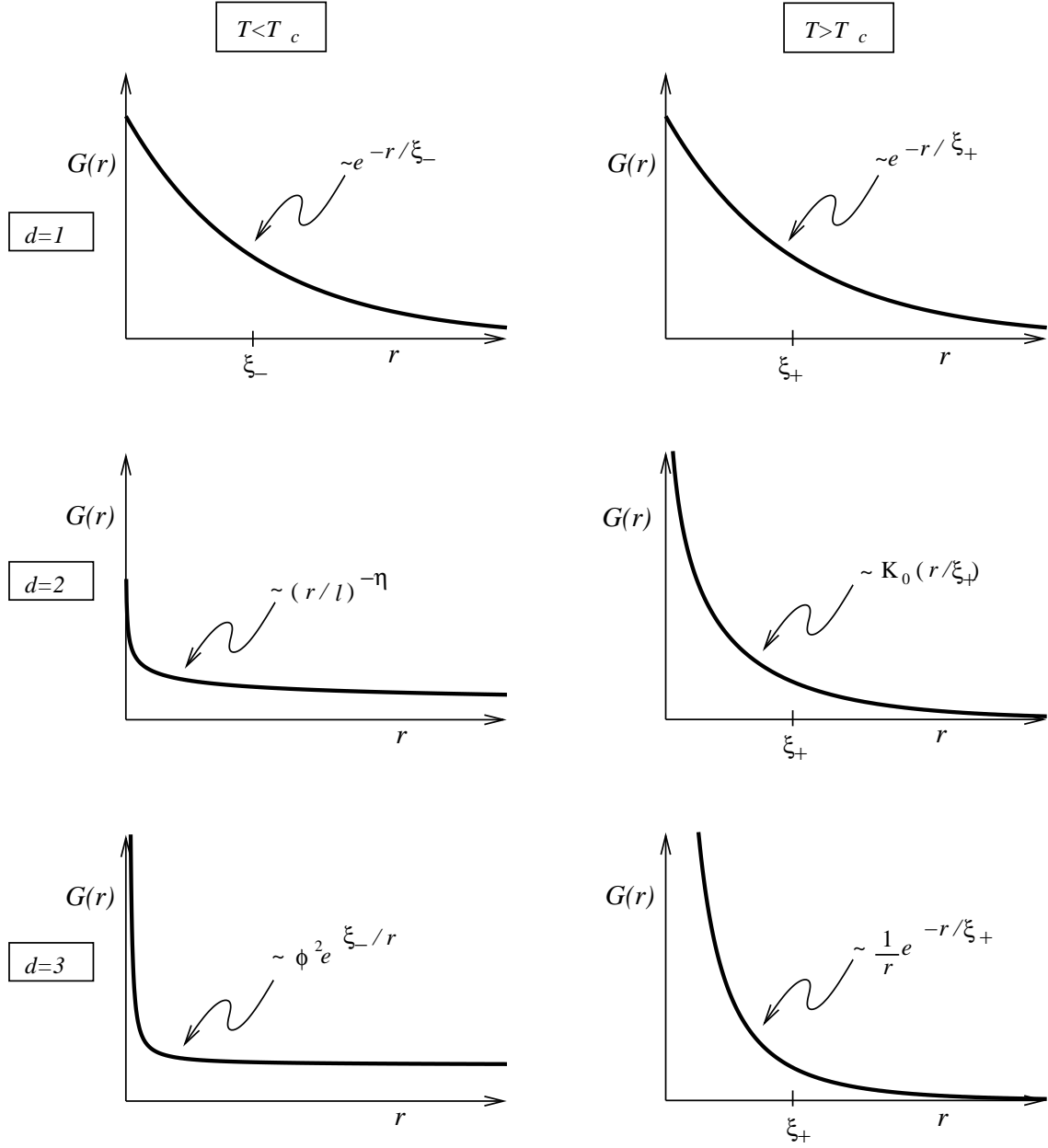


Figure 11: The propagator  $G(r) = \langle \phi(\mathbf{r}) \phi^*(0) \rangle$  of the complex-scalar order parameter within the Gaussian approximation. The results are shown for temperatures below and above the mean-field transition temperature  $T_c$  where the quadratic prefactor  $a$  changes sign. Results are shown for one, two and three dimensions. Note that only for three dimensions at low temperatures does the propagator go to a non-zero value at large  $r$  (i.e. there is an ordered phase.) Above  $T_c$  there is always a finite correlation length above which the propagator goes exponentially to zero. This is also true at low temperatures for  $d = 1$ . For low temperatures in the two dimensional case, while the propagator goes to zero, it has an algebraic dependence with no characteristic length; this behaviour is known as quasi-long range ordered.

to the correlations at high temperature,

$$G_{T \rightarrow \infty}(\mathbf{r}) = \frac{T}{\pi a \xi^2} K_0(r/\xi) \sim \frac{T}{\pi a \xi^2} e^{-r/\xi}, \quad (88)$$

where there is a characteristic length scale,  $\xi = \sqrt{g/a}$ . This means that there must be a phase transition between the two forms. Either the transition is sharp, occurring at a particular value of  $\xi$ , or the transition is continuous if  $\xi$  goes to infinity at some temperature (from above).<sup>12</sup> The continuous transition is known as the Berezinskii-Kosterlitz-Thouless transition, and is discussed in Lecture 6.

---

<sup>12</sup>This was first pointed out by Berezinskii, Sov. Phys. JETP **32**, 493 (1971).

# Lecture Four

## 4 Field Theory of Phase Transitions

In this lecture we first look at the effect of fluctuations within the Gaussian approximation as we get closer to  $T_c$ . We will find that these fluctuations do not change the predictions of mean-field theory close to  $T_c$  only if the dimension is greater than 4. When fluctuations are important, we need then to look at the corrections to the Gaussian model. We therefore develop the perturbation theory in the quartic term of the Landau free energy for  $T > T_c$ . By analysing the diagrams that represent this perturbation series, we will see that the series is divergent close enough to  $T_c$  for  $d < 4$ , which ruins our chance for a straightforward analysis of the phase transition.

### 4.1 Destruction of mean-field theory by fluctuations near the critical point

#### 4.1.1 Gaussian approximation below $T_c$ and above $d_l$

We will look at the Landau free energy for a real scalar order parameter,

$$F_L[\phi(\mathbf{r})] = \int d^d r \left[ \frac{a}{2} \phi^2 + \frac{b}{4} \phi^4 + \frac{g}{2} |\partial_{\mathbf{r}} \phi|^2 \right]. \quad (89)$$

Let us assume we are above the lower critical dimension and there is a spontaneous symmetry breaking below  $T_c$ . We break the symmetry by choosing the minimum of  $F_L$ ,

$$\phi_0 = +\sqrt{a/b} \quad (90)$$

We write  $\phi(\mathbf{r}) = \phi_0 + u(\mathbf{r})$  in the Landau free energy,

$$F_L = F_0 + \int d^d r \left[ |a| u^2 + b \phi_0 u^3 + \frac{b}{4} u^4 + |\partial_{\mathbf{x}} u|^2 \right]. \quad (91)$$

The Gaussian approximation is then just,

$$F_G = \int d^d r \left[ |a| u^2 + g |\partial_{\mathbf{x}} u|^2 \right], \quad (92)$$

and the propagator for fluctuations  $u$  is,

$$G_u(\mathbf{r}) = T \int \frac{d^d k}{(2\pi)^d} \frac{e^{i\mathbf{k} \cdot \mathbf{r}}}{2|a| + gk^2} \approx \frac{T}{g} \frac{c_d}{r^{d-2}} e^{-r/\xi_u}, \quad (93)$$

with correlation length  $\xi_u^2 = g/2|a|$ . For the full propagator we then have,

$$G(\mathbf{r}) = \langle \phi(r) \phi(0) \rangle = \phi_0^2 + C_d \frac{T}{g} \frac{e^{-r/\xi_u}}{r^{d-2}}. \quad (94)$$

consistent with an ordered phase for  $d \geq 2$ .

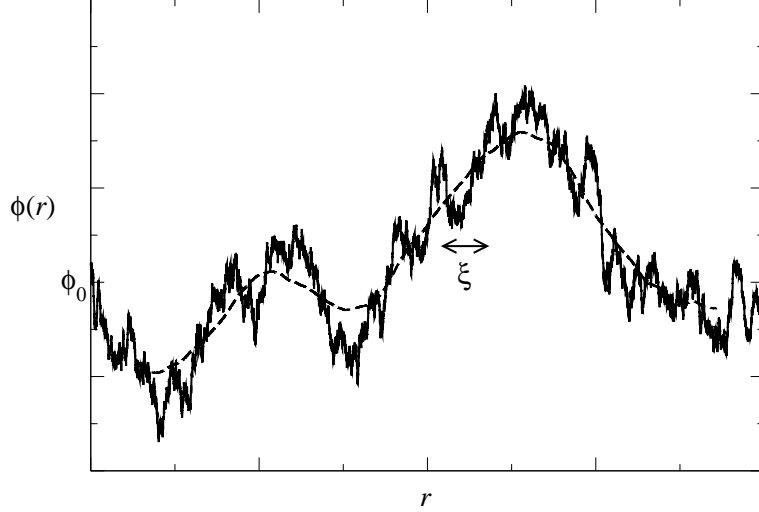


Figure 12: Snapshot of the profile of the order parameter in the ordered phase at some nonzero temperature. The random fluctuations are characterized by a typical length scale  $\xi$  over which the order parameter tends to return to the average value. The dashed line shows the value of  $\phi_{\text{coh}}$ , the value when coarse-grained over the length  $\xi$ .

#### 4.1.2 Gaussian fluctuations in the ordered phase

A typical snapshot of the fluctuating order parameter in the ordered phase is shown as the full line in Fig. 12. Notice the extent to which the fluctuations are correlated, so that a typical excursion away from the mean value occurs over a length scale of order  $\xi$ . Also shown as the dashed line is the same order parameter when “coarse-grained” up to the length scale  $\xi$ . We define this as the “coherent” order parameter,

$$\phi_{\text{coh}}(\mathbf{r}) = \xi^{-d} \int_{|\mathbf{r}' - \mathbf{r}| < \xi} d^d r' \phi(\mathbf{r}'). \quad (95)$$

Notice that the mean-square fluctuations of  $\phi_{\text{coh}}$  will be less than that of the original order parameter  $\phi$ .

Depending on the temperature, the fluctuations will occasionally take the order parameter into the “wrong” phase. As long as we are not in one dimension, the resulting droplets might not destroy the ordered phase. Because we know that  $\xi$  is the important length over which a domain-wall can relax from one phase to another (i.e., from  $\phi_0$  to  $-\phi_0$ ) we can estimate when the effect of these droplets becomes important by calculating when the width of fluctuations of  $\phi_{\text{coh}}$  becomes of the order of  $\phi_0$ . So when

$$\langle (\delta \phi_{\text{coh}})^2 \rangle > \phi_0^2, \quad (96)$$

the effect of Gaussian fluctuations should become more important than the mean-field predicted properties from just sitting in the minimum. From our results for the Gaussian approximation, we can calculate this condition using,<sup>13</sup>

$$\begin{aligned} \langle (\delta \phi_{\text{coh}})^2 \rangle &= \xi^{-2d} \int_{|\mathbf{r}' - \mathbf{r}| < \xi} d^d r' \int_{|\mathbf{r}'' - \mathbf{r}| < \xi} d^d r'' \langle \delta \phi(\mathbf{r}') \delta \phi(\mathbf{r}) \rangle \\ &= \xi^{-d} \int_{r' < \xi} d^d r' G_u(\mathbf{r}') \\ &= A_d \frac{T}{g} \xi^{-(d-2)}. \end{aligned} \quad (97)$$

<sup>13</sup>Compare this result to the total fluctuation width,  $\langle (\delta \phi^2) \rangle \sim T/g l^{d-2} \gg \langle (\delta \phi_{\text{coh}})^2 \rangle$ .

Inserting this in condition (96), with  $\xi^2 = g/2|a|$  and  $\phi_0^2 = |a|/b$  gives,

$$A_d \frac{T}{g} (g/2|a|)^{-(d-2)/2} > |a|/b, \quad (98)$$

or

$$A'_d T b g^{-d/2} > |a|^{(4-d)/2}, \quad (99)$$

as the regime where Gaussian fluctuations will become important. Remembering that  $|a| = a'(T_c - T)$ , we see that for  $d < 4$  there will always be a regime close enough to  $T_c$  so that fluctuations *change the predictions* of mean-field theory. On the other hand, for  $d > 4$  the left hand side of (99) will always be smaller than the right hand side close enough to  $T_c$ , so that the effect of fluctuations can be *ignored* close to the critical point.

#### 4.1.3 Specific heat from Gaussian fluctuations

The important effect of fluctuations below four dimensions is also seen in the specific heat contribution of these fluctuations. Above  $T_c$  we have in the Gaussian model,

$$f = -\frac{T}{2} \int \frac{d^d k}{(2\pi)^d} \ln \left( \frac{T l^{-d}}{(a + g k^2)} \right). \quad (100)$$

##### Question 5

Show that as  $T \rightarrow T_c$  from above, the most singular part of the specific heat  $c = -\partial^2 f / \partial T^2$  is given by,

$$c_s = \frac{1}{2} \int \frac{d^d k}{(2\pi)^d} \frac{a'^2 T}{(a + g k^2)^2}. \quad (101)$$

Evaluate the integral for the cases  $d < 4$ ,  $d = 4$ , and  $d > 4$  to show the following behaviours,

$$c_s \propto \begin{cases} (T - T_c)^{-(4-d)/2}, & \text{for } d < 4 \\ \ln[(T - T_c)/T_c], & \text{for } d = 4 \\ \text{const.}, & \text{for } d > 4 \end{cases} \quad (102)$$

Therefore there is a diverging specific heat as  $T \rightarrow T_c^+$  for  $d \leq 4$ . Below  $T_c$ , the results are broadly similar, but now we can compare to the specific heat due to the condensation of the order parameter in mean-field theory (this is zero above  $T_c$ ). Remember that in mean-field Landau theory we had (27),

$$c_0 = \frac{a'^2 T}{2b}, \quad \text{for } T < T_c. \quad (103)$$

Now the Gaussian fluctuations have a free energy contribution,<sup>14</sup>

$$f = -\frac{T}{2} \int \frac{d^d k}{(2\pi)^d} \ln \left( \frac{T l^{-d}}{(2|a| + g k^2)} \right). \quad (104)$$

---

<sup>14</sup>If we had any soft transverse modes, we can show that they do not give singular contributions to the specific heat as long as  $d > d_{lc}$



The same procedure then leads to the singular contribution to the specific heat,

$$\begin{aligned} c_s &= \frac{a'^2 T^2}{2|a|^2} \int \frac{d^d k}{(2\pi)^d} \frac{1}{(1 + \xi_u^2 k^2)^2} \\ &= \frac{I_d}{2\xi_0^d} \frac{T^2}{T_c^2} \left[ \frac{(T_c - T)}{T_c} \right]^{-(4-d)/2} \quad \text{for } d < 4, \end{aligned} \quad (105)$$

where we have defined the zero temperature correlation length by  $\xi(T) = \xi_0(T_c - T)/T_c$ , and  $I_d = (2\pi)^{-d} \int d^d q \, 1/(1 + q^2)$ . We have a specific heat contribution,  $c_s$ , that will always become larger than the contribution from condensing to the ordered phase,  $c_0$ , close enough to the critical point.

#### 4.1.4 Upper critical dimension and the Ginzburg criterion

Using the above results we can define a temperature,  $T_G$ , close to, but below  $T_c$ , above which the Gaussian fluctuations become more important than the mean-field condensation of the order parameter. We call this criterion the Ginzburg criterion after such a temperature was defined for superconductors (Ginzburg 1960). Both of the above arguments give a Ginzburg criterion of the same form. Using the specific heat results, we define the Ginzburg temperature as the point where the singular specific heat from fluctuations is equal to the mean-field specific heat, which gives,

$$T_G = T_c - T_c \left[ \frac{I_d}{2\xi_0^d c_0} \right]^{2/(4-d)}. \quad (106)$$

This is also often written as the relative width of the “critical region” over which fluctuations are important,  $\tau_G = (T_c - T_G)/T_c$ , which is,

$$\tau_G = \left[ \frac{I_d}{2\xi_0^d c_0} \right]^{2/(4-d)}. \quad (107)$$

This goes some way to explaining why experimental and theoretical results for continuous phase transitions in dimensions two and three may have different exponents than predicted by Landau mean-field theory. However, notice that a very large value of the zero-temperature correlation length, or indeed, a large mean-field specific heat step, will lead to a very narrow region where fluctuations are important. This is especially the case for most superconductors, where the correlation length from the zero temperature theory (Bardeen-Cooper-Schrieffer 1957) is orders of magnitude larger than atomic spacing. On the other hand, using experimental values for superfluid Helium gives a very large value of  $\tau_G$ , so that fluctuations are nearly always important. This is why the so-called “lambda transition” (a log-divergence in specific heat) was first found in the superfluid to normal transition of Helium.

## 4.2 Perturbation theory

Having demonstrated that Gaussian fluctuations become important near  $T_c$  for  $d < 4$ , we then have to worry about whether the corrections to the Gaussian model become important. We will therefore develop the perturbation theory for the quartic term in the Landau free energy that we ignored in the Gaussian approximation. As the statistical averages for any physical quantity, will contain  $F_L$  in the exponent, our

expansion around the Gaussian model (for  $a > 0$ , i.e., as in Section 3.3.1, but for a scalar  $\phi$ ) consists of expanding the exponential,

$$e^{-\beta(F_G+F_4)} = e^{-\beta F_G} \left[ \sum_{m=0}^{\infty} \frac{(-\beta)^m}{m!} (F_4)^m \right], \quad (108)$$

where  $F_G$  is given in (92), and

$$\begin{aligned} F_4 &= \frac{b}{4} \int d^d r \phi^4(\mathbf{r}) \\ &= \frac{b}{4} \int \frac{d^d k_1}{(2\pi)^d} \frac{d^d k_2}{(2\pi)^d} \frac{d^d k_3}{(2\pi)^d} \phi_{\mathbf{k}_1} \phi_{\mathbf{k}_2} \phi_{\mathbf{k}_3} \phi_{-\mathbf{k}_1-\mathbf{k}_2-\mathbf{k}_3}. \end{aligned} \quad (109)$$

As  $F_4 \propto b$ , we might think this a good expansion as long as  $b/T$  is small. (This is of course wrong, as we still have to include the integral in the expansion. We will consider this later.)

We can now write the partition function using this expansion,

$$\begin{aligned} Z &= \int D\phi e^{-\beta(F_G[\phi]+F_4[\phi])} \\ &= Z_0 \langle e^{-\beta F_4} \rangle_0 = Z_0 \sum_{m=0}^{\infty} \frac{(-\beta)^m}{m!} \langle (F_4)^m \rangle_0, \end{aligned} \quad (110)$$

where  $Z_0$  is the partition function of the Gaussian model, and  $\langle \dots \rangle_0$  represents an average within this Gaussian model. Similarly, we can write the average of a general quantity  $A[\phi]$

$$\begin{aligned} \langle A \rangle &= \int D\phi A[\phi] e^{-\beta(F_G[\phi]+F_4[\phi])} \\ &= \frac{\langle A e^{-\beta F_4} \rangle_0}{\langle e^{-\beta F_4} \rangle_0} = \frac{\sum_{m=0}^{\infty} \frac{(-\beta)^m}{m!} \langle A (F_4)^m \rangle_0}{\sum_{m=0}^{\infty} \frac{(-\beta)^m}{m!} \langle (F_4)^m \rangle_0} \end{aligned} \quad (111)$$

#### 4.2.1 Calculating the average of products of $\phi$ in the Gaussian model

We have already calculated the average of pairs of fields in the Gaussian model. For example,

$$\langle \phi_{\mathbf{k}_1} \phi_{\mathbf{k}_2} \rangle_0 = (2\pi)^d \delta^d(\mathbf{k}_1 + \mathbf{k}_2) \frac{T}{a + gk_1^2} \equiv (2\pi)^d \delta^d(\mathbf{k}_1 + \mathbf{k}_2) G_0(\mathbf{k}_1), \quad (112)$$

where we define  $G_0(\mathbf{k}_1)$  as the propagator in the Gaussian model. Now consider the average arising in the first-order correction to the partition function,

$$\langle F_4 \rangle_0 = \frac{b}{4} \int \frac{d^d k_1}{(2\pi)^d} \int \frac{d^d k_2}{(2\pi)^d} \int \frac{d^d k_3}{(2\pi)^d} \int d^d k_4 \delta^d(\mathbf{k}_1 + \mathbf{k}_2 + \mathbf{k}_3 + \mathbf{k}_4) \langle \phi_{\mathbf{k}_1} \phi_{\mathbf{k}_2} \phi_{\mathbf{k}_3} \phi_{\mathbf{k}_4} \rangle_0. \quad (113)$$

We therefore need the Gaussian average of a product of four  $\phi$ 's. We can find this using the general rule for a product of  $n$  terms,

$$g_n \equiv \langle \phi_{\mathbf{k}_1} \phi_{\mathbf{k}_2} \dots \phi_{\mathbf{k}_n} \rangle_0 = \begin{cases} 0, & \text{if } n \text{ is odd.} \\ \text{sum of products of pairwise averages for all possible} \\ \text{pairings, if } n \text{ is even.} \end{cases} \quad (114)$$

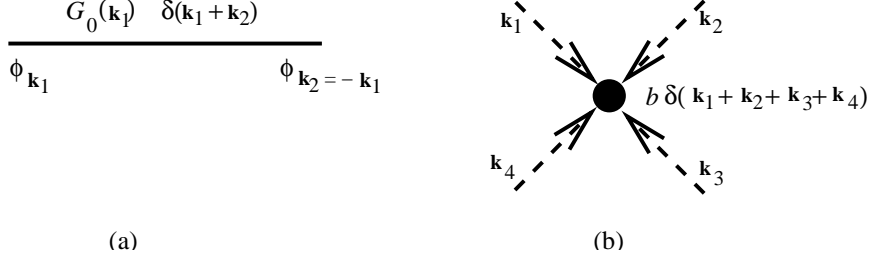


Figure 13: Definition of the building blocks of the diagrammatic representation of perturbation theory. (a) shows a line that represents the pairing of two fields. (b) is the vertex from an instance of  $F_4$ , with a constraint on the sum of the momenta entering.

$$Z = Z_0 \left( 1 + \text{diagram} \right)$$

Figure 14: Diagrammatic representation of the first-order expansion of the partition function.

(The proof is through the properties of a Gaussian distribution.) We therefore have, using (112),

$$\langle \phi_{\mathbf{k}_1} \phi_{\mathbf{k}_2} \phi_{\mathbf{k}_3} \phi_{\mathbf{k}_4} \rangle_0 = (2\pi)^{2d} \left[ G_0(\mathbf{k}_1) \delta^d(\mathbf{k}_1 + \mathbf{k}_2) G_0(\mathbf{k}_3) \delta^d(\mathbf{k}_3 + \mathbf{k}_4) + \dots (3 \text{ permutations}) \right]. \quad (115)$$

As the labels on the integrals in (113) can be swapped, each permutation gives the same contribution so that we get,

$$\langle F_4 \rangle_0 = \frac{3b}{4} \int \frac{d^d k}{(2\pi)^d} \int \frac{d^d k'}{(2\pi)^d} G_0(\mathbf{k}) G_0(\mathbf{k}') = \frac{3b}{4} \left[ \int \frac{d^d k}{(2\pi)^d} G_0(\mathbf{k}) \right]^2. \quad (116)$$

Note that the integral is convergent at the lower limit as  $a \rightarrow 0$  as long as  $d > 2$ .

#### 4.2.2 Diagrammatic representation of perturbation theory

For higher order terms it is clearly going to be difficult to keep track of the different pairing of  $\phi$ 's. The human brain finds it easier to view the problem topologically, i.e. by drawing diagrams. The convention is that a straight line represents the pairing of two fields, forcing them to carry equal and opposite momenta (see Fig. 13a). The other condition comes from the delta function in the quartic term [seen in (113)], which forces a conservation of momentum for the four fields that “belong” to a given interaction term. This constraint is given diagrammatically by a vertex with four legs (Fig. 13b), where we know that the sum of momenta coming out of the vertex must be zero. For example the diagrammatic representation of the perturbation series for the partition function to first order is given in Fig. 14. The only diagram corresponds to the result (116).

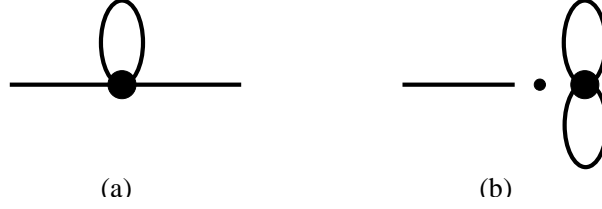


Figure 15: The two diagrams appearing to first order in the numerator of the propagator expansion. (a) The “connected” diagram where the two external fields are paired with fields inside  $F_4$ . (b) The “disconnected” diagram where the external fields pair with each other.

$$\begin{aligned}
 \underline{\underline{G(k)}} &= \underline{\underline{G_0(k)}} + \text{diagram (a)} \\
 &+ \text{diagram (two loops)} + \text{diagram (three loops)} \\
 &+ \text{diagram (bubble)}
 \end{aligned}$$

Figure 16: The perturbation series for the propagator to second order in  $b$ .

#### 4.2.3 Perturbation expansion for the propagator

We now use the above results to calculate the propagator,

$$\langle \phi_{\mathbf{k}_1} \phi_{\mathbf{k}_2} \rangle = \frac{\sum_{m=0}^{\infty} \frac{(-\beta)^m}{m!} \langle \phi_{\mathbf{k}_1} \phi_{\mathbf{k}_2} (F_4)^m \rangle_0}{\sum_{m=0}^{\infty} \frac{(-\beta)^m}{m!} \langle (F_4)^m \rangle_0}. \quad (117)$$

Consider the first term in the numerator. We see that we can either pair the two external fields  $\phi_{\mathbf{k}_1}$  and  $\phi_{\mathbf{k}_2}$  with each other, or each one must be paired with a field inside the expression for  $F_4$ . In each case there are 12 permutations that give the same result, so we finally get,

$$\begin{aligned}
 \langle \phi_{\mathbf{k}_1} \phi_{\mathbf{k}_2} F_4 \rangle &= (2\pi)^d \delta^d(\mathbf{k}_1 + \mathbf{k}_2) 3b \left[ G_0(\mathbf{k}_1) G_0(\mathbf{k}_1) \int \frac{d^d k'}{(2\pi)^d} G_0(\mathbf{k}') \right. \\
 &\quad \left. + G_0(\mathbf{k}_1) \int \frac{d^d k'}{(2\pi)^d} G_0(\mathbf{k}') \int \frac{d^d k''}{(2\pi)^d} G_0(\mathbf{k}'') \right] \quad (118)
 \end{aligned}$$

The two contributions are shown as diagrams in Fig. 15. To be consistent, we also need to expand the denominator to the same order, where we pick up the contribution of (116). When we also expand this denominator using  $(1+x)^{-1} = 1 - x + \mathcal{O}(x^2)$ , we see that the product of this partition function correction with the Gaussian propagator exactly cancels the contribution of the term in (118) corresponding to the diagram in Fig. 15b, i.e., the term in the expansion of the numerator which has separate parts disappears when we include corrections to the partition function. It turns out that this is a general rule,<sup>15</sup> that all of the denominator corrections just have the effect to cancel

<sup>15</sup>We don’t prove this “linked-cluster theorem” here, but see, S.-K. Ma, *Modern Theory of Critical Phenomena* (Addison-Wesley 1976) p. 293; D.J. Amit, *Field Theory, the Renormalization Group, and Critical phenomena* (World Scientific, 1984) p. 60.



those diagrams in the numerator made from a product of “disconnected diagrams”. The end result is a diagrammatic series of all possible “connected diagrams”. For example in Fig. 16 we show the diagrammatic series to order  $b^2$  for the propagator,  $G(\mathbf{k})$ .

Consider the 1st-order correction to  $G(\mathbf{k})$ , i.e., the term arising from diagram 15a. This is,

As  $a \rightarrow 0$  the integral is convergent for  $d > 2$ , to give,

which diverges faster than the zeroth-order term  $G_0(0) = T/a \sim (T-T_c)^{-1}$ . The same factor of  $1/a$  will appear in higher order diagrams as extra  $G_0$ 's are inserted. Therefore the series is apparently divergent as  $T \rightarrow T_c$ . However, this form of divergence is easily *resummed*, as it basically takes the form of a geometric series, as is shown in Fig. 17a. The building block that repeats itself is known as the self-energy  $\Sigma(\mathbf{k})$ . After resumming, the perturbation series takes the form (as in Fig. 17b),

Multiplying both sides by  $G^{-1}G_0^{-1}$  tells us that the correction to the *inverse* of the propagator is just the self-energy,

(where  $G_0^{-1}(\mathbf{k}) = (a + gk^2)/T$ ). This is known as the Dyson equation. The first two orders in the expansion of the self-energy are shown in Fig. 17c. The problem of

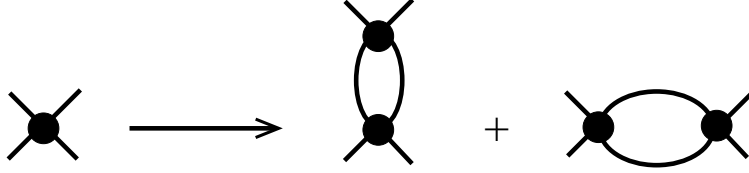


Figure 18: Demonstration of the procedure to generate *some* of the next-higher order diagrams from a given diagram. The extra factor that results diverges as  $T \rightarrow T_c$  for  $d \leq 4$ .

finding the propagator in the presence of a quartic interaction is therefore reduced to the problem of finding the self-energy. However, we notice that the extra factor of  $G_0$  has miraculously disappeared from the correction to the inverse propagator. For example, the first-order correction to  $G^{-1}(\mathbf{k})$  is,

$$\Sigma^{(1)}(\mathbf{k}) = b \int \frac{d^d k'}{(2\pi)^d} \frac{1}{(a + gk'^2)}, \quad (123)$$

which stays finite as  $a \rightarrow 0$  as long as  $d > 2$ .

#### 4.2.5 Relative divergence of successive terms in self-energy expansion near $T_c$ : reappearance of Ginzburg criterion

Consider the second and third term in the self-energy expansion in Fig.17c. Notice how they each contain the same factors as the first diagram, together with an extra “bubble” that contains two factors of  $G_0$  and a vertex. Seeing as the vertex only makes one constraint on momenta, this means that we have one extra integral over two propagators. In fact, from any diagram, we will be able to construct new higher-order diagrams by replacing each vertex with such a bubble (see Fig. 18), thus always introducing more and more factors of,

$$b\beta \int \frac{d^d k'}{(2\pi)^d} [G_0(\mathbf{k}')]^2 \sim \left[ \frac{(T - T_c)}{T_c} \right]^{(d-4)/2}. \quad (124)$$

Therefore, as  $T \rightarrow T_c$ , each order in perturbation theory has terms with an extra factor of  $(T - T_c)^{(d-4)/2}$  compared to corresponding diagrams in the order below. Note, however, that we cannot do a similar Dyson resummation in this case, as more topologically complex diagrams are created by this procedure. This means that perturbation theory becomes undefined when this factor is large. We can only use the expansion when  $d > 4$ , or when  $d < 4$  and  $T > T_{Gi}$ .<sup>16</sup>

<sup>16</sup>The case  $d = 4$  is special, as the extra factor from the bubble is only logarithmically divergent. This allows certain resummation tricks to be used to find the behaviour near  $T_c$  at the upper critical dimensions, see A.I. Larkin and D.E. Khmel'nitskii, Sov. Phys. JETP **29**, 1123 (1969).

# Lecture Five

## 5 Scaling and Renormalization Group Approach

In this lecture we start with an overview of the concept of scale invariance in the context of the critical point, and its relation to the result of coarse-graining. We then review the definition of critical exponents near a continuous phase transition, and relate the existence of universal non-mean-field exponents. Finally we introduce the renormalization group (RG) transformations, the knowledge of which allows one in principle to calculate the critical exponents. As examples we shall derive the RG equations for the Gaussian model, and look at the corrections to lowest order in an  $\epsilon = 4 - d$  expansion.

### 5.1 Power laws and scale-invariance

Consider the power-law decay of the correlation function for a  $U(1)$  order-parameter in two dimensions at low temperatures [see the  $d = 2$  result in (86)],

$$G(r) = A \left( \frac{r}{l} \right)^{-\eta}. \quad (125)$$

If we consider a scale transformation with  $\mathbf{r} \rightarrow \mathbf{r}' = \mathbf{r}/\lambda$ , then we can write the correlation function  $G'(r') \equiv G(r)$  as

$$G'(r') = A\lambda^{-\eta} \left( \frac{r'}{l} \right)^{-\eta}, \quad (126)$$

i.e. the two functions are the same to within a multiplicative factor,  $G'(r) = \lambda^{-\eta}G(r)$ .

Now consider the correlation function in three dimensions above the transition temperature [see (79)],

$$G(r) = \frac{C}{r} e^{-r/\xi}. \quad (127)$$

This function clearly does not have the same scale-invariant properties, as there is a characteristic length  $\xi$ . On the other hand, for distances much less than  $\xi$  we do seem to have effectively scale-invariant correlations.

These ideas are visualized in Figs. 19 and 20,<sup>17</sup> where we see snapshots of a 2D Ising model, and successive “coarse-grainings”. In Fig. 19a we see the system just above  $T_c$  with no net magnetization, but correlated fluctuations. As the system is coarse-grained, the correlation length flows towards the cut-off scale, and the system looks more like a very high temperature state. Similarly in Fig. 19b the first picture shows a snapshot just below  $T_c$ . Here there is a net magnetization, but with domains of opposite sign with a typical scale. As we coarse-grain, this typical scale flows to zero, and the system looks like its low temperature limit.

Finally, Fig. 20 shows repetitive coarse-graining at exactly the critical temperature. This is a state with power-law correlations, so that the general properties of the system are not changing with the coarse-graining. We see that the low-temperature and high temperature limits (with zero correlation length) and the critical temperature (with infinite correlation length) are “fixed points” of the coarse-graining procedure.

---

<sup>17</sup>Taken from A. Bruce and D. Wallace, in *The New Physics*, ed. P. Davies (Cambridge University Press, 1989).

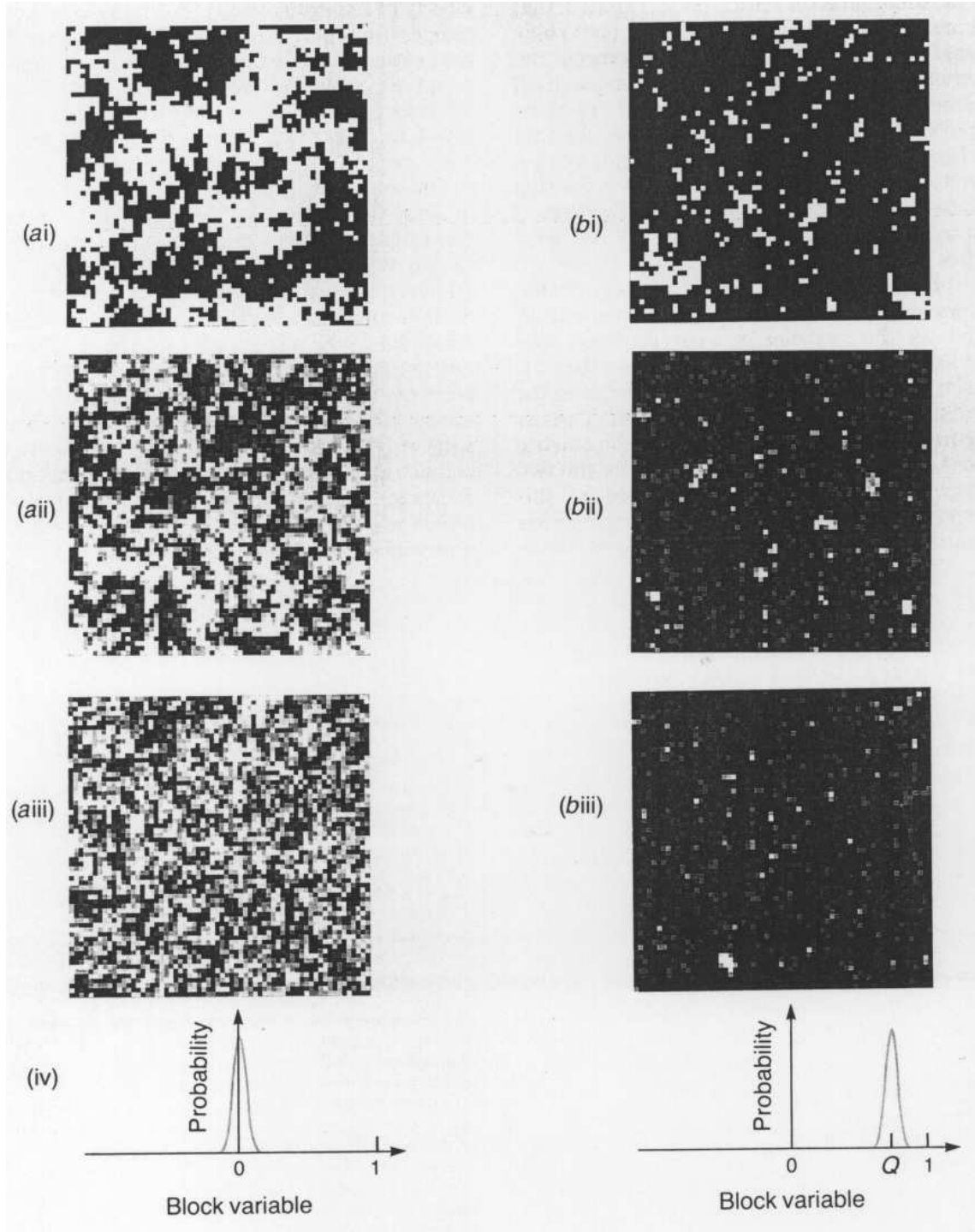


Figure 19: Coarse-graining procedure on snapshot configurations in the 2D Ising model (a) for  $T > T_c$  and (b) for  $T < T_c$ . Note how after many coarse-grainings the system starts to look more like the zero or infinite temperature limit.



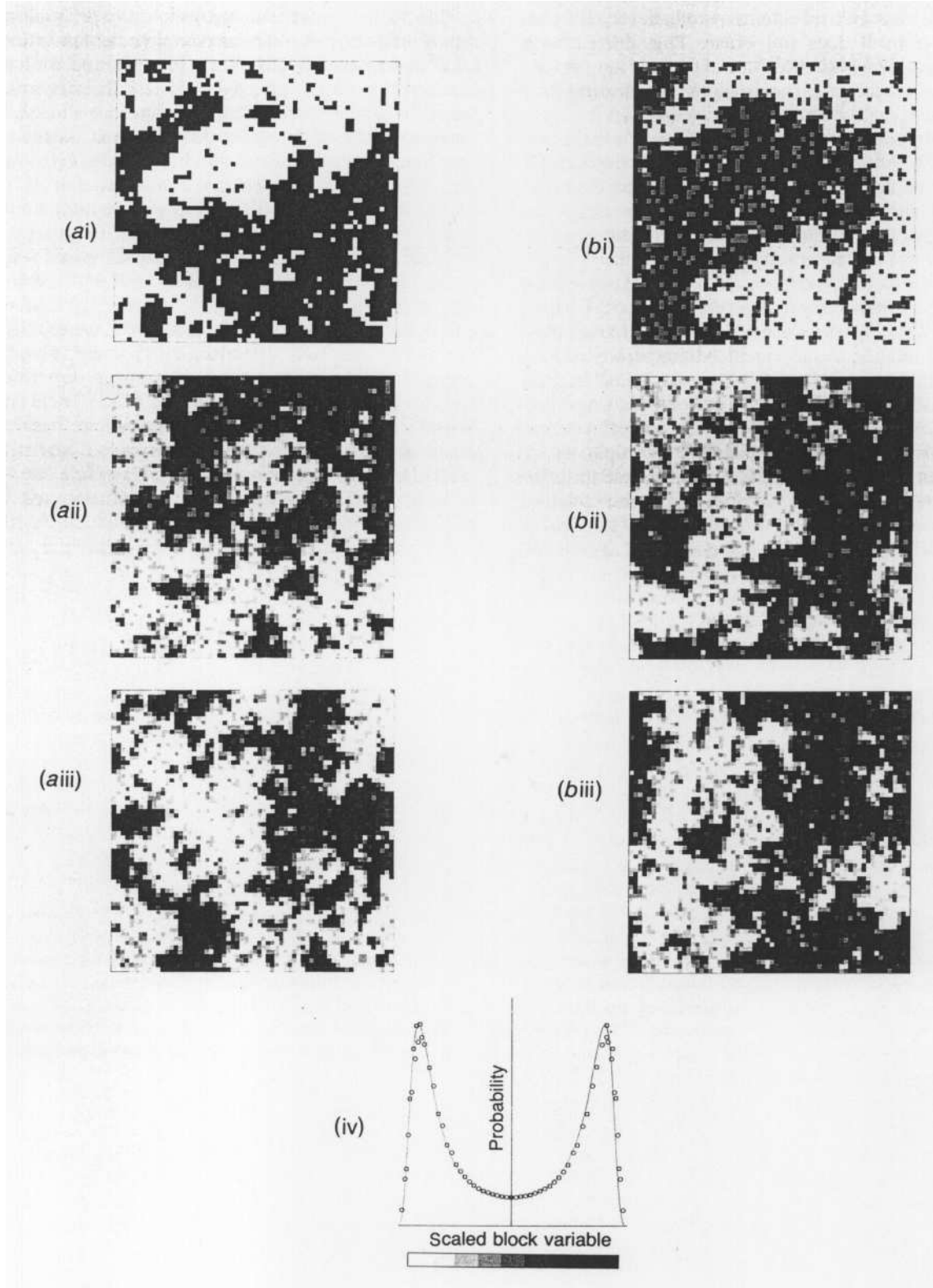


Figure 20: Same coarse-graining procedure but on a snapshot configuration at exactly  $T = T_c$  for the 2D Ising model. This demonstrates the “self-similarity” of the critical state, with its power-law correlations, i.e. each successive coarse-grained picture looks qualitatively the same as previous pictures, and there is not a single characteristic length scale.

## 5.2 Critical Exponents

So far we have mostly looked at mean-field theory or the Gaussian approximation. However, in these examples we saw the general property of continuous phase transitions, which is the power-law dependence on critical parameters of many physical quantities. Therefore, continuous transitions are characterized by exponents, which we know are often different from the “classical” (i.e. mean-field) values. Notice that these power-law dependences also hint at some “scale-invariance” of the critical parameters.

### 5.2.1 Mean-field exponents

Let us remind ourselves of the characteristic exponents in the Landau mean-field theory, and at the same time define the conventional notation of greek symbols for these exponents.

*Spontaneous magnetization exponent,  $\beta$*

We have seen that the order parameter vanishes at  $T_c$  with the behaviour,

$$|\phi| = \left( \frac{a'(T_c - T)}{b} \right)^{1/2}. \quad (128)$$

Writing this in the general form,

$$|\phi| = A\tau^\beta, \quad (129)$$

where  $\tau = (T_c - T)/T_c$ , defines the exponent  $\beta$ , which therefore has the Landau mean-field value,

$$\beta = \frac{1}{2}. \quad (130)$$

*Susceptibility exponent,  $\gamma$*

Similarly, if we define an exponent  $\gamma$  by,

$$\chi \equiv \left. \frac{\partial \phi}{\partial h} \right|_{h \rightarrow 0} = C\tau^{-\gamma}, \quad (131)$$

then the Landau mean-field theory has the value,

$$\gamma = 1. \quad (132)$$

*Critical isotherm magnetization exponent,  $\delta$*

If we remain at  $T = T_c$ , and consider how  $\phi$  vanishes as  $h \rightarrow 0$ , we can write,

$$\lim_{h \rightarrow 0, T=T_c} \phi = Dh^{1/\delta}, \quad (133)$$

and the Landau theory gives

$$\delta = 3. \quad (134)$$

*Correlation length exponent,  $\nu$*

We have also seen the characteristic length  $\xi$  diverging at  $T_c$ . In general we write this as

$$\xi = \xi_0 \left( \frac{T - T_c}{T_c} \right)^{-\nu}, \quad (135)$$

and within Landau theory,

$$\nu = \frac{1}{2}. \quad (136)$$

*Heat capacity exponent,  $\alpha$*

Although there is only a step in the specific heat at the critical point in Landau theory, in general we will see that there can be a divergence in  $c$ . We therefore define  $\alpha$  by,

$$c \propto \tau^{-\alpha}, \quad (137)$$

but with the trivial value in mean-field theory,

$$\alpha = 0. \quad (138)$$

### 5.2.2 Exponents from mean-field theory plus Gaussian fluctuations

Within the Gaussian approximation that we have considered in the previous lectures, there is no correction to the size of the order parameter. Also, the correlation length characterizing the fluctuations has the same temperature dependence of the mean-field coherence length. On the other hand, the fluctuations do give a diverging specific heat for  $d < 4$ . Therefore the Gaussian exponents below the upper critical dimension are,

$$\alpha = \frac{4-d}{2}, \quad \beta = \frac{1}{2}, \quad \gamma = 1, \quad \delta = 3, \quad \nu = \frac{1}{2}. \quad (139)$$

### 5.2.3 Exponents from exact solution of 2D Ising Model

The exact solution of the 2D Ising model (Onsager 1944) gives the following exponents (defined in the same way as the above mean-field results),

$$\beta = \frac{1}{8}, \quad \gamma = \frac{7}{4}, \quad \delta = 15, \quad \nu = 1. \quad (140)$$

All of these are different from their mean-field counterparts. In addition, the specific heat of the 2D Ising model has the behaviour near the transition temperature,

$$c \approx c_0 \ln |1 - T/T_c|. \quad (141)$$

While this strictly corresponds to an “exponent” of  $\alpha = 0$ , this log divergence is very different behaviour from the mean-field result of a jump in specific heat.

Clearly the mean-field Landau theory cannot hope to describe the real properties of this continuous transition. Onsager’s results do not follow the “universal” prescription that we saw in Lecture 1. We will see why in this lecture by looking at the importance of fluctuations near the critical point. Nevertheless it turns out that the exponents of the 2D Ising model are still in some sense universal: they apply for all two-dimensional phase transitions with the same broken symmetry (e.g. the lattice gas, or Ising models on different lattices, or different interactions.)

### 5.2.4 Experimental exponents

While the Onsager solution destroyed the previous faith in mean-field theory and its universal application, a new puzzle then arrived: There is still some universality in the value of these exponents: they only depend on the order-parameter symmetry and the dimension, but not on details of the system. Certainly by 1967 this was accepted knowledge when the review<sup>18</sup> by Kadanoff et al. tabulated exponents from many

---

<sup>18</sup>L. P. Kadanoff et al., Rev. Mod. Phys. bf 39, 395 (1967);

different experiments. The most striking result were those from different liquid-gas critical points, where despite large variations in  $T_c$ , the same exponents are found, and which are markedly different from the classical values derived in the Van der Waals model in Lecture 1. Magnetic systems also show exponents very different from the Weiss model predictions, although there is some variation between different ferromagnets<sup>19</sup> which may depend on the different anisotropies of the local moments. Even so, the magnetization exponent  $\beta$  is always less than 0.38 in three-dimensional ferromagnets. Therefore the task that the renormalization group approach solved was to understand in a systematic way how exponents are determined universally, while being very different to the classical values.

### 5.3 Renormalization Group Transformations

The RG (Renormalization Group) transformation is just a way to formalize the coarse-graining we saw in Figs. 19 and 20. The basic idea is that after coarse-graining the system is transformed to a new system with different values of parameters (external, such as temperature and field, or internal, such as the coupling constants that go into the Landau free energy). The first attempt to actually calculate this procedure was due to Kadanoff,<sup>20</sup> who invented the concept of block spins as a way of mapping a coarse-grained system on to a system with the original Hamiltonian. The general formulation and significance of the RG procedure was first given by Wilson.<sup>21</sup>

If we define (abstractly for now) a coarse-graining procedure  $R_\lambda$  (where  $\lambda$  is the ratio of new cut-off length to old cut-off length), then we should have a “semi-group” structure,

$$R_{\lambda_1} R_{\lambda_2} = R_{\lambda_2} R_{\lambda_1} = R_{\lambda_1 \lambda_2}. \quad (142)$$

(It is a semi-group because the inverse can not be defined.) Now, suppose we have a system with a Landau free energy of very general form,

$$\beta F_L[\phi] = \sum_n K_n f_n[\phi], \quad (143)$$

where  $K_n$  are the coupling constants for different local functions  $f_n$  of the field  $\phi$  [e.g.,  $\beta a$ ,  $\beta b$ , and  $\beta g$  in the Landau free energy (40)]. Then under a RG transformation, each coupling constant will change in a prescribed way depending on the value of all the  $K_n$ ,

$$\{K'_n\} = R_\lambda [\{K_n\}]. \quad (144)$$

One example, which is very illustrative is the 2D Ising model, where we consider the flow under RG operations of the couplings  $J/T$  and  $h/T$ . The schematic result is shown in Fig. 21 Note the presence of five “fixed points” in the RG flow (defined as where the RG transformation leaves the coupling constants with the same values,  $\{K_n^*\} = R_\lambda [\{K_n^*\}]$ ). These are: C– the critical point of the 2D Ising model where all flows in the vicinity of this point take you away; F– ferromagnetic fixed point at  $(h = 0, T = 0)$ , to which all points at  $h = 0$  and  $T < T_c$  flow to; P– paramagnetic fixed point at  $(h = 0, T = \infty)$ . to which all points at  $h = 0$  and  $T > T_c$  flow to; 2×S– sink points which all points with non-zero  $h$  eventually flow to.

<sup>19</sup>E.g. compare Fe and Ni in Tanaku and Miyatori, J. Appl. Phys. 82, 5658 (1997).

<sup>20</sup>L.P. Kadanoff, Physics **2**, 263 (1966)

<sup>21</sup>K.G. Wilson, Phys. Rev. B **4**, 3174 (1971); Phys. Rev. B **4**, 3184 (1971).

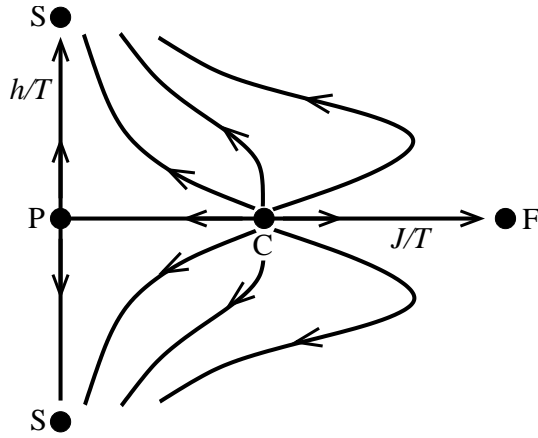


Figure 21: RG flow diagram for 2D Ising model (taken from Goldenfeld's book).

### 5.3.1 Fixed Points

We will now see what we can do with an unstable fixed point. By linearizing in the vicinity of a fixed point we will find that the eigenvalues of the RG flow give us the critical behaviour, and therefore the critical exponents, of the system near its critical point.

First we make a general statement on the correlation length at a fixed point. In general after a transformation  $\{K'_n\} = R_\lambda[\{K_n\}]$ , the correlation length will have shrunk by a factor  $\lambda$ ,

$$\xi(K') = \lambda^{-1}\xi(K), \quad (145)$$

but at the fixed point  $\{K_n^*\}$  we must have  $K'_n = K_n^*$ , so that the only solution for the correlation length is,

$$\xi(K^*) = 0 \text{ or } \infty. \quad (146)$$

For example in the 2D Ising model we have  $\xi(K^*) = 0$  for S, F, and P, but  $\xi(K^*) = \infty$  for C.

Now we expand the coupling constants near the fixed point,

$$K_n = K_n^* + \delta K_n. \quad (147)$$

Then we can write in general the RG transformation as a linear function of  $\{\delta K_n\}$ ,

$$\delta K'_n = \sum_m \left. \frac{\partial K'_n}{\partial K_m} \right|_{K=K^*} \delta K_m + \mathcal{O}(\delta K_m^2). \quad (148)$$

The linear transformation for a given  $\lambda$  is therefore defined by the matrix

$$M_{nm}^\lambda = \left. \frac{\partial K'_n}{\partial K_m} \right|_{K=K^*}. \quad (149)$$

Supposing this matrix to have eigenvectors  $\mathbf{e}_i$  with eigenvalues  $\Lambda_i$  we can write (148) as

$$\delta \mathbf{K}' = \sum_i a_i \Lambda_i^\lambda \mathbf{e}_i, \quad (150)$$

with  $a_i = \mathbf{e}_i \cdot \delta \mathbf{K}$ , and the RG transformation is determined by the eigenvalues  $\Lambda_i^\lambda$ . Note that because of the semi-group structure, we must have the general form,

$$\Lambda_i^\lambda = \lambda^{y_i}. \quad (151)$$

If the eigenvalue exponent  $y_i$  is positive, then  $a_i$  grows with  $\lambda$  and the component of  $\delta\mathbf{K}$  in the  $\mathbf{e}_i$  direction is a *relevant* perturbation. If  $y_i$  is negative, then the component in the  $\mathbf{e}_i$  direction is *irrelevant*.

### 5.3.2 Unstable fixed point, scaling laws and critical exponents

Consider a fixed point with one relevant direction, e.g. temperature. We have  $T^* = R_\lambda(T^*)$ , and linearizing,

$$R_\lambda(T^* + \delta T) = T^* + \delta T' \quad (152)$$

gives

$$\delta T' = \lambda^{y_t} \delta T. \quad (153)$$

We can also write this in terms of the reduced temperature,  $t = (T - T^*)/T^*$  to give

$$t' = \lambda^{y_t} t. \quad (154)$$

Now consider the correlation length, which should follow the rule under the RG transformation  $T' = R_\lambda(T)$ ,

$$\xi(T) = \lambda \xi(T'). \quad (155)$$

Writing this as a function of reduced temperature, and using (154) gives,

$$\xi(t) = \lambda \xi(t') = \lambda \xi(\lambda^{y_t} t). \quad (156)$$

Note that this is a *scaling law*. We want to remove the  $t$  dependence from the argument of the right-hand side. We can do this as the result is true for any  $\lambda$  (as long as  $l < \lambda l < \xi$ ), so we can choose  $\lambda$  to always take us to the same final temperature, i.e.  $t' = t_0 = \lambda^{y_t} t$ . We can then write,

$$\xi(t) = \left( \frac{t_0}{t} \right)^{\frac{1}{y_t}} \xi(t_0), \quad (157)$$

i.e., the correlation length diverges as  $\xi \sim t^{-\frac{1}{y_t}}$ . In (135) we write this exponent as  $\nu$ , so that,

$$\nu = \frac{1}{y_t}. \quad (158)$$

We can do something similar for the free energy. This should follow the rule under the RG transformation  $T' = R_\lambda(T)$ ,

$$f(T) = \lambda^{-d} f(T'). \quad (159)$$

In the same way, we then get another scaling law,

$$f(t) = \lambda^{-d} f(\lambda^{y_t} t) = \left( \frac{t_0}{t} \right)^{\frac{-d}{y_t}} f(t_0). \quad (160)$$

From this we get the singular specific heat,

$$c_s \sim t^{\frac{d}{y_t} - 2}. \quad (161)$$

The specific heat exponent is usually written as  $\alpha$ , and we can combine results (158) and (161) to find

$$\alpha = 2 - \nu d. \quad (162)$$

This is a *scaling relation* (known as the Josephson hyperscaling relation). There are several such relations relating the different exponents in a given universality class. This particular case depends on  $d$ , and is noticeably not satisfied by the mean-field exponents!

### 5.3.3 Fixed point with two unstable directions

#### Question 6

Consider a fixed point with two unstable directions  $t$  and  $h$  (e.g., C for the 2D Ising model). Write the free energy scaling law in terms of the two eigenvalue exponents  $y_t$  and  $y_h$ , and find the scaling of the magnetization  $M = \partial f / \partial h$  and the susceptibility  $\chi = \partial M / \partial h$ . Combine these results to prove the scaling relation,

$$\alpha + 2\beta + \gamma = 2. \quad (163)$$

It turns out that there are enough such scaling relations that all of the characteristic exponents can be found in terms of just the eigenvalue exponents  $y_h$  and  $y_t$ .

### 5.4 RG for Gaussian model

Although we have already solved the Gaussian model in Lectures 3 and 4, we will use it now as a concrete illustration of the RG method. There are three steps to an RG transformation:

1) Coarse-grain: In this example we will coarse-grain by integrating out the fields  $\phi_{\mathbf{q}}$  for  $\Lambda/\lambda < q < \Lambda$ .

2) Rescale: To get a system of the same form after coarse-graining, we need to push the cut-off back to  $\Lambda$ , which we do by rescaling  $\mathbf{q}' = \lambda \mathbf{q}$ .

3) Renormalize fields: we can include in the transformation a renormalization  $\phi' = \zeta \phi$ , which will give us an extra control on the form of the renormalized system.

First, consider the general problem,

$$Z = \int \prod_{0 < q < \Lambda} d\phi_{\mathbf{q}} e^{-\beta F_L[\phi]}. \quad (164)$$

In order to integrate over short-wavelength modes, we define the fields inside and outside a “momentum shell” by,

$$\phi_{<}(\mathbf{q}) = \begin{cases} \phi(\mathbf{q}), & \text{for } 0 < q < \Lambda/\lambda \\ 0, & \text{otherwise.} \end{cases} \quad (165)$$

$$\phi_{>}(\mathbf{q}) = \begin{cases} \phi(\mathbf{q}), & \text{for } \Lambda/\lambda < q < \Lambda \\ 0, & \text{otherwise.} \end{cases} \quad (166)$$

We then define coarse-graining as the partial trace over the short-wavelength modes, so that,

$$e^{-\beta F'_L[\phi_{<}]} = \int \prod_{\Lambda/\lambda < q < \Lambda} d\phi_{\mathbf{q}} e^{-\beta F_L[\phi]}. \quad (167)$$

For the Gaussian model, the different modes are uncoupled and we have,

$$e^{-\beta F'_G[\phi_{<}]} = Z_{>} \exp \left[ -\beta \int_0^{\Lambda/\lambda} \frac{d^d q}{(2\pi)^2} \frac{1}{2} (a + gq^2) |\phi_{\mathbf{q}}|^2 \right], \quad (168)$$

We now should rescale to recover the correct cut-off. If we also include a field renormalization we get the renormalized Gaussian model,

$$F'_G[\phi'] = \lambda^{-d} \int_0^{\Lambda} \frac{d^d q'}{(2\pi)^2} \frac{1}{2} (a + g\lambda^{-2} q'^2) \zeta^{-2} |\phi'_{\mathbf{q}}|^2. \quad (169)$$

That is, the coupling constants  $a$  and  $g$  flow to the new values,

$$a' = \lambda^{-d} \zeta^{-2} a \quad (170)$$

$$g' = \lambda^{-2-d} \zeta^{-2} g. \quad (171)$$

Now, the field renormalization defined by  $\zeta$  is quite general, and we are free to choose it. As we are interested in the flow of the critical parameter  $a$  under the scaling transformation, we will choose  $\zeta$  such that  $g$  remains fixed, i.e.,  $\lambda^{-2-d} \zeta^{-2} = 1$ , which leads to the RG equation for the Gaussian model,

$$a' = \lambda^2 a. \quad (172)$$

In other words, the temperature eigenvalue exponent is  $y_t = 2$ . Note that this gives the correlation length exponent  $\nu = \frac{1}{y_t} = \frac{1}{2}$ , as we have previously found for the Gaussian model. Also,  $\alpha = 2 - d\nu = (4 - d)/2$  as we have found before. We can also include a field term to the Gaussian model, as the modes remain uncoupled. It is then straightforward to find

$$h' = \lambda^{-d} \zeta h = \lambda^{\frac{2-d}{2}} h, \quad (173)$$

or  $y_h = 1 - \frac{d}{2}$ . We could use this result to find the exponents  $\beta$  and  $\delta$ , but they won't correspond to the low-temperature Gaussian approximation. The reason<sup>22</sup> is that the above is true for the quartic coupling  $b = 0$ , which is a singular limit when  $a < 0$ .

## 5.5 Including Quartic Coupling to Order $\epsilon = 4 - d$

### 5.5.1 Dimensional analysis on coupling constants

We now repeat the RG procedure as above, but now for the full Landau theory including quartic interactions. As a first estimate, we can look at the flow in the quartic coupling constant from just the rescaling and renormalization procedures (i.e., not properly integrating out the fast modes  $\phi^>$ ). From the quartic energy,

$$F_4[\phi, \Lambda/\lambda] = \frac{b}{4} \int \frac{d^d q_1}{(2\pi)^d} \frac{d^d q_2}{(2\pi)^d} \frac{d^d q_3}{(2\pi)^d} \phi_{\mathbf{q}_1} \phi_{\mathbf{q}_2} \phi_{\mathbf{q}_3} \phi_{-\mathbf{q}_1 - \mathbf{q}_2 - \mathbf{q}_3}, \quad (174)$$

we can rescale to

$$F_4[\phi', \Lambda] = \frac{b}{4} \lambda^{-3d} \int \frac{d^d q_1}{(2\pi)^d} \frac{d^d q_2}{(2\pi)^d} \frac{d^d q_3}{(2\pi)^d} \zeta^4 \phi'_{\mathbf{q}_1} \phi'_{\mathbf{q}_2} \phi'_{\mathbf{q}_3} \phi'_{-\mathbf{q}_1 - \mathbf{q}_2 - \mathbf{q}_3}. \quad (175)$$

In other words, the coupling constant  $b$  scales as,

$$b' = \zeta^4 \lambda^{-3d} b. \quad (176)$$

We fix  $\zeta$  as before so that the constant  $g$  has no flow,  $\zeta^2 = \lambda^{2+d}$ , so that,

$$b' = \lambda^{4-d} b. \quad (177)$$

This simple argument gives an eigenvalue exponent of  $y_b = 4 - d$ . In other words, the coupling constant is irrelevant for  $d > 4$ , but relevant for  $d < 4$ . This means that the Gaussian fixed point ( $b = 0$ ) only controls the phase transition above four dimensions. This is illustrated in Fig. 22.

---

<sup>22</sup>It turns out that for  $a < 0$  the coupling constant  $b$  is “dangerously irrelevant”. See Section 12.2.5 of N. Goldenfeld, *Lectures on Phase Transitions and the Renormalization Group*, (Addison-Wesley, 1992).



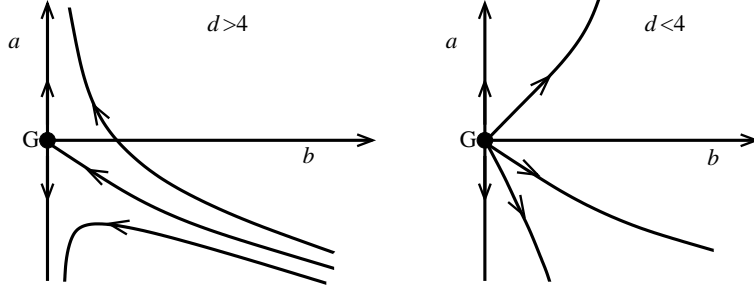


Figure 22: RG flow diagram near the Gaussian fixed point. For  $d > 4$  the flows always send  $b$  to zero, so it is an irrelevant variable (although the lack of a solution at  $a < 0$  makes  $b$  dangerously irrelevant). For  $d < 4$  the flow near the fixed point is always to greater values of  $b$ , so that the coupling constant  $b$  is relevant, and the Gaussian approximation cannot hold.

### 5.5.2 Integrating out fast modes in quartic contribution and expanding in $b$

The full RG procedure first needs to integrate out the modes in the high momentum shell with  $\Lambda/\lambda < q < \Lambda$ , as in (167). Writing  $F_L = F_G + F_4$ , we have

$$\begin{aligned} e^{-\beta F'_L[\phi_<]} &= \int \prod_{\Lambda/\lambda < q < \Lambda} d\phi_{\mathbf{q}} e^{-\beta F_G[\phi] - \beta F_4[\phi]} \\ &= e^{-\beta F'_G[\phi_<]} Z_{0>} \left\langle e^{-\beta F_4[\phi]} \right\rangle_{0>}, \end{aligned} \quad (178)$$

where  $Z_{0>}$  and  $\langle \dots \rangle_{0>}$  are averages over the fast modes  $\phi_>$  with respect to the Gaussian weight,  $e^{-\beta F'_G[\phi_>]}$ .

So as before in Section 4.2, we want to find Gaussian averages of the form  $\langle (F_4)^n \rangle_{0>}$  (after expanding the exponential), the difference being that in this case we only integrate over short-wavelength modes with  $\Lambda/\lambda < q < \Lambda$ . Therefore we will avoid the small  $q$  divergences that appeared in the perturbation series of Section 4.2, and the expansion is well-defined for small  $b$ . In order to find the first correction to the renormalization of  $b$ , we will need to go to second order in the expansion of the exponential,

$$\begin{aligned} \langle e^{-\beta F_4} \rangle_{0>} &= 1 - \beta \langle F_4 \rangle_{0>} + \frac{1}{2} \beta^2 \langle (F_4)^2 \rangle_{0>} + \mathcal{O}(F_4^3) \\ &= e^{-\beta \langle F_4 \rangle_{0>} + \frac{1}{2} \beta^2 [\langle (F_4)^2 \rangle_{0>} - \langle F_4 \rangle_{0>}^2]} + \mathcal{O}(F_4^3). \end{aligned} \quad (179)$$

Inserting this result in (178) gives to second order in  $b$ ,

$$F'_L[\phi_<] = \text{const.} + F'_G[\phi_<] + \langle F_4 \rangle_{0>} - \frac{1}{2} \beta \left[ \langle (F_4)^2 \rangle_{0>} - \langle F_4 \rangle_{0>}^2 \right]. \quad (180)$$

We will again use Wick's theorem to pair up the fields in an average of a product of fields, only this time we use the result,

$$\langle \phi_{\mathbf{q}_1} \phi_{\mathbf{q}_2} \rangle_{0>} = \begin{cases} G_0(\mathbf{q}_1) (2\pi)^d \delta^d(\mathbf{q}_1 + \mathbf{q}_2), & \text{if } \Lambda/\lambda < \{q_1, q_2\} < \Lambda, \\ \phi_{\mathbf{q}_1} \phi_{\mathbf{q}_2}, & \text{if } \{q_1, q_2\} < \Lambda/\lambda. \end{cases} \quad (181)$$

Therefore when we calculate  $\langle F_4 \rangle_{0>}$ , we must pair up the fields, but treat long- and short-wavelength modes differently. Diagrammatically, this is shown in Fig. 23, with

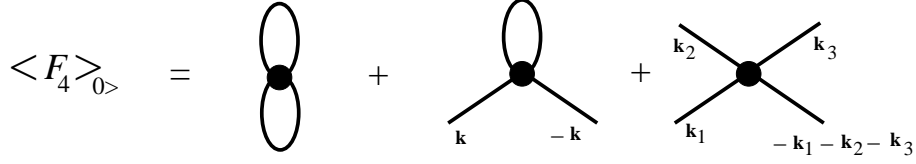


Figure 23: The diagrams that contribute to the coarse-graining average over the quartic coupling energy  $\langle F_4 \rangle_{0>}$ . The fast modes that have been integrated out are represented by the closed loops. The open legs are the fields left over with  $q < \Lambda/\lambda$ .

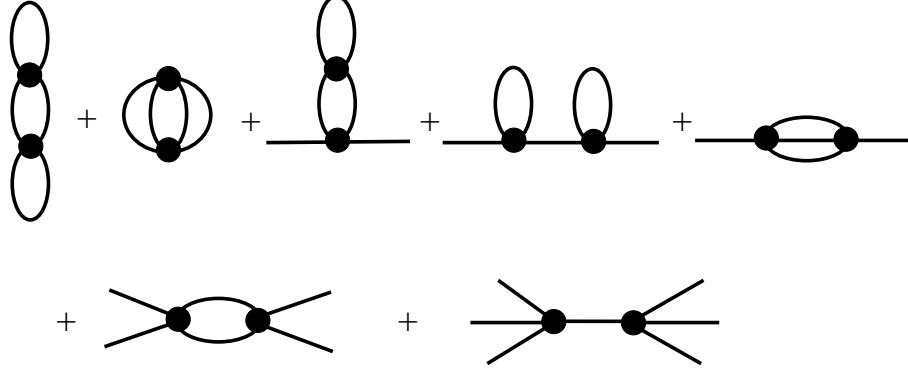


Figure 24: The diagrams that contribute to the coarse-graining average to second order in  $b$ , coming from  $[\langle (F_4)^2 \rangle_{0>} - \langle F_4 \rangle_{0>}^2]$ .

the result,

$$\begin{aligned} \langle F_4 \rangle_{0>} &= \frac{3}{4} b T^2 I_1^2 + \frac{6}{4} b T I_1 \int_{0 < q < \Lambda/\lambda} \frac{d^d q}{(2\pi)^d} \phi_{\mathbf{q}}^< \phi_{-\mathbf{q}}^< \\ &+ \frac{b}{4} \int_{0 < \{q_1, q_2, q_3, q_1+q_2+q_3\} < \Lambda/\lambda} \frac{d^d q_1}{(2\pi)^d} \frac{d^d q_2}{(2\pi)^d} \frac{d^d q_3}{(2\pi)^d} \phi_{\mathbf{q}_1}^< \phi_{\mathbf{q}_2}^< \phi_{\mathbf{q}_3}^< \phi_{-\mathbf{q}_1-\mathbf{q}_2-\mathbf{q}_3}^<, \end{aligned} \quad (182)$$

where

$$I_1 = \int_{\Lambda/\lambda < q < \Lambda} \frac{d^d q}{(2\pi)^d} \frac{1}{(a + gq^2)}. \quad (183)$$

The first term in (182) just adds a constant. The second term is of the form of the quadratic interaction, and should therefore renormalize the coupling constant  $a$ . The third term is just the unrenormalized quartic coupling for the modes with  $q < \Lambda/\lambda$ .

The diagrams that contribute to  $[\langle (F_4)^2 \rangle_{0>} - \langle F_4 \rangle_{0>}^2]$  are shown in Fig. 24. Note that there is a term which gives an interaction over six fields. We will not consider this term, as the flow of this sixth-order coupling constant should be to zero. There are also several diagrams that renormalize the quadratic interaction. However, these are corrections to order  $b^2$ , so we will ignore them to the accuracy of this calculation. Therefore the only diagram we take from Fig. 24 is the one that renormalizes the quartic interaction. We write this as,

$$[\langle (F_4)^2 \rangle_{0>} - \langle F_4 \rangle_{0>}^2] = \frac{9}{2} b^2 T^2 I_2 \int \frac{d^d q_1}{(2\pi)^d} \frac{d^d q_2}{(2\pi)^d} \frac{d^d q_3}{(2\pi)^d} \phi_{\mathbf{q}_1} \phi_{\mathbf{q}_2} \phi_{\mathbf{q}_3} \phi_{-\mathbf{q}_1-\mathbf{q}_2-\mathbf{q}_3} + \text{other terms}, \quad (184)$$

with

$$I_2 = \int_{\Lambda/\lambda < q < \Lambda} \frac{d^d q}{(2\pi)^d} \frac{1}{(a + gq^2)^2}, \quad (185)$$

and we have ignored the momentum dependence of the bubble when  $\mathbf{q}_1 + \mathbf{q}_2 \ll \Lambda$ .

### 5.5.3 Recursion relations for small $b$

From (180), (182) and (184) we get the flow equations,

$$a' = \lambda^2 [a + 3bT I_1(a, \Lambda, \lambda)], \quad (186)$$

and

$$b' = \lambda^{4-d} [b - 9b^2 T I_2(a, \Lambda, \lambda)]. \quad (187)$$

### 5.5.4 Evaluating integrals in $4 - \epsilon$ dimensions

The remaining question is how to evaluate  $I_1$  and  $I_2$  for non-integer dimensions? The answer is that we can perform the solid-angular part of the symmetric integral in integer dimension, to get a result that is a smooth function of  $d$  for non-integer values. For example,

$$I_1 = \int_{\Lambda/\lambda < q < \Lambda} \frac{d^d q}{(2\pi)^d} \frac{1}{(a + gq^2)} \quad (188)$$

$$= \frac{S_d}{(2\pi)^d} \int_{\Lambda/\lambda < q < \Lambda} dq q^{d-1} \frac{1}{(a + gq^2)}, \quad (189)$$

where  $S_d = 2\pi^{d/2}/\Gamma(d/2)$  is an analytic function of  $d$ , and the remaining radial integral can be performed for all  $d$ .

#### Question 7

Show by expanding for small  $a$  and small  $\epsilon = 4 - d$  that,

$$I_1 \frac{(2\pi)^4}{S_4} = \frac{1}{2g} \Lambda^2 \left[ 1 - \frac{1}{\lambda^2} \right] - \frac{a}{g^2} \ln \lambda + \mathcal{O}(a^2, \epsilon), \quad (190)$$

where  $S_4 = 2\pi^2$ . Similarly show that

$$I_2 \frac{(2\pi)^4}{S_4} = \frac{1}{g^2} \ln \lambda + \frac{2a}{g^2} \left[ \frac{1}{\Lambda} - \frac{\lambda}{\Lambda} \right] + \mathcal{O}(a^2, \epsilon). \quad (191)$$

[Hint: use  $\lim_{x \rightarrow 0} (\lambda^x/x) = \ln \lambda$ .]

### 5.5.5 Recursion relations for small $a$ , $b$ and $\epsilon$

We will now substitute results (190) and (191) into the flow equations (186) and (187). We will keep the terms in  $I_1$  up to order  $a$ , as this is the same order as the rest of (186). However, we only keep the first term in  $I_2$ . We discard all terms in  $\epsilon$  as these will only give higher order corrections in  $\epsilon$  to our flow equations:

$$a' = \lambda^2 \left\{ a + \frac{3}{8\pi^2} bT \left[ \frac{1}{2g} \Lambda^2 \left( 1 - \frac{1}{\lambda^2} \right) - \frac{a}{g^2} \ln \lambda \right] \right\}, \quad (192)$$

$$b' = \lambda^\epsilon \left[ b - \frac{9}{8\pi^2} b^2 T \frac{1}{g^2} \ln \lambda \right]. \quad (193)$$

To cast this in a simpler form, we make the substitutions,

$$\tilde{a} = \frac{a}{g}, \quad (194)$$

and

$$\tilde{b} = \frac{bT}{g^2}, \quad (195)$$

to give,

$$\tilde{a}' = \lambda^2 \left\{ \tilde{a} + \frac{3}{8\pi^2} \tilde{b} \left[ \frac{1}{2} \Lambda^2 \left( 1 - \frac{1}{\lambda^2} \right) - \tilde{a} \ln \lambda \right] \right\}, \quad (196)$$

$$\tilde{b}' = \lambda^\epsilon \left[ \tilde{b} - \frac{9}{8\pi^2} \tilde{b}^2 \ln \lambda \right]. \quad (197)$$

Finally, we should expand this last result for small  $\epsilon$  using  $\lambda^\epsilon = e^{\epsilon \ln \lambda} = 1 + \epsilon \ln \lambda + \mathcal{O}(\epsilon^2)$ , to give,

$$\tilde{b}' = (1 + \epsilon \ln \lambda) \left[ \tilde{b} - \frac{9}{8\pi^2} \tilde{b}^2 \ln \lambda \right]. \quad (198)$$

### 5.5.6 A new fixed point

To find the fixed points of (196) and (198) we consider an infinitesimal slice in momentum space so that  $\lambda = 1 + d\lambda$ . We then have

$$\tilde{a}' = \tilde{a} + d\lambda \left[ 2\tilde{a} + \frac{3}{8\pi^2} \tilde{b} (\Lambda^2 - \tilde{a}) \right], \quad (199)$$

$$\tilde{b}' = \tilde{b} + d\lambda \left( \tilde{b}\epsilon - \frac{9}{8\pi^2} \tilde{b}^2 \right). \quad (200)$$

The point  $\tilde{a} = 0, \tilde{b} = 0$  is just the Gaussian fixed point, which we have shown to be unstable to  $\tilde{b}$  for positive  $\epsilon$ . However, we have another fixed point for finite  $\epsilon$  as in (200) there is no flow in  $\tilde{b}$  when  $\tilde{b}\epsilon - \frac{9}{8\pi^2} \tilde{b}^2 = 0$ , or

$$\tilde{b}^* = \frac{8\pi^2}{9} \epsilon. \quad (201)$$

At this value of  $\tilde{b}^*$  the flow in  $\tilde{a}$  in (199) is zero at  $2\tilde{a} + \frac{3}{16\pi^2} \tilde{b} (\Lambda^2 - \tilde{a}) = 0$ , or to order  $\epsilon$ ,

$$\tilde{a}^* = -\frac{1}{6} \epsilon \Lambda^2. \quad (202)$$

Notice that our approximation of small  $a$  and  $b$  is therefore consistent for this fixed point within this  $\epsilon$  expansion.

The existence and position of this new fixed point below four dimensions was found by Wilson and Fisher.<sup>23</sup> Hence it is often called the Wilson-Fisher fixed point. The schematic flow for small  $a$  and  $b$  and  $d < 4$  is shown in Fig. 25. We now see that the phase transition occurs when following a path through the  $a$ - $b$  plane when the path crosses the dashed line in Fig. 25); this is when the flow changes from going to the positive  $a$  sink to the negative  $a$  sink. It should be clear that the critical exponents of this transition are now controlled by the Wilson-Fisher fixed point rather than the Gaussian fixed point.

---

<sup>23</sup>K.G. Wilson and M.E. Fisher, Phys. Rev. Lett. **28**, 240 (1972). See also historical reflections by M.E. Fisher, Rev. Mod. Phys. **70**, 653 (1998). Also note that when  $\epsilon = 0$  the two fixed points overlap, and this is the marginal case first treated by A.I. Larkin and D.E. Khmel'nitskii, Sov. Phys. JETP **29**, 1123 (1969).

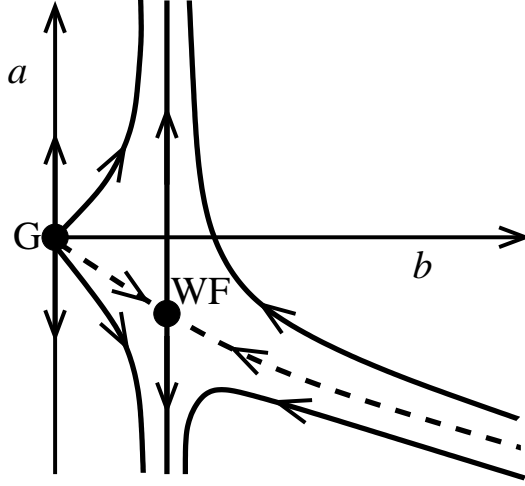


Figure 25: The RG flow diagram within the  $\epsilon$  expansion for  $d < 4$ . The dashed line represents the line of critical points where the phase transition takes place in the  $a$ - $b$  parameter space. The critical exponents are determined by the new Wilson-Fisher fixed point, rather than the unstable Gaussian fixed point.

### 5.5.7 Critical Exponents to order $\epsilon$

To find the critical exponents, we need to linearize about the Wilson-Fisher fixed point. Writing  $\tilde{a} = \tilde{a}^* + \delta\tilde{a}$  and  $\tilde{b} = \tilde{b}^* + \delta\tilde{b}$ , we easily find,

$$\delta\tilde{a}' = d\lambda \left[ \left(2 - \frac{\epsilon}{3}\right)\delta\tilde{a} + \frac{3}{8\pi^2}\Lambda^2\left(1 + \frac{\epsilon}{6}\right)\delta\tilde{b} \right], \quad (203)$$

$$\delta\tilde{b}' = d\lambda \left( -\epsilon\delta\tilde{b} \right). \quad (204)$$

Notice that the resulting transformation matrix is not symmetric (there is no requirement for it to be so). As one off-diagonal element is zero, the eigenvalues characterizing the fixed point are simply,

$$\Lambda_t = \lambda^{2 - \frac{\epsilon}{3}}, \quad (205)$$

for the direction of increasing  $a$  (or  $t$ ), and

$$\Lambda_2 = \lambda^{-\epsilon}, \quad (206)$$

in a direction which is not perpendicular to the first eigenvector. However, we have now found the important result that the eigenvalue exponent  $y_t = 2 - \frac{\epsilon}{3}$ . Notice how the difference from the value at the Gaussian fixed point increases with  $\epsilon$ . It is possible to find all of the critical exponents to first order in  $\epsilon$ . The results are simply quoted here:

$$\nu = \frac{1}{y_t} = \frac{1}{2} + \frac{\epsilon}{12}, \quad (207)$$

$$\alpha = 2 - \nu d = \frac{\epsilon}{6}, \quad (208)$$

$$\gamma = 1 + \frac{\epsilon}{6}, \quad (209)$$

$$\beta = \frac{1}{2} - \frac{\epsilon}{6}, \quad (210)$$

$$\delta = 3 + \epsilon. \quad (211)$$

While these results are only valid for small  $\epsilon = 4 - d$ , if we insert the value  $\epsilon = 1$  we do get exponents which are closer to the correct value in three dimensions (from experiments and numerical calculations) than the mean-field predictions. It is hoped that further orders in  $\epsilon$  will take the results closer to the correct values (although life is not always so straightforward...).

# Lecture Six

## 6 Vortex-Unbinding Transition in the 2D-XY Model

In this lecture we concentrate on a specific model: the XY model in two dimensions. As this model has a continuous symmetry, we know from Lecture 3 that there will only be quasi-long-range order at low temperatures. However there is still a phase transition from this state to the high-temperature state with short-range correlations, and this transition is known as the Kosterlitz-Thouless vortex-unbinding transition. We will see that a vortex is the important topological defect in the XY system, and that when free vortices proliferate due to thermal fluctuations, the system loses “spin-stiffness” and is short-range ordered. Finally we will look at the RG treatment of this phase transition, and derive a non-trivial flow diagram which gives us the critical properties near the Kosterlitz-Thouless transition. We will find this RG flow by first mapping the system of vortices to the so-called Sine-Gordon model, on which we can use a similar method of coarse-graining to that used in Lecture 5.

### 6.1 The XY model in two dimensions

Consider a lattice of fixed-length spins  $\mathbf{S}_\mathbf{r}$  constrained to rotate only in two dimensions. With nearest-neighbour interactions the classical energy of configurations is,

$$F_{\text{XY}} = -K \sum_{\langle \mathbf{r}, \mathbf{r}' \rangle} \mathbf{S}_\mathbf{r} \cdot \mathbf{S}_{\mathbf{r}'} = -K \sum_{\langle \mathbf{r}, \mathbf{r}' \rangle} \cos(\theta_\mathbf{r} - \theta_{\mathbf{r}'}), \quad (212)$$

where  $\theta_\mathbf{r}$  is the angle of the spin relative to some fixed axis. (Note that this is the same as the discrete version of a  $U(1)$  Landau theory when we are at low enough temperatures to ignore amplitude fluctuations.) It is important to state that there is no exact solution of this model in two dimensions (unlike the case for the 2D Ising model). Nevertheless, through a series of reasonable approximations, some detailed and fascinating predictions have been made.

#### 6.1.1 Spin-wave expansion at low temperatures

At small  $T/K$  there will only be small distortions between neighbouring sites, and we can expand the cosine,

$$F_{\text{XY}} = \text{const.} - \frac{K}{2} \sum_{\mathbf{r}} \sum_{\mathbf{l}} (\Delta_{\mathbf{l}} \theta_\mathbf{r})^2 + \mathcal{O}(T^2/K), \quad (213)$$

where  $\mathbf{l}$  label the neighbouring sites and,  $\Delta_{\mathbf{l}} \theta_\mathbf{r} = \theta_{\mathbf{r}+\mathbf{l}} - \theta_\mathbf{r}$ . This is now a quadratic theory, and therefore solvable. With the Fourier transform,  $\theta_\mathbf{r} = (2\pi)^{-2} \int d^2k e^{i\mathbf{k} \cdot \mathbf{r}} \theta_\mathbf{k}$  we have,

$$F_{\text{XY}} = \text{const.} + K \int \frac{d^2k}{(2\pi)^2} l^2 \sum_{\mathbf{l}} (1 - \cos \mathbf{k} \cdot \mathbf{l}) |\theta_\mathbf{k}|^2. \quad (214)$$

Taking the long-wavelength limit gives the elastic form,

$$F_{\text{SW}} = \frac{K}{2} \int \frac{d^2k}{(2\pi)^2} k^2 |\theta_\mathbf{k}|^2. \quad (215)$$

Note that we have already studied this problem in Section ?? . Using the elastic energy (83) we found the propagators (86) for different dimensions. In two dimensions this gave the result for the spin correlation function,

$$\langle \mathbf{S}_{\mathbf{r}} \cdot \mathbf{S}_{\mathbf{r}'} \rangle = \left( \frac{|\mathbf{r} - \mathbf{r}'|}{l} \right)^{-T/2\pi K}. \quad (216)$$

Therefore there is only quasi-long-range order at low temperatures. Note that the scale invariance of this correlation function implies that each value of  $T/K$  is a fixed point, and there is a *line* of fixed points at low temperatures.

### 6.1.2 High temperature expansion

We briefly review the high-temperature expansion of the XY model, to show that there is short-range order.<sup>24</sup> To take the high-temperature limit, we want to expand in powers of  $\beta$ . The XY partition function is,

$$\begin{aligned} Z_{\text{XY}} &= \int \prod_{\mathbf{r}''} d\theta_{\mathbf{r}''} e^{\beta K \sum_{\langle \mathbf{r}, \mathbf{r}' \rangle} \cos(\theta_{\mathbf{r}} - \theta_{\mathbf{r}'})} \\ &= \int \prod_{\mathbf{r}''} d\theta_{\mathbf{r}''} \prod_{\langle \mathbf{r}, \mathbf{r}' \rangle} e^{\beta K \cos(\theta_{\mathbf{r}} - \theta_{\mathbf{r}'})}. \end{aligned} \quad (217)$$

The function  $e^{\beta K \cos x}$  is a periodic, even function of  $x$ , and can be written in a Fourier series. It is straightforward to show that,

$$e^{\beta K \cos x} = \sum_{n=0}^{\infty} I_n(\beta K) e^{inx}, \quad (218)$$

where  $I_n(x)$  is a modified Bessel function with the series expansion,

$$I_n(x) = \sum_{k=0}^{\infty} \frac{1}{k!(n+k)!} \left( \frac{x}{2} \right)^{n+2k}. \quad (219)$$

If we only keep the lowest order term in  $\beta K$  for each Bessel function, we find the high-temperature limit of the partition function,

$$\lim_{\beta K \rightarrow 0} Z_{\text{XY}} = \int \prod_{\mathbf{r}''} d\theta_{\mathbf{r}''} \prod_{\langle \mathbf{r}, \mathbf{r}' \rangle} \left[ 1 + \sum_{n_{\mathbf{r}, \mathbf{r}'}=1}^{\infty} \frac{1}{n_{\mathbf{r}, \mathbf{r}'}!} \left( \frac{\beta K}{2} \right)^{n_{\mathbf{r}, \mathbf{r}'}} e^{in_{\mathbf{r}, \mathbf{r}'}(\theta_{\mathbf{r}} - \theta_{\mathbf{r}'})} \right] \quad (220)$$

Performing the integrals over  $\theta_{\mathbf{r}''}$  will only get non-zero results for configurations satisfying  $\nabla \cdot \mathbf{n} \equiv \sum_{\mathbf{l}} n_{\mathbf{r}, \mathbf{r}+\mathbf{l}} = 0$ . The partition function is then a constrained sum over possible configurations of the integers  $n_{\mathbf{r}, \mathbf{r}'}$  defined on each bond between neighbours,

$$Z_{\text{XY}} = \text{Tr}_{\mathbf{n}} \prod_{\langle \mathbf{r}, \mathbf{r}' \rangle} \frac{1}{n_{\mathbf{r}, \mathbf{r}'!}} \left( \frac{\beta K}{2} \right)^{n_{\mathbf{r}, \mathbf{r}'}}. \quad (221)$$

In the same way we can calculate the correlation function,

$$\langle \mathbf{S}_{\mathbf{r}_1} \cdot \mathbf{S}_{\mathbf{r}_2} \rangle = \left\langle e^{i(\theta_{\mathbf{r}_1} - \theta_{\mathbf{r}_2})} \right\rangle = \frac{1}{Z_{\text{XY}}} \text{Tr}'_{\mathbf{n}} \prod_{\langle \mathbf{r}, \mathbf{r}' \rangle} \frac{1}{n_{\mathbf{r}, \mathbf{r}'!}} \left( \frac{\beta K}{2} \right)^{n_{\mathbf{r}, \mathbf{r}'}}. \quad (222)$$

---

<sup>24</sup>See section 4.2.1 of C. Itzykson and J.-M. Drouffe, *Statistical Field Theory*, Vol. 1 (Cambridge University Press, 1989).



where the trace  $\text{Tr}'$  is over configurations satisfying  $\nabla \cdot \mathbf{n} = \delta_{\mathbf{r}, \mathbf{r}_1} - \delta_{\mathbf{r}, \mathbf{r}_2}$ . The main contribution (lowest order in  $\beta$ ) comes from the links on the shortest path between the two points  $\mathbf{r}_1$  and  $\mathbf{r}_2$  having  $n = 1$  with all other links zero. This gives,

$$\langle \mathbf{S}_{\mathbf{r}_1} \cdot \mathbf{S}_{\mathbf{r}_2} \rangle = \prod_{\langle \mathbf{r}, \mathbf{r}' \rangle} \left( \frac{\beta K}{2} \right) = \left( \frac{\beta K}{2} \right)^{|\mathbf{r}_1 - \mathbf{r}_2|/l} = e^{-|\mathbf{r}_1 - \mathbf{r}_2|/\xi}. \quad (223)$$

Therefore we have an exponential decay in the correlation function, with  $\xi = l/\ln(2T/K)$ .

The different functional forms of the correlation functions at high and low temperatures implies that there must be a phase transition between the two behaviours, as was first pointed out by Berezinskii,<sup>25</sup> who also showed that the low temperature phase has an infinite magnetic susceptibility and a rigidity to long-wavelength spin distortions (spin-stiffness).

### 6.1.3 Separation of longitudinal and transverse fluctuations (spin-waves and vortices)

Consider the change in spin-angle as we follow a path  $C$ ,

$$\Delta\theta = \sum_{\langle \mathbf{r}, \mathbf{r}' \rangle}^C (\theta_{\mathbf{r}} - \theta_{\mathbf{r}'}) \approx \int_C d\mathbf{r} \cdot \nabla \theta_{\mathbf{r}}. \quad (224)$$

If  $C$  is a closed path, then the change in angle must be a multiple of  $2\pi$ ,

$$\oint_C d\mathbf{r} \cdot \nabla \theta_{\mathbf{r}} = 2n_c\pi. \quad (225)$$

Note that the fact that this result must be unchanged for small deformations in the path  $C$ , together with Stokes' theorem tells us that (except for isolated points),

$$\nabla \times \nabla \theta_{\mathbf{r}} = 0. \quad (226)$$

Within this continuum limit, this means that a non-zero result for (225) can only be obtained from singular points, which define the “core” of a topological defect, the vortex. Therefore we should generalize (226) to include singularities of strength  $n_i$  located at points  $\mathbf{r}_i$ , so that

$$\nabla \times \nabla \theta_{\mathbf{r}} = 2\pi \hat{\mathbf{z}} \sum_i n_i \delta^2(\mathbf{r} - \mathbf{r}_i) \equiv 2\pi \mathbf{n}(\mathbf{r}). \quad (227)$$

This defines the vortex density  $\mathbf{n}(\mathbf{r})$ .

In the continuum limit, the energy of the system only depends on the spatially varying gradient of phase,  $\nabla \theta_{\mathbf{r}}$ . By a quantum-mechanical analogy, this gradient looks a bit like a velocity, so we write  $\mathbf{v}_{\mathbf{r}} \equiv \nabla \theta_{\mathbf{r}}$ . It will be useful to write this velocity as a sum of “longitudinal” and “transverse” parts,  $\mathbf{v}_{\mathbf{r}} = \mathbf{v}_{\mathbf{r}}^l + \mathbf{v}_{\mathbf{r}}^t$  defined by,

$$\begin{aligned} \nabla \times \mathbf{v}_{\mathbf{r}}^l &= 0, \\ \nabla \cdot \mathbf{v}_{\mathbf{r}}^t &= 0. \end{aligned} \quad (228)$$

Note that this means that there are no vortex contributions to the longitudinal part, while the transverse part is entirely determined by the positions of the vortex cores,

$$\mathbf{v}_{\mathbf{r}}^t = 2\pi \int d^d r' G_L(\mathbf{r} - \mathbf{r}') \nabla \times \mathbf{n}(\mathbf{r}'), \quad (229)$$

---

<sup>25</sup>V.L. Berezinskii, Sov. Phys. JETP **32**, 493 (1971); Sov. Phys. JETP **34**, 610 (1971).

where  $G_L(\mathbf{r} - \mathbf{r}')$  is the Green's function for the Laplacian operator  $-\nabla^2$ .

In the low  $T$  regime where we have expanded the cosine, we can then separate the contributions of transverse and longitudinal parts to the energy  $F_{XY} = F_{XY}^l + F_{XY}^t$ . We then get a “spin-wave” contribution,

$$F_{XY}^l = \int d^2r \frac{K}{2} |\mathbf{v}_r^l|^2 = \int d^2r \frac{K}{2} |\nabla \theta_r^l|^2, \quad (230)$$

and a “vortex” contribution,

$$F_{XY}^t = \frac{(2\pi)^2 K}{2} \int d^2r \int d^2r' G_L(\mathbf{r} - \mathbf{r}') \mathbf{n}(\mathbf{r}) \cdot \mathbf{n}(\mathbf{r}'). \quad (231)$$

This contribution is sometimes called the “Coulomb gas” because of the form of the pairwise interactions.

Our general approach then will be to treat separately the spin-wave part from the Coulomb gas (this is only a good approximation at low temperatures). Therefore the XY model reduces to the problem of solving for the Coulomb gas. We will rephrase the Coulomb gas in a discrete form, with a general configuration given by the number  $n_r$  of charges at the site  $\mathbf{r}$ , so that the partition function is

$$Z_{CG} = \prod_{\mathbf{r}} \sum_{n_r=-\infty}^{\infty} e^{-\beta F_{CG}[n_r]}, \quad (232)$$

with the configuration energy,

$$F_{CG}[n_r] = \frac{(2\pi)^2 K}{2} \sum_{\mathbf{r}} \sum_{\mathbf{r}'} n_r n_{r'} G_L(\mathbf{r} - \mathbf{r}') + \sum_{\mathbf{r}} \varepsilon_c n_r^2 \quad (233)$$

where we have included the core correction to the energy of each vortex  $\varepsilon_c$ , due to details in the lattice not captured by the continuum approximation.

#### 6.1.4 Spin-stiffness and vortex density

The spin-stiffness of the system can be defined by the response to a force that tries to impose a relative twist of the spins at the boundary of the system. We can define a force  $\mathbf{f}$  by including a linear energy gain for the spin twist,  $-f\Delta\theta$ , with a relative twist,

$$\Delta\theta \equiv \langle (\theta_L - \theta_0) \rangle = \int_0^L dx \langle \partial_x \theta_x \rangle. \quad (234)$$

The spin stiffness  $K_{\text{eff}}$  is then defined by,

$$\Delta\theta = \frac{f}{K_{\text{eff}}}. \quad (235)$$

Also note that the energy change in the presence of the force will be

$$\Delta F = \frac{f^2}{2K_{\text{eff}}}. \quad (236)$$

For an elastic (or harmonic) theory such as (215) for the spin-wave part, the response is easily derived to find a temperature independent spin stiffness  $K$ . However, the XY model also has higher-order (anharmonic) terms, which for our purposes are

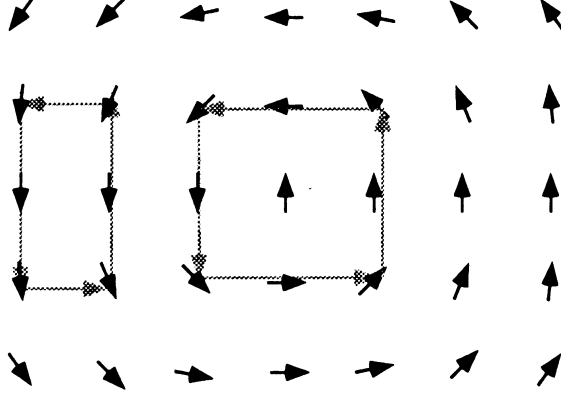


Figure 26: An example spin-configuration in a vortex in the XY model. Notice the change in angle by  $2\pi$  for a path that encloses the vortex core.

captured in the transverse (vortex) modes (233). By treating longitudinal and transverse modes separately, it is straightforward to derive the free energy change in the presence of a twisting force,

$$F(\mathbf{f}) = F(0) + \frac{f^2}{2K} + \frac{f^2}{2TL^2} \int d^2r_1 \int d^2r_2 \langle \mathbf{v}_{\mathbf{r}_1}^t \cdot \mathbf{v}_{\mathbf{r}_2}^t \rangle + \mathcal{O}(f^4) \quad (237)$$

$$= F(0) + \frac{f^2}{2K} + \frac{2\pi^2 f^2}{T} \int d^2r r^2 \langle \mathbf{n}(\mathbf{r}) \cdot \mathbf{n}(\mathbf{0}) \rangle + \mathcal{O}(f^4), \quad (238)$$

where the last line uses the vortex density  $\mathbf{n}(\mathbf{r}) = (2\pi)^{-1} \nabla \times \mathbf{v}_{\mathbf{r}}^t$ . Therefore the effective stiffness must be given by,

$$\frac{1}{K_{\text{eff}}} = \frac{1}{K} + \frac{4\pi^2}{T} \int d^2r r^2 \langle \mathbf{n}(\mathbf{r}) \cdot \mathbf{n}(\mathbf{0}) \rangle. \quad (239)$$

It turns out that the integral of the vortex-density correlation function is negative (due to vortex-dipole correlations) so that the net effect of a finite density of vortex-anti-vortex pairs is to reduce the effective spin-stiffness. One can also show that the same  $K_{\text{eff}}$  appears in the exponent for the correlation function when we include the transverse modes.

### 6.1.5 Structure and energy of a vortex

We now look at the vortex solution in more detail. For example, consider a vortex centred at the origin. The phase-field will be the solution to,

$$\nabla \times \nabla \theta_{\mathbf{r}} = 2\pi \delta^2(r), \quad (240)$$

which has the solution

$$\theta_{\mathbf{r}}^1 = \tan^{-1}(y/x), \quad (241)$$

with a “velocity” of,

$$\mathbf{v}_{\mathbf{r}}^1 = \nabla \theta_{\mathbf{r}}^1 = \frac{\hat{\mathbf{z}} \times \hat{\mathbf{r}}}{r}. \quad (242)$$

An example is shown in Fig. 26. The energy of such a configuration is given by,

$$F_{\text{XY}}^v = \frac{K}{2} \int d^2r |\nabla \theta_{\mathbf{r}}^1|^2 = \frac{K}{2} \int d^2r \frac{1}{r^2} = \pi K \ln(L/l), \quad (243)$$

where we must include the cut-offs in the limits of the integral as the system size,  $L$ , and the lattice length  $l$ . Notice that a vortex costs an infinite energy in an infinitely big system.

For more than one vortex, we just add the solutions to (240) for different source terms. This leads to the pairwise dependence of the energy given above in (233). As an example consider a pair of oppositely charged vortices each with a strength  $n$ . Writing  $\mathbf{v}_\mathbf{r} = \mathbf{v}_{\mathbf{r}-\mathbf{r}_1}^1 - \mathbf{v}_{\mathbf{r}-\mathbf{r}_2}^1$  and using (242) gives the energy of the pair,

$$\begin{aligned} F_{\text{XY}}^{\text{pair}}(\mathbf{r} - \mathbf{r}_2) &= \frac{n^2 K}{2} \int d^2 r \left| \frac{\mathbf{r} - \mathbf{r}_1}{|\mathbf{r} - \mathbf{r}_1|^2} - \frac{\mathbf{r} - \mathbf{r}_2}{|\mathbf{r} - \mathbf{r}_2|^2} \right|^2 \\ &= \frac{n^2 K}{2} \int \frac{d^2 k}{(2\pi)^2} \frac{|e^{i\mathbf{k}\cdot\mathbf{r}_1} - e^{i\mathbf{k}\cdot\mathbf{r}_2}|^2}{k^2} \\ &= 2\pi n^2 K \ln(|\mathbf{r} - \mathbf{r}_2|/l). \end{aligned} \quad (244)$$

So we see that oppositely charged vortices attract, and that a pair only costs a finite energy (the diverging energy from currents at far distances has cancelled). This result agrees with the general form of (233), when we take the continuum limit  $G_L(r) = (2\pi)^{-1} \ln(r/L)$ .

### 6.1.6 Single-vortex derivation of Kosterlitz-Thouless transition

Naively, we might suggest that because a vortex costs an infinite energy to put into an infinite system, there will never be a finite density of these objects from thermal fluctuations. However, this is seen not to be the case when we consider the *free energy* change to add a vortex.<sup>26</sup> Assuming that the entropy of a vortex is just the logarithm of the number of places we can put it, we get

$$S_v = k_B \ln[(L/l)^2], \quad (245)$$

and

$$F_v = (\pi K - 2k_B T) \ln(L/l). \quad (246)$$

Therefore we can reduce the free energy by adding a vortex to a vortex-free system as long as the temperature is above,

$$T_{\text{KT}} = \frac{\pi}{2} K. \quad (247)$$

Although the real system becomes much more complicated when we need to consider more than one vortex, this argument certainly shows that there is an instability towards vortex proliferation at this “Kosterlitz-Thouless” temperature.

The fuller picture that has emerged of this Kosterlitz-Thouless transition is one where at low temperatures there is a small but finite density of bound vortex-pairs, which may renormalize the spin-stiffness, but do not destroy the quasi-long-range order. Above the transition however, each vortex is essentially “free”, so that its wanderings lead to violent phase fluctuations that kill the algebraic order and reduce it to a short-range order with correlation length of order the average spacing of the vortices.

A detailed derivation of the transition was given by Kosterlitz,<sup>27</sup> who used a real-space RG scaling in the low temperature phase to integrate out small length scales.

<sup>26</sup>This argument is due to J.M. Kosterlitz and D.J. Thouless, J. Phys. C **6**, 1181 (1973).

<sup>27</sup>J.M. Kosterlitz, J. Phys. C **7**, 1046 (1974).

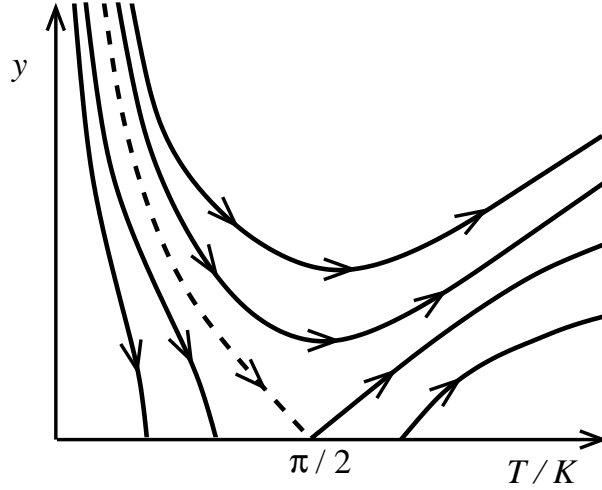


Figure 27: Schematic RG flow diagram for the XY model, for the parameters  $y = e^{-\varepsilon_c/T}$  and  $T/K$ . Note that  $y = 0$  is a line of fixed points, which are stable for  $T < \pi K/2$ . The dashed line marks the actual phase boundary between a low-temperature phase with no vortices and a high-temperature phase with free vortices.

The effect of the coarse-graining is to renormalize the core energy of a vortex. In the low temperature phase, this core-energy flows to infinity, and the effective coarse-grained system has no vortices. Above the transition, however, the core energy flows to zero, which implies a rush of vortices and a breakdown of the ordered phase. Rather than following the Kosterlitz procedure, we will derive the same RG flow diagram in the next section by mapping the vortex problem to a different model, where a momentum-space RG method can be used. For now we just look at the resulting schematic RG flow diagram for parameters  $T/K$  versus  $y \equiv e^{-\varepsilon_c/T}$  in Fig. 27. Note how the line  $y = 0$ , corresponding to no vortices, is a line of fixed points. Below the temperature  $T = \pi K/2$  these fixed points are stable to small values of  $y$ , whereas above this temperature the fixed points are unstable. For non-zero  $y$ , the flow is always to larger temperatures. Note the critical line that flows to the point  $(y = 0, T = \pi K/2)$ . This marks the actual phase transition: as the real system parameters cross through this line in the  $(y, T)$  plane, the behaviour swaps from the low-temperature phase with no vortices to the high temperature phase with vortices.

## 6.2 The Sine-Gordon model in two dimensions

Starting from the partition function for the Coulomb gas of (232), we will find that in a certain limit it is equivalent to the partition function for the so-called Sine-Gordon model, defined by the energy functional,

$$\beta F_{\text{SG}}[\phi] = \int d^2r \left[ \frac{g}{2} |\partial_{\mathbf{r}} \phi|^2 - J \cos \phi_{\mathbf{r}} \right]. \quad (248)$$

### 6.2.1 Duality transformation from Coulomb gas to Sine-Gordon

We first rewrite the interaction part of the Coulomb gas energy (233) in Fourier space,

$$e^{-\frac{1}{2}(2\pi)^2 \beta K \sum_{\mathbf{r}, \mathbf{r}'} n_{\mathbf{r}} n_{\mathbf{r}'} G_L(\mathbf{r} - \mathbf{r}')} = e^{-\frac{1}{2}(2\pi)^2 \beta K \frac{1}{L^{2/d}} \sum_{\mathbf{k}} |n_{\mathbf{k}}|^2 G_L(\mathbf{k})}, \quad (249)$$

with  $G_L(\mathbf{k}) = l^2 / \sum_{\mathbf{l}} (1 - \cos \mathbf{k} \cdot \mathbf{l})$ . Then we introduce an auxiliary phase,

$$e^{-\frac{1}{2}(2\pi)^2 \beta K \frac{1}{L^2 l^4} |n_{\mathbf{k}}|^2 G_L(\mathbf{k})} = A_{\mathbf{k}} \int_{-\infty}^{\infty} d\phi e^{\frac{1}{L^2} \left( -\frac{1}{2} \frac{|\phi|^2}{(2\pi)^2 \beta K G_L(\mathbf{k})} + i \frac{1}{l^2} \phi n_{\mathbf{k}} \right)}. \quad (250)$$

Doing this for each  $\mathbf{k}$  vector, and then transforming back to real space gives the identity for the partition function of (232),

$$Z_{CG} = A' \left( \prod_{\mathbf{r}'} \sum_{n_{\mathbf{r}'}=-\infty}^{\infty} \right) \left( \int_{-\infty}^{\infty} \prod_{\mathbf{r}''} d\phi_{\mathbf{r}''} \right) e^{-\frac{1}{2} \frac{1}{(2\pi)^2 \beta K} \sum_{\mathbf{r}, \mathbf{l}} (\Delta_{\mathbf{l}} \phi_{\mathbf{r}})^2 + \sum_{\mathbf{r}} \phi_{\mathbf{r}} n_{\mathbf{r}} - \beta \varepsilon_c \sum_{\mathbf{r}} n_{\mathbf{r}}^2}. \quad (251)$$

The Kosterlitz RG results were obtained in the limit of very large core energy. Therefore we will consider the same limit, the effect of which is first to restrict the allowed values of  $n_{\mathbf{r}}$  to be only  $[0, \pm 1]$ . (the density of sites with  $|n_{\mathbf{r}}| = 2$  will be a factor of  $\exp(-\beta \varepsilon_c)$  smaller). This allows us to complete the trace over  $n_{\mathbf{r}}$  in (251),

$$\sum_{n=-1}^1 e^{i\phi n - \beta \varepsilon_c n^2} = 1 + 2e^{-\beta \varepsilon_c} \cos \phi. \quad (252)$$

We will label the exponentially small factor as  $e^{-\beta \varepsilon_c} \equiv y$  (this is known as the fugacity), and after reexponentiating we have,

$$\sum_n e^{i\phi n - \beta \varepsilon_c n^2} = e^{2y \cos \phi} + \mathcal{O}(y^2). \quad (253)$$

Including this result in (251) gives the partition function as a trace over the auxiliary phase only,

$$Z_{CG} = A' \int_{-\infty}^{\infty} \prod_{\mathbf{r}''} d\phi_{\mathbf{r}''} e^{-\frac{1}{2} \frac{1}{(2\pi)^2 \beta K} \sum_{\mathbf{r}, \mathbf{l}} (\Delta_{\mathbf{l}} \phi_{\mathbf{r}})^2 + \sum_{\mathbf{r}} 2y \cos \phi_{\mathbf{r}}}. \quad (254)$$

This is just the form of the partition function for the discrete version of the Sine-Gordon model (248). In fact, we can write the relationship between the Coulomb gas defined by  $Z_{CG}(\beta K, \beta \varepsilon_c)$  and the Sine-Gordon model  $Z_{SG}(g, J)$  as,

$$Z_{CG}(\beta K, \beta \varepsilon_c) = A' Z_{SG}\left(\frac{1}{(2\pi)^2 \beta K}, \frac{2}{l^2} e^{-\beta \varepsilon_c}\right) \quad (255)$$

This is known as a duality transformation, where every point in the low-temperature phase of the Coulomb gas maps to a point in the high-temperature phase in the Sine-Gordon model, and vice-versa.

Our knowledge that there is a phase-transition in the 2D-XY model tells us that there must be a phase transition in the 2D-Sine-Gordon model. However, in the second case the high-temperature phase must be the one with algebraic correlations and quasi-long-range order. This is clearly true for the model (248) if  $J$  can be ignored. So at high temperatures, thermal fluctuations in the Sine-Gordon model drive the effective  $J$  to zero (just as the fugacity  $e^{-\beta \varepsilon_c}$  flows to zero in the low-temperature Coulomb gas). Similarly, at low temperatures we expect a finite correlation length in the Sine-Gordon model, which in this case is in an ordered phase, with  $J$  remaining “relevant” (this corresponds to a relevant fugacity, or small effective vortex-core energy in the high temperature phase of the Coulomb gas). We will now substitute this hand-waving discussion for an RG calculation of the Sine-Gordon model.

### 6.2.2 Momentum-space RG for Sine-Gordon model

First we note that the continuum action (248) should be defined only down to a small-length cut-off  $l = 2\pi\Lambda^{-1}$ . We will coarse-grain in the same way as in Lecture 5, by separating a shell of small-wavelength modes out of the Fourier transform, i.e.  $\phi_{\mathbf{r}} = \phi_{\mathbf{r}}^< + \phi_{\mathbf{r}}^>$ , with,

$$\begin{aligned}\phi_{\mathbf{r}}^< &= \int_{0 < q < \Lambda/\lambda} \frac{d^2 q}{(2\pi)^2} e^{i\mathbf{q}\cdot\mathbf{r}} \phi_{\mathbf{q}}, \\ \phi_{\mathbf{r}}^> &= \int_{\Lambda/\lambda < q < \Lambda} \frac{d^2 q}{(2\pi)^2} e^{i\mathbf{q}\cdot\mathbf{r}} \phi_{\mathbf{q}}.\end{aligned}\tag{256}$$

Then we can write the Sine-Gordon action as a functional of the fast and slow modes,

$$\beta F_{\text{SG}}[\phi^<, \phi^>] = \int d^2 r \left[ \frac{g}{2} |\partial_{\mathbf{r}} \phi^<|^2 + \frac{g}{2} |\partial_{\mathbf{r}} \phi^>|^2 - J \cos(\phi_{\mathbf{r}}^< + \phi_{\mathbf{r}}^>) \right]. \tag{257}$$

To coarse-grain, we take a partial trace over the fast modes to leave an effective action of the slow modes,

$$\begin{aligned}e^{-\beta F'_{\text{SG}}[\phi^<]} &= \int \prod_{\Lambda/\lambda < q < \Lambda} d\phi_{\mathbf{q}}^> e^{-\beta F_{\text{SG}}[\phi^<, \phi^>]} \\ &= e^{-\int d^2 r \frac{g}{2} |\partial_{\mathbf{r}} \phi^<|^2} \int \prod_{\Lambda/\lambda < q < \Lambda} d\phi_{\mathbf{q}}^> e^{-\int d^2 r \frac{g}{2} |\partial_{\mathbf{r}} \phi^>|^2 - J \cos(\phi_{\mathbf{r}}^< + \phi_{\mathbf{r}}^>)} \\ &= e^{-\int d^2 r \frac{g}{2} |\partial_{\mathbf{r}} \phi^<|^2} Z_{>} \left\langle e^{\int d^2 r J \cos(\phi_{\mathbf{r}}^< + \phi_{\mathbf{r}}^>)} \right\rangle_{>},\end{aligned}\tag{258}$$

where  $Z_{>}$  and  $\langle \dots \rangle_{>}$  are averages over the fast modes with respect to the Gaussian weight  $\exp(-\int d^2 r \frac{g}{2} |\partial_{\mathbf{r}} \phi^>|^2)$ . We have written it in this form so as to be able to attempt the Gaussian averages.

### 6.2.3 Important averages over the fast modes

As we are interested in the small  $J$  limit, we will expand the average in (258) to get,

$$\begin{aligned}\left\langle e^{\int d^2 r J \cos(\phi_{\mathbf{r}}^< + \phi_{\mathbf{r}}^>)} \right\rangle_{>} &= 1 + J \int d^2 r \langle \cos(\phi_{\mathbf{r}}^< + \phi_{\mathbf{r}}^>) \rangle_{>} \\ &\quad + \frac{J^2}{2} \int d^2 r_1 \int d^2 r_2 \langle \cos(\phi_{\mathbf{r}_1}^< + \phi_{\mathbf{r}_1}^>) \cos(\phi_{\mathbf{r}_2}^< + \phi_{\mathbf{r}_2}^>) \rangle_{>} + \mathcal{O}(J^3) \\ &= e^{J \int d^2 r \langle \cos(\phi_{\mathbf{r}}^< + \phi_{\mathbf{r}}^>) \rangle_{>}} + \frac{J^2}{2} \int d^2 r_1 \int d^2 r_2 \left[ \langle \cos(\phi_{\mathbf{r}_1}^< + \phi_{\mathbf{r}_1}^>) \cos(\phi_{\mathbf{r}_2}^< + \phi_{\mathbf{r}_2}^>) \rangle_{>} - \langle \cos(\phi_{\mathbf{r}_1}^< + \phi_{\mathbf{r}_1}^>) \rangle_{>} \langle \cos(\phi_{\mathbf{r}_2}^< + \phi_{\mathbf{r}_2}^>) \rangle_{>} \right].\end{aligned}\tag{259}$$

We therefore need the cosine average,

$$\begin{aligned}\langle \cos(\phi_{\mathbf{r}}^< + \phi_{\mathbf{r}}^>) \rangle_{>} &= \frac{1}{2} e^{i\phi_{\mathbf{r}}^<} \langle e^{i\phi_{\mathbf{r}}^>} \rangle_{>} + \frac{1}{2} e^{-i\phi_{\mathbf{r}}^<} \langle e^{-i\phi_{\mathbf{r}}^>} \rangle_{>} \\ &= e^{-\frac{1}{2}g >^{(0)}} \cos \phi_{\mathbf{r}}^<,\end{aligned}\tag{260}$$

where we defined the “fast” propagator,

$$g_{>}(\mathbf{r}) = \int_{0 < q < \Lambda/\lambda} \frac{d^2 q}{(2\pi)^2} \frac{e^{i\mathbf{q}\cdot\mathbf{r}}}{g q^2}.\tag{261}$$

We also need the double cosine average,

$$\begin{aligned}
\left\langle \cos(\phi_{\mathbf{r}_1}^< + \phi_{\mathbf{r}_1}^>) \cos(\phi_{\mathbf{r}_2}^< + \phi_{\mathbf{r}_2}^>) \right\rangle_{>} &= \frac{1}{4} \left\{ e^{i(\phi_{\mathbf{r}_1}^< + \phi_{\mathbf{r}_2}^<)} \langle e^{i(\phi_{\mathbf{r}_1}^> + \phi_{\mathbf{r}_2}^>)} \rangle_{>} + e^{-i(\phi_{\mathbf{r}_1}^< + \phi_{\mathbf{r}_2}^<)} \langle e^{-i(\phi_{\mathbf{r}_1}^> + \phi_{\mathbf{r}_2}^>)} \rangle_{>} + \right. \\
&\quad \left. + e^{i(\phi_{\mathbf{r}_1}^< - \phi_{\mathbf{r}_2}^<)} \langle e^{i(\phi_{\mathbf{r}_1}^> - \phi_{\mathbf{r}_2}^>)} \rangle_{>} + e^{-i(\phi_{\mathbf{r}_1}^< - \phi_{\mathbf{r}_2}^<)} \langle e^{-i(\phi_{\mathbf{r}_1}^> - \phi_{\mathbf{r}_2}^>)} \rangle_{>} \right\} \\
&= \frac{1}{2} \left[ e^{-[g_{>}(0) + g_{>}(\mathbf{r}_1 - \mathbf{r}_2)]} \cos(\phi_{\mathbf{r}_1}^< + \phi_{\mathbf{r}_2}^<) \right. \\
&\quad \left. + e^{-[g_{>}(0) - g_{>}(\mathbf{r}_1 - \mathbf{r}_2)]} \cos(\phi_{\mathbf{r}_1}^< - \phi_{\mathbf{r}_2}^<) \right]. \tag{262}
\end{aligned}$$

Including these results in the expansion (259) gives,

$$\begin{aligned}
\ln \left[ \left\langle e^{\int d^2 r J \cos(\phi_{\mathbf{r}}^< + \phi_{\mathbf{r}}^>)} \right\rangle_{>} \right] &= J \int d^2 r e^{-\frac{1}{2} g_{>}(0)} \cos \phi_{\mathbf{r}}^< \\
&\quad + \frac{J^2}{4} \int d^2 r_1 \int d^2 r_2 \left\{ e^{-g_{>}(0)} \left[ e^{-g_{>}(\mathbf{r}_1 - \mathbf{r}_2)} - 1 \right] \cos(\phi_{\mathbf{r}_1}^< + \phi_{\mathbf{r}_2}^<) \right. \\
&\quad \left. + e^{-g_{>}(0)} \left[ e^{g_{>}(\mathbf{r}_1 - \mathbf{r}_2)} - 1 \right] \cos(\phi_{\mathbf{r}_1}^< - \phi_{\mathbf{r}_2}^<) \right\}. \tag{263}
\end{aligned}$$

At first sight, the double integral that appears to second order in  $J$  does not look like it can lead to a renormalized action of the form of (248). However, we note that the function  $g_{>}(r)$  should become very small as  $r$  gets larger than the new cut-off scale, as only Fourier modes with  $q > \Lambda/\lambda$  have any weight in the definition (261). Therefore the combination  $[e^{\pm g_{>}(\mathbf{r}_1 - \mathbf{r}_2)} - 1]$  is small everywhere but  $|\mathbf{r}_1 - \mathbf{r}_2| \sim \lambda/\Lambda$ , and we can expand it in the difference of  $\mathbf{r}_1$  and  $\mathbf{r}_2$ . We do this using the transformations

$$\begin{aligned}
\mathbf{u} &= \frac{1}{2}(\mathbf{r}_1 + \mathbf{r}_2) \\
\mathbf{v} &= (\mathbf{r}_1 - \mathbf{r}_2). \tag{264}
\end{aligned}$$

Then for small  $v$  we write,

$$\begin{aligned}
\phi_{\mathbf{r}_1}^< + \phi_{\mathbf{r}_2}^< &\approx 2\phi_{\mathbf{u}}^< \\
\phi_{\mathbf{r}_1}^< - \phi_{\mathbf{r}_2}^< &\approx \mathbf{v} \cdot \partial_{\mathbf{u}} \phi_{\mathbf{u}}^<. \tag{265}
\end{aligned}$$

We can then approximate (263) as,

$$\begin{aligned}
\ln \left[ \left\langle e^{\int d^2 r J \cos(\phi_{\mathbf{r}}^< + \phi_{\mathbf{r}}^>)} \right\rangle_{>} \right] &= J \int d^2 r e^{-\frac{1}{2} g_{>}(0)} \cos \phi_{\mathbf{r}}^< \\
&\quad + \frac{J^2}{2} \int d^2 r \left\{ I_1 \cos(2\phi_{\mathbf{r}}^<) + I_2 |\partial_{\mathbf{r}} \phi_{\mathbf{r}}^<|^2 + \text{const.} \right\}, \tag{266}
\end{aligned}$$

with

$$\begin{aligned}
I_1 &= \frac{1}{2} e^{-g_{>}(0)} \int d^2 v \left[ e^{-g_{>}(\mathbf{v})} - 1 \right], \\
I_2 &= -\frac{1}{4} e^{-g_{>}(0)} \int d^2 v v^2 \left[ e^{g_{>}(\mathbf{v})} - 1 \right]. \tag{267}
\end{aligned}$$

Now, we will only consider the lowest-order corrections in  $J$  to the two terms appearing in the action (248). Therefore we ignore for now the term in  $\cos(2\phi_{\mathbf{r}}^<)$ , and get the result,

$$e^{-\beta F'_{\text{SG}}[\phi^<]} = X e^{-\int d^2 r \left[ \frac{1}{2} (g + J^2 I_2) |\partial_{\mathbf{r}} \phi_{\mathbf{r}}^<|^2 - J e^{-\frac{1}{2} g_{>}(0)} \cos \phi_{\mathbf{r}}^< \right]}. \tag{268}$$



### 6.2.4 RG equations for Sine-Gordon model

Eq. (268) tells us the effect on  $J$  and  $g$  after coarse-graining. Of course for the RG procedure, we should also rescale to get a coarse-grained system with the original cut-off. After doing this we easily find the following RG equations for a given coarse-graining of  $\lambda$ ,

$$\begin{aligned} J' &= \lambda^2 J e^{-\frac{1}{2}g_{>}(0)}, \\ g' &= g + J^2 I_2(\lambda, g). \end{aligned} \quad (269)$$

with  $I_2$  defined in (267).

We can make more sense of the dependence of  $I_2$  if we take the infinitesimal limit of an RG procedure, i.e., we only take out the fastest modes in an infinitesimal slice of width  $d\Lambda$ , so that

$$\begin{aligned} g_{>}(r) &= \int_{\Lambda-d\Lambda < q < \Lambda} \frac{d^2 q}{(2\pi)^2} \frac{e^{i\mathbf{q}\cdot\mathbf{r}}}{g q^2}, \\ &= \frac{1}{2\pi g} J_0(\Lambda r) \frac{d\Lambda}{\Lambda}, \end{aligned} \quad (270)$$

with  $J_0(x)$  the zeroth-order Bessel function. Substituting this in (267) gives,

$$I_2 = \frac{1}{g} \frac{d\Lambda}{\Lambda^5} \alpha_2, \quad (271)$$

with the dimensionless constant  $\alpha_2 = (8\pi)^{-1} \int d^2 x x^2 J_0(x)$ . We then get the infinitesimal form of the flow equations,

$$\begin{aligned} J' &= J \left( 1 + 2 \frac{d\Lambda}{\Lambda} \right) \left( 1 - \frac{1}{4\pi g} \frac{d\Lambda}{\Lambda} \right), \\ g' &= g \left( 1 + \frac{J^2 \alpha_2}{g^2} \frac{d\Lambda}{\Lambda^5} \right). \end{aligned} \quad (272)$$

Writing  $J' = J + dJ$  and  $g' = g + dg$  turns this into,

$$\begin{aligned} \frac{dJ}{J} &= \left( 2 - \frac{1}{4\pi g} \right) \frac{d\Lambda}{\Lambda}, \\ gdg &= J^2 \alpha_2 \frac{d\Lambda}{\Lambda^5}. \end{aligned} \quad (273)$$

Physically we see that the coarse-graining process leads to an effective system with either larger or smaller  $J$  depending on the sign of  $(g - 8\pi)$ . For small enough  $g$ , the flow is to smaller  $J$ , and successive RG transformations take the system to a  $J = 0$  fixed point, corresponding to a system with logarithmic roughness in the correlations in  $\phi(\mathbf{r})$ . For large enough  $g$ , the flow is to larger  $J$ , and the flow is to a bulk fixed point with zero correlation length. Also note that the flows always increase the value of  $g$ , i.e., the effective phase stiffness increases with the coarse-graining.

### 6.2.5 Kosterlitz flow diagram

We now make a few substitutions to cast the flow equations in a simpler form, as well as to make them look more like the form that Kosterlitz first found. We substitute

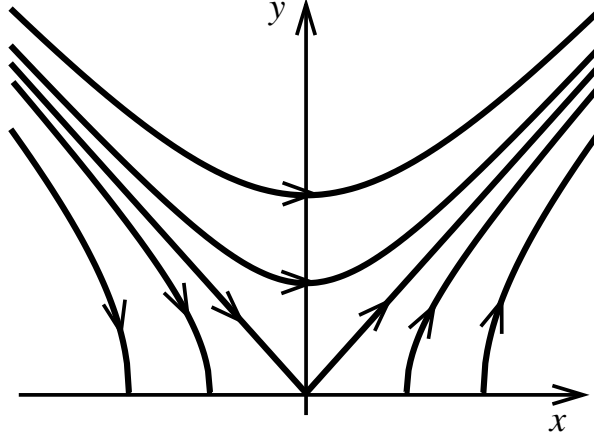


Figure 28: Calculated RG flow for small  $x$  and  $y$  satisfying the equation  $x^2 - y^2 = \text{const.}$ , where the constant depends on the initial parameters before renormalization. If the constant is negative, the flow is eventually to large values of  $y$ . The critical line is when the constant is zero. For a positive constant, and with  $x < 0$ , the flow is to  $y = 0$ .

the change in q-space cut-off  $d\Lambda$  for the change in real-space cut-off  $dl$ . Then we get,

$$\begin{aligned} \frac{dJ}{J} &= \left(2 - \frac{1}{4\pi g}\right) \frac{dl}{l}, \\ gdg &= J^2 \alpha_2 l^3 dl. \end{aligned} \quad (274)$$

Now we write  $x = (1/4\pi g) - 2$ , to give

$$\begin{aligned} \frac{dJ}{J} &= -x \frac{dl}{l}, \\ \frac{dx}{(x+2)^3} &= -(4\pi)^2 J^2 \alpha_2 l^3 dl. \end{aligned} \quad (275)$$

Finally we substitute  $y = 4\pi\sqrt{8\alpha_2}l^2J$ , so that

$$\begin{aligned} \frac{dy}{y} &= -x \frac{dl}{l}, \\ \frac{dx}{(x+2)^3} &= -\frac{1}{8}y^2 \frac{dl}{l}. \end{aligned} \quad (276)$$

The two important things to notice about this set of flow equations is that  $y = 0$  is a fixed point for all  $x$  (i.e. a *line* of fixed points), and that  $x = 0$  is also special in that it makes  $dy = 0$ , (although not  $dx$ ). For this reason we zoom in on the vicinity of  $(x, y) = (0, 0)$ , where we can solve the equations. Replacing  $(x+2)$  with 2, allows us to write,

$$-xy^2 \frac{dl}{l} = xdx = ydy, \quad (277)$$

so that solutions must be of the form

$$x^2 = y^2 + \text{const.} \quad (278)$$

In other words, the flow near the origin follows the curve of a hyperbola. The particular constant depends on the initial conditions, and its sign determines whether the

system flows to  $y = 0$ , or to infinite  $y$ . To demonstrate this, the flow lines are drawn in Fig. 28.

Therefore the phase transition between these two behaviours occurs when the constant is zero, or when the initial conditions,

$$\begin{aligned} x_0 &= \frac{1}{4\pi g} - 2, \\ y_0 &= 4\pi\sqrt{8\alpha_2}l^2J \end{aligned} \quad (279)$$

satisfy  $x_0^2 = y_0^2$ . The critical value of  $g$  for the phase transition is therefore,

$$g_c = 1/8\pi - \sqrt{\alpha_2/2}l^2J + \mathcal{O}(J^2). \quad (280)$$

Notice the strange result that in the limit  $J \rightarrow 0$ , the phase transition only depends on the value of  $g$ . This means that for  $g < 1/8\pi$ ,  $J$  is always a relevant perturbation, as is seen in the RG flow we have derived.

### 6.3 Properties of Kosterlitz-Thouless transition from RG

We should now think about what the flow diagram we have derived for the Sine-Gordon model implies for the XY model. Remember that we have shown the partition functions to be the same if we take  $g = 1/(2\pi)^2\beta K$  and  $J = 2l^{-2}e^{-\beta\epsilon_c}$ . Therefore we can write the dimensionless flow variables

$$\begin{aligned} x &= \pi\beta K - 2, \\ y &= be^{-\beta\epsilon_c}, \end{aligned} \quad (281)$$

with  $b = 8\pi\sqrt{8\alpha_2}$ . The flow diagram of Fig. 28 is then seen to represent either flows to zero fugacity at low temperature or to large fugacity at high temperature as in Fig. 27. The critical value of temperature where the two different behaviours are separated is given by, using (280),

$$T_{\text{KT}} = \frac{\pi K}{2} \left[ 1 - \frac{b}{2}e^{-\epsilon_c/T_{\text{KT}}} \right]. \quad (282)$$

This is a self-consistent relation for  $T_{\text{KT}}$ , that needs to be solved numerically. Notice how, in the limit of very large core energy, this result converges on the simple result from the free energy consideration of a single vortex in Section 6.1.6.

In fact, a much more complete picture emerges, if we write the effective spin-stiffness as given in (239). It turns out that evaluating the vortex-density correlation function leads to a correction of exactly the same form as in (282), so that the simple Kosterlitz-Thouless result is recovered, only with the *effective* spin-stiffness in the formula,

$$T_{\text{KT}} = \frac{\pi}{2}K_{\text{eff}}(T_{\text{KT}}). \quad (283)$$

Therefore, if we can measure this stiffness, it should have a universal ratio to temperature at the point where it jumps to zero. This is seen experimentally, for instance in the value of the superfluid density for thin-films of Helium at the point of the transition from superfluid to normal liquid.

What does the RG flow tell us about the correlations in the XY model? Clearly, below  $T_{\text{KT}}$ , the system flows under renormalization to a critical fixed point with

an algebraic correlation function, and an exponent equal to  $T/2\pi K_{\text{eff}}$ . Above  $T_{\text{KT}}$ , however, the system flows to a high-temperature fixed point where the correlation length becomes equal to the short-scale cut-off length. The actual correlation length must then be found by integrating back the flow equations, which we will now do: For  $T > T_{\text{KT}}$  we have the initial condition  $x_0^2 - y_0^2 = -\chi^2 < 0$ , where  $\chi$  can be written,

$$\chi = (y_0^2 - x_0^2)^{1/2} = [b^2 e^{-2\beta\epsilon_c} - (\pi\beta\epsilon - 2)^2]^{1/2} \approx c \left[ \frac{(T - T_{\text{KT}})}{T_{\text{KT}}} \right]^{1/2}, \quad (284)$$

where the last result is the limiting form close enough to  $T_{\text{KT}}$ . Now using the RG flow equation (277) we have,

$$\begin{aligned} dx &= -y^2 \frac{dl}{l}, \\ &= -(\chi^2 + x^2) \frac{dl}{l}, \\ \frac{dx}{x^2 + \chi^2} &= -\frac{dl}{l}, \end{aligned} \quad (285)$$

with solution,

$$\frac{1}{\chi} \tan^{-1} \frac{x}{\chi} - \frac{1}{\chi} \tan^{-1} \frac{x_0}{\chi} = \ln(l/l_0). \quad (286)$$

Inverting this shows us how the length-scale  $l$  changes with the RG flow,

$$l = l_0 e^{-\frac{1}{\chi}(\tan^{-1} \frac{x}{\chi} - \tan^{-1} \frac{x_0}{\chi})}. \quad (287)$$

Note that we expect  $x$  to flow to large positive values. However the  $\tan^{-1}$  function will be limited to  $\pi$  as  $x \gg \chi$ , so that the limit of  $l$  will be

$$\xi(T) = l(x \rightarrow \infty) = l_0 e^{\pi/\chi} = l_0 e^{b \left[ \frac{T_{\text{KT}}}{(T - T_{\text{KT}})} \right]^{1/2}}. \quad (288)$$

Therefore we see an incredibly sudden divergence of the correlation length as the Kosterlitz-Thouless transition is approached from above. Note that while the exponent of  $1/2$  that appears is universal, the factor  $b$ , which also appears in the exponential, is non-universal, i.e. it depends on initial conditions.

We can now use a simple scaling argument to find the singular contribution to the free energy near the phase transition. Assuming that the free-energy density scales as  $f_s \sim \xi^{-d}$  we get,

$$f_s \propto e^{-bd \left[ \frac{T_{\text{KT}}}{(T - T_{\text{KT}})} \right]^{1/2}}. \quad (289)$$

(This result is backed up by a more careful RG analysis of the free energy.) Intriguingly, all orders of derivatives of this free energy are zero as  $T \rightarrow T_{\text{KT}}$ . Therefore there are no discontinuities in any derivative of the free energy at the Kosterlitz-Thouless transition!

## 6.4 Physical examples

Apart from the quite beautiful theory, partially described above, of this Kosterlitz-Thouless phase transition, the interest in the problem also comes from its applicability

to many important condensed matter systems. Apart from an easy-plane 2D ferromagnet, the same transition can occur in thin-film superfluids and superconductors (although in the latter the extra property of magnetic screening will kill the phase transition on very long lengths). Also, the dynamical phase transition of phase-slips in a very thin superconducting wire has been described as a KT transition using the quantum  $d$ -dimension to classical  $(d + 1)$ -dimension mapping.

Other two-dimensional systems with a goldstone mode, such as crystals, can also be expected to have analagous topological defects to the vortex. For a crystal the relevant defect is a dislocation, and the theory describing unbinding of dislocation pairs is known as the Kosterlitz-Thouless-Halperin-Nelson-Young theory of 2D melting. The theory is more complicated as dislocations can only destroy some of the quasi-long-range order in a crystal: the system can retain orientational order, which is only destroyed if extra defects known as disclinations can proliferate. Whether there are two such transitions, of KT type, or if there is a single first-order transition, remains a question of controversy.

Finally, an interesting system arises when we have an external magnetic field perpendicular to a thin-film superconductor. The field forces a finite density of vortices (of same orientation) in to the film, and their mutual repulsion means that a lattice is formed at low enough temperatures. This system should therefore have both a unbinding transition of vortex-anti-vortex pairs, and an unbinding transition of dislocations in the vortex lattice. It turns out that the melting transition happens at a considerably lower temperature due to the smaller energy cost of a dislocation than a vortex (there is an extra factor of  $1/4\pi$  in the prefactor of the logarithm!).

# Statistical Physics of Phase Transitions

## Problem Sheet

Matthew J. W. Dodgson

November 28, 2001

Lecture One: Early understanding of phase transitions

Section 1.2: Van der Waals theory of a liquid-gas transition

### Question 1

**Find the location of the critical point  $P_c = P(v_c, T_c)$ , defined by setting the first and second derivatives of (16) to zero. Show that near the critical point,**

$$\frac{v - v_c}{v_c} = - \left[ \frac{2}{3} \frac{(P - P_c)}{P_c} \right]^{1/3}. \quad (1)$$

**on the critical isotherm  $T = T_c$  (note, the same exponent of  $1/3$  is found for the mean-field ferromagnet on the critical isotherm.) Show that on the coexistence line,**

$$v = v_c \pm 2v_c \left( \frac{T_c - T}{T} \right)^{1/2}, \quad (2)$$

**with the plus sign for approaching from the gas phase and the minus sign corresponding to the liquid. We see that the density difference  $\Delta v$  between gas and liquid falls continuously to zero at the critical point (again, the same exponent of  $1/2$  is found for the spontaneous magnetic moment in a mean-field ferromagnet). Finally, show that the compressibility**

$$\kappa = -\frac{1}{v} \left. \frac{\partial v}{\partial P} \right|_T. \quad (3)$$

**diverges at the critical point. Therefore we can expect violent density fluctuations at criticality (observed in carbon dioxide as “critical opalescence” by Andrews in 1863).**

Lecture Two: Statistical mechanics of phase transitions

Section 2.1.1: Simple model of a first-order transition

### Question 2

**We can illustrate the above points with an extremely simple model. Consider a system with a choice of  $2^N + 1$  configurations, one of which has zero**

energy, while the other  $2^N$  configurations all cost an energy  $\epsilon N$ . Write down the partition function and find the free energy as  $N \rightarrow \infty$ . Find the transition temperature, and the latent heat. Find the zeros of the partition function in the complex- $\beta$  plane. What happens to the zeros as  $N \rightarrow \infty$ ?

Section 2.3.1: Solution of Ising model in one dimension

### Question 3

Find the magnetization of the 1D Ising model in a field  $h$ , and show that the susceptibility follows the Curie law at high temperatures, but has a much stronger divergence as  $T \rightarrow 0$ .

Lecture Three: Thermal fluctuations in the ordered phase

Section 3.3.3: Gaussian approximation at low temperatures

### Question 4

Show that in the small  $\delta$  and  $\theta$  limit,

$$F_L^G[\delta, \theta] = \int d^d r \frac{|a|^2}{b} \delta^2 + \frac{g|a|}{2b} \left\{ |\partial_{\mathbf{x}} \delta|^2 + |\partial_{\mathbf{x}} \theta|^2 \right\}, \quad (4)$$

so that the elastic stiffness of the phase fluctuations is  $\varepsilon = g|a|/b$ . Calculate the propagator for the phase

$$G_\theta(\mathbf{r}) = \langle \theta(\mathbf{r}) \theta(\mathbf{0}) \rangle = \frac{T}{\varepsilon} \int \frac{d^d k}{(2\pi)^d} \frac{e^{i\mathbf{k} \cdot \mathbf{r}}}{k^2}. \quad (5)$$

for dimensions 1, 2, and higher. Then, ignoring the contribution from  $G_\delta(\mathbf{r})$  and using the property of Gaussian distributions<sup>1</sup> to write  $\langle e^{i[\theta(\mathbf{r}) - \theta(\mathbf{0})]} \rangle = e^{-\frac{1}{2} \langle [\theta(\mathbf{r}) - \theta(\mathbf{0})]^2 \rangle}$ , show that,

$$G(\mathbf{r}) = \begin{cases} \phi_0^2 e^{-\frac{T}{\varepsilon \pi} r}, & d = 1, \\ \phi_0^2 \left( \frac{r}{l} \right)^{-\frac{T}{2\pi\varepsilon}}, & d = 2, \\ \phi_0^2 \exp \left[ \frac{T}{\varepsilon} \frac{c_d}{r^{d-2}} - \frac{T}{\varepsilon} \frac{c_d}{l^{d-2}} \right], & d \geq 3. \end{cases} \quad (6)$$

---

<sup>1</sup>If we have a distribution  $P(x) = e^{-x^2/2\sigma}$  so that  $\langle x^2 \rangle = \sigma$  then we can write  $\langle e^{ix} \rangle = z^{-1} \int dx e^{-x^2/2\sigma} e^{ix} = z^{-1} \int dx e^{-\frac{1}{2\sigma}(x-i\sigma)^2} e^{-\sigma/2} = e^{-\langle x^2 \rangle/2}$ .

## Lecture Four: Field Theory of Phase Transitions

### Section 4.1.3: Specific heat from Gaussian fluctuations

#### Question 5

**Show that as  $T \rightarrow T_c$  from above, the most singular part of the specific heat  $c = -\partial^2 f / \partial T^2$  is given by,**

$$c_s = \frac{1}{2} \int \frac{d^d k}{(2\pi)^d} \frac{a'^2 T}{(a + gk^2)^2}. \quad (7)$$

**Evaluate the integral for the cases  $d < 4$ ,  $d = 4$ , and  $d > 4$  to show the following behaviours,**

$$c_s \propto \begin{cases} (T - T_c)^{-(4-d)/2}, & \text{for } d < 4 \\ \ln[(T - T_c)/T_c], & \text{for } d = 4 \\ \text{const.}, & \text{for } d > 4 \end{cases} \quad (8)$$

## Lecture Five: Scaling and Renormalization Group Approach

### Section 5.3.3: Fixed point with two unstable directions

#### Question 6

**Consider a fixed point with two unstable directions  $t$  and  $h$  (e.g., C for the 2D Ising model). Write the free energy scaling law in terms of the two eigenvalue exponents  $y_t$  and  $y_h$ , and find the scaling of the magnetization  $M = \partial f / \partial h$  and the susceptibility  $\chi = \partial M / \partial h$ . Combine these results to prove the scaling relation,**

$$\alpha + 2\beta + \gamma = 2. \quad (9)$$

## Lecture Six: Vortex-Unbinding Transition in the 2D-XY Model

### Section 6.2 The Sine-Gordon model in two dimensions

#### Question 7

**We ran out of time in the last lecture, so the final problem is to go over the derivation given in the lecture notes of the RG flow equations for the 2D Sine-Gordon model.**